# Novel Robust Adaptive Beamforming Algorithms with Improved Estimation of Array Covariance Matrix and Signal Steering Vector

**Saeed Mohammadzadeh**

Submitted to the
Institute of Graduate Studies and Research
in partial fulfillment of the requirements for the degree of

Doctor of Philosophy
in
Electrical and Electronic Engineering

Eastern Mediterranean University
January 2019
Gazimağusa, North Cyprus

Approval of the Institute of Graduate Studies and Research

Assoc. Prof. Dr. Ali Hakan Ulusoy
Acting Director

I certify that this thesis satisfies all the requirements as a thesis for the degree of Doctor of Philosophy in Electrical and Electronic Engineering.

Prof. Dr. Hasan Demirel
Chair, Department of Electrical and Electronic Engineering

We certify that we have read this thesis and that in our opinion it is fully adequate in scope and quality as a thesis for the degree of Doctor of Philosophy in Electrical and Electronic Engineering.

Prof. Dr. Osman Kükrer
Supervisor

Examining Committee

1. Prof. Dr. Feza Arıkan
2. Prof. Dr. Tolga Çiloğlu
3. Prof. Dr. Osman Kükrer
4. Prof. Dr. Hüseyin Özkaramanlı
5. Asst. Prof. Dr. Rasime Uyguroğlu

# ABSTRACT

Robust adaptive beamforming has long been an attractive research topic over several decades due to wide applications in vast fields of signal processing such as, radar, sonar, wireless communications, medical imaging, microphone array speech processing and other areas. Adaptive beamforming improves the reception of desired signals in the presence of interference signals automatically by sensing the presence of interferences and suppressing them while simultaneously enhancing desired signal reception without prior knowledge of the signal and interference environment. However, under certain circumstances, adaptive beamformers suffer performance degradation due to several reasons which include small sample size, the presence of the desired signal in the training data, the presence of nonstationary interference, or imprecise knowledge of the steering vector of the desired signal. Moreover, conventional approaches are very sensitive to these types of mismatches, do not provide sufficient robustness and may suffer from severe performance degradation in such situations.

In this thesis, we propose three different types of novel adaptive beamforming techniques to resolve the effects caused by some of the aforementioned difficulties.

A general goal in adaptive beamforming is to adaptively steer a beam towards a desired signal, while placing nulls at interference directions. The well-known minimum variance distortionless response (MVDR) adaptive beamformer is designed to linearly combine the outputs of the sensors in order to minimize the array output power, while maintaining a fixed response towards the desired signal. However, it is

well known that the MVDR beamformer is quiet sensitive to the mismatch between the actual steering vector and the assumed one, which could be caused by any array imperfection. In the first approach, a robust adaptive beamforming technique based on a modification of the robust Capon beamforming approach is introduced which estimates the steering vector using eigenspace projection-based approximation. The steering vector is estimated as a reasonable approximation for the orthogonal projection of the presumed steering vector of the desired signal onto the signal-plus-interference subspace. In this approach, the optimal diagonal loading factor corresponds to the minimum of the estimated beamformer output power. Also, estimation of the desired signal's direction-of-arrival is utilized to update the presumed steering vector.

On the other hand, during the past decade, many approaches based on the processing of the sample covariance matrix have been proposed. However, since the desired signal component is usually included in this matrix, the beamformer is sensitive to slight mismatches. Although, some techniques have been proposed to remove the signal-of-interest (SOI) component from the signal covariance matrix using the reconstruction of the interference-plus-noise covariance (IPNC) matrix, these have a number of drawbacks. In the second approach, we introduce a low complexity procedure for IPNC matrix construction. The main motivation of this algorithm is to simplify the estimation of the IPNC matrix using its theoretical expression which is based on projection processing for covariance matrix construction and desired-signal steering vector estimation. In this accordance, the optimal minimum variance distortion-less response beamformer is closely achieved through approximating the interference-plus-noise covariance matrix by utilizing the eigenvalue decomposition

of the received signal's covariance matrix. Moreover, the direction-of-arrival (DOA) of the desired signal is estimated by maximizing the beamformer output power in a certain angular sector. In particular, the proposed beamformer utilizes the aforementioned DOA in order to estimate the desired-signal's steering vector for general steering vector mismatches.

In addition, adaptive beamforming methods are sensitive to underlying assumptions on the environment, sources, or sensor array violation, especially when interferences are moving fast. In recent years, research efforts have been devoted to the development of beamforming using covariance matrix taper (CMT) or additional constraints in the optimization programming for suppression of pre-defined angular ranges. This research presents an innovative beamforming approach in which the nonstationary interference source is estimated during the period in which snapshots are taken. Then, a new interference-plus-noise covariance matrix reconstruction is introduced which is derived from a simplified power spectral density function that can be used to shape the directional response of the beamformer. Finally, the beamformer is designed to impose nulls toward the regions of the moving interference based on the reconstructed covariance matrix. The essence of the proposed method is to express the inverse of the reconstructed covariance matrix in such a way that significantly reduces computational complexity.

Theoretical analysis and simulation results indicate the superior performance of the introduced proposed approaches in the presence of mismatches relative to other some existing methods.

**Keywords**: Covariance matrix reconstruction, Diagonal loading, Fast moving

interference, Orthogonal projection, Robust Capon beamforming, Steering vector estimation.

# ÖZ

Dayanıklı uyarlanır demet oluşturucular, radar, sonar, telsiz haberleşme, tıbbi görüntüleme, mikrofon dizileri gibi işaret işlemenin çeşitli alanlarındaki uygulamalarından dolayı son zamanlarda ilgi çeken bir araştırma alanı olmuştur. Uyarlanır demet oluşturma, istenen işaret ve girişimlerden oluşan ortam hakkında önbilgi olmadan, girişimlerin varlığını otomatik olarak algılayıp istenen işaretlerin alınmasını iyileştirir ve girişimlerin bastırılmasını mümkün kılar. Fakat uyarlanır demet oluşturucular, küçük örnek miktarı, eğitim verisi içinde istenen işaretin bulunması, girişimlerin durağan olmaması ve istenen işaretin yönlendirme vektörü hakkında yeterli bilgi olmaması gibi durumlarda başarım kaybına uğramaktadır. Ayrıca, geleneksel yaklaşımlar bu gibi uyumsuzluklara karşı çok hassas olup yeterli dayanıklılık sağlamaktan uzaktırlar. Bu yaklaşımlar, bu gibi durumlarda ağır başarım kaybına uğrayabilir.

Bu tezde, yukarıda bahsedilen zorlukları aşmak amacı ile üç farklı ve yeni uyarlanır demet oluşturma yöntemi önerilmektedir.

Uyarlanır demet oluşturmanın genel amacı, girişimlerin yönünde dizilim yanıtını sıfırlamak suretiyle dizilimin esas demetini uyarlanır bir şekilde istenen işarete yönlendirmektir. Çok iyi bilinen bozunumsuz yanıtlı en az değişintili (MVDR) uyarlanır demet oluşturucu, dizilim çıkış gücünü en aza indirgemek amacıyla duyargaç çıkışlarını doğrusal olarak birleştirecek şekilde tasarlanır. Fakat, MVDR demet oluşturucunun, dizilimin kusurlarından kaynaklanabilen ve istenen işaretin gerçek ve varsayılan yönlendirme vektörleri arasındaki uyumsuzluğa karşı çok hassas

olduğu iyi bilinmektedir. Önerilen birinci yaklaşımda, yaklaşık özuzay izdüşümüne dayalı yönlendirme vektörü kestirimi yapan ve dayanıklı Capon demet oluşturma yaklaşımının değiştirilmiş bir şeklinden oluşan bir uyarlanır demet oluşturma yöntemi tanıtılmaktadır. İstenen işaretin varsayılan yönlendirme vektörünün işaret-girişim altuzayına dikey izdüşümünü yaklaşıklayan bir vektör kestirimi yapılmaktadır. Bu yaklaşımda, en iyi köşegen yükleme oranı demet oluşturucunun kestirilen çıkış gücünün en az değerine karşılık gelir. Ayrıca, varsayılan yönlendirme vektörünü güncellemek için istenen işaretin geliş yönü kestirimi kullanılır.

Diğer yandan, geçen on yılda, örnek özdeğişinti matrisini işlemeye dayalı yöntemler önerilmiştir. Fakat, bu matrise istenen işaret bileşeni de dahil edildiği için, demet oluşturucu hafif uyumsuzluklara karşı hassastır. Girişim-gürültü özdeğişinti (IPNC) matrisini yeniden yapılandırarak istenen işareti özdeğişinti matrisinden dışlamak amacı güden yöntemler önerilmiş olmasına ragmen, bu yöntemlerin bir takım zorlukları vardır. İkinci yöntemde, düşük karmaşıklığa sahip bir IPNC matris yapılandırma yöntemi önerilmektedir. Bu algoritmanın hareket noktası, IPNC matrisinin kuramsal ifadesini kullanmak suretiyle kestirimini basitleştirmektir. Bu da özdeğişinti matrisinin özuzay izdüşümünün işlenmesine ve istenen işaret yönlendirme vektörü kestirimine dayanmaktadır. Bu şekilde IPNC matrisini yaklaşıklama ve alınan işaretin özdeğişinti matrisinin özdeğer ayrışımını kullanmak yoluyla en iyi MVDR demet oluşturucu yaklaşık olarak gerçekleştirilmiştir. Ek olarak, demet oluşturucunun çıkış gücünü belirli bir açı aralığında enbüyüterek istenen işaretin geliş yönü kestirilmektedir. Bu kestirim, özellikle genel yönlendirme vektörü uyumsuzluk durumlarında istenen işaret yönlendirme vektörünün kestirimi için kullanıldı.

Uyarlanır demet oluşturma yöntemleri, ortam, kaynaklar veya duyargaç dizilimine ait yapılan varsayımlara karşı, özellikle girişimlerin hızlı hareket etmesine karşı duyarlıdırlar. Son yıllarda, araştırma gayretleri özdeğişinti matrisi konikleştirme veya önceden tanımlanmış açısal aralıkları bastırmaya yönelik eniyileştirme programlarına ek kısıtlar getirme konularına adanmaktadır. Bu araştırmada durağan olmayan girişim kaynağının hereketinin işaret enstantanelerinin alındığı aralık süresince takip edilip kestirildiği yenilikçi bir demet oluşturma yaklaşımı da sunulmaktadır. Bu yaklaşımda, basitleştirilmiş bir güç izge yoğunluğundan elde edilen bir IPNC matris yapılandırması üzerinde durulmaktadır. Sözkonusu basitleştirilmiş güç izge yoğunluğu işlevi, demet oluşturucunun yönsel yanıtını şekillendirmek için de kullanılır. Sonuç olarak demet oluşturucu, girişim kaynağının hareket ettiği açısal aralıkta dizilim yanıtını sıfırlayacak şekilde tasarlanır.

Önerilen yöntemin özünde yeniden yapılandırılmış özdeğişinti matrisinin tersinin, hesaplama karmaşıklığını önemli ölçüde azaltacak bir şekilde elde ediliyor olmasıdır.

**Anahtar Kelimeler**: Özdeğişinti matris yeniden yapılandırma, köşegen yükleme, hızlı hareketli girişim, dikey izdüşüm, dayanıklı Capon demet oluşturma, yönlendirme vektör kestirimi.

# DEDICATION

**To My Dear Son Artin**

# ACKNOWLEDGMENT

Firstly, I would like to express my sincere gratitude to my advisor Prof. Dr. Osman Kukrer for the continuous support of my Ph.D study and related research, for his patience, motivation, and immense knowledge. His guidance helped me in all the time of research and writing of this thesis. I could not have imagined having a better advisor and mentor for my Ph.D study.

I would like to extend my gratitude to the committee members for their academic guidance. I would also like to thank all faculty members at the department of electrical and electronic engineering, and specially the chairman Prof. Dr. Hasan Demirel.

My deepest gratitude goes to my love Noushin Hajarolasvadi who supported me in writing, and incented me to strive towards my goal.

Last but not the least, I would like to thank my family: my parents and to my brothers and sisters for supporting me spiritually throughout writing this thesis and my life in general.

# TABLE OF CONTENTS

# LIST OF FIGURES

# LIST OF SYMBOLS AND ABBREVIATIONS

| | |
|---|---|
| $\varepsilon$ | Uncertainty factor |
| $\zeta$ | Diagonal loading factor |
| $\lambda$ | Eigenvalue |
| $\sigma^2$ | Variance |
| $\mathbf{a}$ | Array steering vector |
| $\mathbf{e}$ | Eigenvector |
| $d$ | Interelement spacing |
| H | Hermitian operator |
| $N$ | Number of sensors |
| $M$ | Number of training data |
| $\mathbf{Q}$ | Noise covariance matrix |
| $\mathbf{R}$ | Autocorrelation matrix |
| T | Transposition operator |
| $\mathbf{w}$ | Weights vector |
| $\mathbf{x}$ | Received signal vector |
| AOA | Angle of Arrival |
| AUIRCB | Adaptive Uncertainty Iterative Robust Capon Beamformer |
| CMT | Covariance matrix Taper |
| CS | Compressive Sensing |
| DL | Diagonal Loading |
| DOA | Direction of Arrival |
| EVD | Eigenvalue Decomposition |

| | |
|---|---|
| ESB | Eigespace Baesd Beamformer |
| FIR | Finite Impulse Response |
| INR | Interference to Noise Ratio |
| IPNC | Interference plus Noise Covariance |
| LCMV | Linearly Constrainted Minimum Variance |
| MDDR | Minimum Dispersion Distortionless Response |
| MVDR | Minimum Variance Distortionless Response |
| MUSIC | Multiple Signal Channel |
| QCQP | Quadratically Constrainted Quadratic Programming |
| RCB | Robust Capon Beamformer |
| SINR | Signal to Interference plus Noise |
| SMI | Sample covaraince Matrix |
| SNR | Signal-to-Noise Ratio |
| SOI | Signal of Interest |
| SPSS | Spatial Power Spectrum Sampling |
| SVD | Singular Value Decomposition |
| ULA | Uniform Linear Array |

# Chapter 1

# INTRODUCTION

## 1.1 Introduction

Array processing is an area of signal processing that deals with techniques for extracting information from signals collected using an array of sensors. The desired information in the signal corresponds to either reflection that produces the signal in radar and sonar systems or the content of spatially propagating signal from a certain direction as often found in communication applications [2]. These signals are broadcast spatially over a space, such as, air, and the samples are collected from the wavefront by the sensor array. Then, the useful information is extracted by processing the sensor array data. Some approaches, including adaptive beamforming and parameter estimation are extended to sensor array application. Amongst the most interesting topics of array processing techniques are beamforming and the estimation of the DOA of signals. Adaptive beamforming and estimation of direction of arrival of signals are spatial filtering techniques for Uniform Linear Array (ULA) of sensors with widespread applications in a large number of fields like sonar [3], radar [4], wireless communications [5, 6], seismology and imaging [7].

## 1.2 Uniform Linear Array

An array of sensors has long been an attractive solution for severe reception problems that commonly involve signal detection and estimation. One of the most famous arrays is the Uniform Linear Array. ULA is an antenna array configured of individual beam elements with equal spacing between the elements and can be employed to

produce a directional radiation array. Every single element antenna has beampatterns that are broad and they have low directivity that is not appropriate for long distance communications. A high directivity can still be achieved with single element antennas by increasing the electrical dimensions with respect to the wavelength and the physical size of the antenna. Antenna arrays come in different geometrical structures, the most common being linear arrays. Arrays commonly use identical antenna elements. The beam pattern of the array depends on the configuration, the distance between the elements, the amplitude and phase excitation of the elements, and also the radiation pattern of every sensor. Figure 1.1 shows the ULA, where interelement spacing is defined by $d$ and a single propagation signal impinges on the ULA from angle θ.

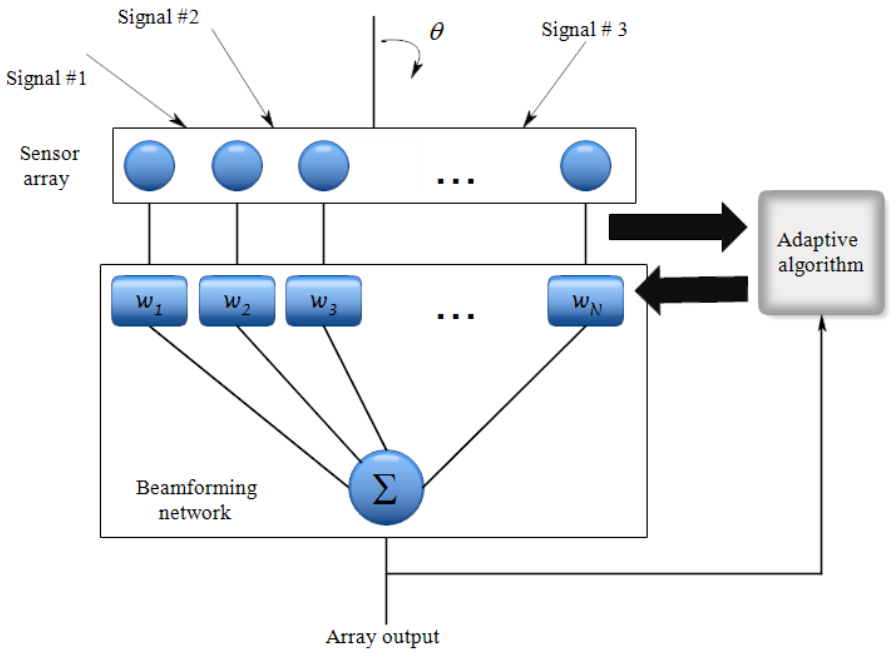


Figure 1.1: Uniform Linear Array in a Beamforming Configuration [1]

However, one of the drawbacks of the ULA sensors is the presence of the left-right ambiguity. Single line array receivers are cylindrically symmetric and, therefore, cannot discriminate left from right, port from starboard (Port and starboard are

nautical terms for left and right, respectively. Port is the left-hand side of or direction from a vessel, facing forward. Starboard is the right-hand side, facing forward). Such an ambiguity complicates the detection and tracking algorithms and may cause severe performance degradation.

## 1.3 Beamforming

Generally, an array receives spatially propagating signals and processes them to emphasize signals arriving from a certain direction. To this end, we want to linearly combine the signals from all the sensors in a manner, that is, with a certain weighting, so as to examine signals arriving from a specific angle. This operation is known as beamforming [2, 8] since the weighting process emphasizes signals from a particular direction while attenuating those from other directions, which can be regarded as casting or forming a beam. In beamforming, an array processor steers a beam to a particular direction by computing a properly weighted sum of the individual sensor signals just as a Finite Impulse Response (FIR) filter generates an output (at a frequency of interest) that is the weighted sum of time samples.

Beamforming is classified into two types, data independent and data dependent. The weights in a data independent beamformer are designed so the beamformer response approximates a desired response independent of the array data or data statistics. The approximation of a desired response is the same as that for classical FIR filter design [9]. In statistically optimum (data dependent) beamforming, the weights are selected to obtain a desired response based on the statistics of data received at the array. The goal is to optimize the beamformer response so the output contains minimal contributions due to noise and interfering signals and maximize the Signal to Interference plus Noise Ratio (SINR) [10].

## 1.4 Thesis Objectives

Adaptive beamforming has found numerous applications in the field of signal processing like radar, sonar, wireless communications, sonar, seismology and diagnostic ultrasound. However, in practice the assumptions on the source, environment and antenna array become imprecise, due to non-ideal conditions such as mismatch in the direction-of-arrival of SOI, array calibration errors and finite sample approximation of the array covariance matrix. Therefore, the adaptive beamforming algorithm's performance degrades substantially. Also, the adaptive weight vector is quite sensitive to error of the signal steering vector and inaccurate estimation of the covariance matrix, especially when the SOI component is present in the training data.

In this study, new approaches for adaptive beamforming are proposed which address the aforementioned problems as follow:

1) Approximation of the eigenspace projection beamformer by using the Robust Capon Beamforming (RCB) algorithm.

2) Estimation of the SOI's steering vector as the orthogonal projection of the presumed steering vector on the signal-plus-interference subspace.

3) Development of a method for determining the diagonal loading factor that optimizes the steering vector estimate.

4) IPNC matrix is closely approximated by using the eigenvalue decomposition of the received signal's covariance matrix.

5) The DOA of the desired signal is estimated by maximizing the beamformer output power in a certain angular sector.

6) Estimation of the desired-signal's steering vector which is based on signal-plus-noise covariance matrix.

## 1.5 Thesis Contribution

This study is mainly focused on problems of adaptive beamforming such as estimation of the DOA and steering vector of the desired signal, reconstruction of the IPNC matrix and suppression of fast moving interference signals.

In this thesis, we first introduce a novel low complexity approach based on modifying the robust Capon beamforming algorithm, which is proposed in an attempt to approximate the eigenspace projection beamformer. This approach leads to an estimate of the SOI's steering vector which is shown to be a reasonably good approximation for the orthogonal projection of the presumed steering vector on the signal-plus-interference subspace. The proposed approach is also based on diagonal loading of the covariance matrix. However, a new method is developed for determining the diagonal loading factor that optimizes the steering vector estimate. This method utilizes the beamformer output power calculated using the steering vector estimate as a function of the diagonal loading factor. It is demonstrated that as the diagonal loading factor increases, the beamformer output power approaches the optimal output power that corresponds to an effective suppression of the interference-plus-noise.

The main contributions of this method may be summarized as follows:

**a**) Desired signal's steering vector estimate is considerably improved with respect to the RCB estimate.

**b**) A new approach to the determination of the diagonal loading factor is introduced, based on the beamformer output power.

**c**) A clear advantage of the proposed beamformer is that it overcomes the subspace swap problem encountered in the eigenspace-based beamformer at low Signal to

Noise Ratio (SNR)s, thus ensuring the validity of the orthogonal projection at all SNRs.

**d**) The availability of an approximate orthogonal projection of the SOI's presumed steering vector onto the signal subspace enables the estimation of the SOI's direction-of arrival in a way similar to the Multiple Signal Classification (MUSIC) methodology.

In some non-ideal situations, the performance of the adaptive beamforming methods severely degrades since the desired signal component is present in the training snapshots. Therefore, in order to remove the SOI component from the signal covariance matrix, an approach based on the reconstruction of the IPNC matrix is introduced. The main motivation of the proposed method is to simplify the estimation of the IPNC matrix using its theoretical expression and the DOA estimate of the desired signal.

The main focus of this approach is summarized as:

**a**) Avoidance of the estimation of the IPNC matrix based on reconstruction in terms of the integral of rank-one matrices weighed by the corresponding incident power, obtained using the Capon spectral estimator.

**b**) The IPNC matrix can be efficiently estimated under certain conditions by utilizing the eigenvalue decomposition of the received signal's covariance matrix.

**c**) Avoidance of desired signal steering vector estimation by formulating the problem as a constrained optimization problem.

**d**) Estimation of the steering vector in a subspace corresponding to the desired signal and the noise. This subspace can be accurately identified if the interference powers

are much larger than the SOI's and the noise powers

On the other hand, the capability of adaptive antenna array lies in forming higher gain in the user directions and lower gain in the interferer directions. Therefore, when the interference waveform or distribution change with time or location by antenna platform vibration, propagation channel variation, the conventional adaptive beamforming algorithm's performance degrades drastically. Hence, it is then desired to maintain a suppressed angular region in the beampattern for such moving interferences. In this research, a novel method is proposed that is capable of creating notches in the directional response of the array with sufficient widths and depths so that interference signals from moving sources can be effectively suppressed.

The aim and contribution of the proposed method can be expressed as:

**a**) The time-varying DOA of a moving interference source is estimated during the period in which snapshots are taken.

**b**) The null region is designed that spans the directions in which the interfering source moves.

**c**) The IPNC matrix is replaced by another one derived from a simplified power spectral density function that can be used to shape the directional response of the beamformer.

**d**) An expression for the inverse of IPNC matrix is developed which facilitates fast calculation of the beamformer weight given the interference signal DOAs.

## 1.6 Thesis Outline

The structure of the thesis is arranged as follows:

In Chapter 2, adaptive beamforming applications, aims and difficulties will be reviewed. Then, the array signal model is presented and the optimum beamformer is

formulated. Finally, we will consider several adaptive beamforming techniques which have been proposed during the past decades.

In Chapter 3, the modification of the robust Capon beamformer is introduced. We develop a new technique that leads to an estimate of the orthogonal projection of the presumed steering vector of SOI onto the signal plus interference subspace. Also, the minimum of the beamformer output power is utilized to find the optimal diagonal loading factor which provides the possibility to estimate the DOA of the desired signal.

In Chapter 4, the beamformer is designed according to projection processing for covariance matrix construction and desired signal steering vector estimation. IPNC matrix approximation is achieved by using the eigenvalue decomposition of the received signal's covariance matrix. Besides, the maximum of the beamformer output power is utilized to estimate the DOA of the desired signal.

In Chapter 5, a robust adaptive beamformer is investigated in practical problems where the interference waveform can rapidly change in time. The time-varying DOA of a moving interference source is estimated during the period in which snapshots are taken. Besides, inverse of the IPNC matrix is proposed which is derived from simplified power spectral density function that leads to shape the directional response of the beamformer.

In Chapter 6, summary of conclusions and a discussion on possibilities for the future work are presented.

# Chapter 2

# ADAPTIVE BEAMFORMING STRUCTURE

## 2.1 Overview

Adaptive beamforming is a spatial filtering technique for array of sensors with numerous applications in the areas of sensor array processing such as radar, sonar and communications. The main goal of adaptive beamforming is to detect and estimate the SOI in the presence of interference and noise by means of data-adaptive spatial filtering. Most of the existing adaptive beamforming methods depend on some assumption and the exact knowledge of the array manifold. Moreover, some of them are related directly to signal or interference source and thermal noise. Practically, if problems exist in the form of non-ideal conditions such as the signal propagation model, antenna array parameters and their underlying assumptions, the adaptive beamformer's performance degrades substantially. The main reason for such degradation is sensitivity of adaptive beamforming algorithms to signal model and array manifold mismatches.

In this chapter, the array signal model is presented and the optimum beamformer is formulated. Then, we will consider several adaptive beamforming techniques which have been proposed during the past decades.

## 2.2 Signal Model

It is assumed that a uniform linear array with $N$ sensors and half wavelength spacing $d$ receives narrowband signals from $R$ point signal sources located at distinct directions.

The $N \times 1$ received signal vector of the array at discrete time $t$ which is corrupted by additive noise can be expressed as follows:

$$\mathbf{x}(t) = s(t)\mathbf{a}(\theta_\circ) + \sum_{i=0}^{L} \mathbf{a}(\theta_i)s_i(t) + \mathbf{n}(t) \tag{2.1}$$

where $s(t) = H(f_c)s_\circ(t)$ is the impulse response of SOI to nth sensor and $s_i(t)(i = 1,\ldots,L)$ is the corresponding interference signals, respectively. $\theta_\circ$ is the desired signal and $\theta_i$ is the $i$th interference directions and the corresponding steering vectors are $\mathbf{a}(\theta_\circ)$, $\mathbf{a}(\theta_i)$, respectively. $\mathbf{n}(t)$ is the $N \times 1$ vector of unknown sensor noise, and $(\cdot)^{\mathrm{T}}$ denotes the transpose.

The spatial signal has a different propagation between two sensors because the space of elements is equal so the result of time delay can be:

$$\tau(\theta) = \frac{d\sin\theta}{c} \tag{2.2}$$

Where $c$ is the speed of propagation for signal. To end up the delay to the nth element (sensor) will be

$$\tau(\theta) = (N-1)\frac{d\sin\theta}{c} \tag{2.3}$$

It should be mentioned that full possible range for angle $\theta$ is $-90^\circ \leq \theta \leq 90^\circ$, the space for sensor must be $d \leq \lambda/2$, it will not let ambiguities. where $\lambda = c/f_c$ is the wavelength and the carrier frequency $f_c$ determines the wavelength of the propagated wavefront.

For sonar systems, frequencies in the range 100–100,000 Hz are commonly employed, whereas for radar systems the range can extend from a few megahertz up into the optical and ultraviolet regions, although most equipment is designed for

microwave bands between 1 and 40 GHz. The wavelength of the propagated wavefront is important because the array element spacing (in units of $\lambda$) is an important parameter in determining the array pattern.

Assuming that the sources and noise are statistically uncorrelated and the interference steering vectors are linearly independent, the theoretical covariance matrix of the received signal can be expressed as

$$\mathbf{R} = \mathrm{E}\{\mathbf{x}(t)\mathbf{x}^{\mathrm{H}}(t)\} = \sigma_{\mathrm{s}}^2\mathbf{a}(\theta_\circ)\mathbf{a}^{\mathrm{H}}(\theta_\circ) + \sum_{i=1}^{L}\sigma_i^2\mathbf{a}(\theta_i)\mathbf{a}^{\mathrm{H}}(\theta_i) + \mathbf{Q} \tag{2.4}$$

where $\sigma_{\mathrm{s}}^2$ and $\sigma_i^2$ are signal and $i$th interference power, respectively. $\mathbf{Q} = \mathrm{E}\{\mathbf{n}(t)\mathbf{n}^{\mathrm{H}}(t)\}$ is the $N \times N$ full-rank covariance matrix of sensor noise, $\mathrm{E}\{\cdot\}$ is the statistical expectation, and $(\cdot)^{\mathrm{H}}$ stands for the Hermitian transpose. It is assumed that sensor noises are temporally and spatially white complex Gaussian random processes, that is,

$$\mathrm{E}\{\mathbf{n}(t)\mathbf{n}^{\mathrm{H}}(t)\} = \sigma_{\mathrm{n}}^2\mathbf{I}_{\mathrm{N}} \tag{2.5}$$

where $\sigma_{\mathrm{n}}^2$ is the noise variance. In matrix form (2.4) is simplified as

$$\mathbf{R} = \sigma_{\mathrm{s}}^2\mathbf{a}_\circ\mathbf{a}_\circ^{\mathrm{H}} + \mathbf{A}_i\mathbf{D}_i\mathbf{A}_i^{\mathrm{H}} + \sigma_{\mathrm{n}}^2\mathbf{I}_{\mathrm{N}} \tag{2.6}$$

where $\mathbf{A}_i = [\mathbf{a}_1\ \mathbf{a}_2\ \ldots\ \mathbf{a}_L]$ is the $N \times L$ interference direction matrix which contains the steering vectors of the interference signals, and the diagonal elements of the diagonal matrix $\mathbf{D}_i$ are the interference signal powers.

The ultimate aim of the adaptive beamformer is to combine the sensor signals in such a way that the interference signals and noise are rejected while the desired signal is

preserved. We would like to maximize the ratio of the signal power to that of the interference plus noise, which is known as the SINR. The beamformer's performance is usually measured using SINR as

$$\mathrm{SINR} = \frac{\sigma_{\mathrm{s}}^2 |\mathbf{w}^{\mathrm{H}} \mathbf{a}_{\circ}|^2}{\mathbf{w}^{\mathrm{H}} \mathbf{R}_{\mathrm{i+n}} \mathbf{w}} \tag{2.7}$$

where $\mathbf{w}$ is the beamformer weight vector and

$$\mathbf{R}_{\mathrm{i+n}} = \sigma_{\mathrm{n}}^2 \mathbf{I}_{\mathrm{N}} + \mathbf{A}_i \mathbf{D}_i \mathbf{A}_i^{\mathrm{H}} \tag{2.8}$$

is the interference-plus-noise covariance matrix. It is easy to find the optimal weight vector by minimizing the interference-plus-noise output power while maintaining a distortionless response toward the desired signal. Therefore, the maximization of SINR is equivalent to

$$\min_{\mathbf{w}} \mathbf{w}^{\mathrm{H}} \mathbf{R}_{\mathrm{i+n}} \mathbf{w} \quad \text{s.t.} \quad \mathbf{w}^{\mathrm{H}} \mathbf{a}_{\circ} = 1 \tag{2.9}$$

$$\mathbf{w}_{\mathrm{opt}} = \frac{\mathbf{R}_{\mathrm{i+n}}^{-1} \mathbf{a}_{\circ}}{\mathbf{a}_{\circ}^{\mathrm{H}} \mathbf{R}_{\mathrm{i+n}}^{-1} \mathbf{a}_{\circ}} \tag{2.10}$$

Correspondingly, the optimal output SINR is given by

$$\mathrm{SINR}_{\mathrm{opt}} = \sigma_{\mathrm{s}}^2 \mathbf{a}_{\circ}^{\mathrm{H}} \mathbf{R}_{\mathrm{i+n}}^{-1} \mathbf{a}_{\circ} \tag{2.11}$$

In most applications, the precise interference-plus-noise covariance matrix is not available. Hence, it is usually replaced by the covariance matrix of the received signal which in practice is calculated using the finite sample approximation as

$$\hat{\mathbf{R}} = \frac{1}{K} \sum_{t=1}^{K} \mathbf{x}(t) \mathbf{x}^{\mathrm{H}}(t) \tag{2.12}$$

where $K$ is the number of snapshots. Note that $\hat{\mathbf{R}}$ includes the desired signal component.

## 2.3 Review of Adaptive Beamforming Methods

An adaptive beamforming algorithm can automatically optimize the array pattern by adjusting the elemental control weights until a prescribed objective function is satisfied. Unfortunately, it is possible that mismatches occur between adaptive weights and data, due to perturbation in the assumptions, imperfect knowledge of source characteristics, environment or antenna array. Throughout this section we review methods and techniques from the literature to provide insight into various aspects of spatial filtering with a beamformer.

Several adaptive beamforming methods have been developed in research topics to enhance robustness against beamformer's difficulties in past decades; see, e.g. [11, 12]. These could be divided into the following categories:

The first category covers methods that do not reconstruct the covariance matrix and process the sample covariance matrix directly: The diagonal loading (DL) methods [13], [14] are aimed at eliminating covariance matrix uncertainty. Diagonal loading mitigates the effects of signal contamination, where the presence of the SOI in the training snapshots degrades the beamformer's performance and the effects of the finite sample approximation of the covariance matrix [15, 16]. The diagonal loading approaches are derived by imposing an additional quadratic constraint either on the Euclidean norm of the weight vector itself or on its difference from a desired weight vector [17, 18]. However, in this technique there is no rule as to how the loading factor should be chosen. In the robust Capon beamformer developed in [19], the DL factor is related to the uncertainty level and can be calculated by solving an

optimization problem which has an equivalent solution in [20]. In order to calculate the DL factor inclusion of an uncertainty set-based technique is used to process the spherical or ellipsoidal steering vector estimation uncertainty set by solving an optimization problem [19, 21]. The main disadvantage of these methods is that in the presence of a large steering vector mismatch the set has to be expanded to cope with the increased uncertainty at the cost of reduced output SINR [21]. Hence, its performance will degrade as the input SNR increases. To decrease the computational complexity, in [22] a generalized Hermitian matrix is estimated in which the directional response of the array is modified and SOI is rejected. This matrix is added to the sample covariance matrix in order to remove the SOI component from the sample covariance matrix of the array input with low computational complexity. In [23] the steering vector of the SOI is estimated under the requirement that the estimate does not converge to any steering vector of the interferences.

In the shrinkage method, an enhanced covariance matrix is obtained instead of the sample covariance matrix to improve robustness against steering vector errors [24, 25]. However, the improvement in performance is very limited and the method cannot completely solve the problems in theory. To improve this, a shrinkage-based mismatch estimation algorithm has been addressed in [26], which estimates the covariance matrix by using the Oracle Approximating Shrinkage method only with prior knowledge of the antenna array geometry and the angular sector, in which the actual steering vector is located.

In subspace based beamformers, only the signal subspace information is retained. Their principle is that by utilizing the subspace component for signal plus interference

of the sample covariance matrix and discarding the noise subspace the SNR is effectively enhanced. In the Eigenspace-based projection approaches [27–29] the desired signal steering vector is obtained by projecting the presumed steering vector on the signal-plus-interference subspace where the signal subspace may be corrupted by the noise subspace [30]. However, the error component lying in the interference signal subspace cannot be eliminated and performance is dramatically degraded at low SNRs. Also, in practical applications determining the number of sources is a challenging issue to estimate the signal-plus-interference subspace. In [31] a modified projection approach is proposed to increase the performance at low SNRs. However, there is no clear guideline on how to choose the parameters in order to find the projection of the presumed steering vector on the eigenvectors of the correlation matrix. Besides, it is sensitive to large steering vector mismatches.

Although these algorithms improve robustness against covariance matrix uncertainty or steering vector mismatches of the SOI, the effectiveness of the beamformer's performance would degrade at different input SNRs. Moreover, many approaches have shown that even for small mismatch between the presumed and the desired signal's steering vector, the output SINR deviates from the optimal one. Since, in these algorithms the sample covariance matrix is exploited directly.

The second category covers approaches which try to remove the SOI components by reconstruction of the covariance matrix instead of using the sample covariance matrix. Adaptive beamforming techniques are proposed in [32–36] based on IPNC matrix reconstruction. A beamformer proposed in [37] attempts to remove the effect of the desired signal by using a vector space projection algorithm and desired signal power

to form the desired-signal-free covariance matrix. In the algorithm of [33], the IPNC matrix is reconstructed by integrating the Capon spectral estimator over an angular sector that excludes the sector containing the direction-of-arrival of the desired signal. Moreover, the desired signal's steering vector is estimated by solving a quadratically constrained optimization problem using quadratic programming methods (QCQP). However, authors in [34] pointed out that the approach based on reconstructing the IPNC matrix in [33] may have some theoretical difficulties. More importantly, these algorithms are sensitive to large DOA and any other kind of steering vector mismatches of the interferences, such as errors due to coherent local scattering and random steering vector [38].

The beamformer in [39] reconstructs both IPNC and the desired signal covariance matrices based on Capon spectral estimation. Then, a subspace is constructed that is orthogonal to the interference subspace. The obtained subspace is rotated in order to attain the optimal weight vector which maximizes the output power of the SOI. To improve robustness of the adaptive beamformer against array steering vector mismatch, the method in [40] utilizes closed-form formula to estimate the array steering vector which lies within the intersection of two subspaces. Then, the covariance matrix is reconstructed by using the eigenvalue corresponding to the desired signal.

In [41], first, covariance matrices of the interference and SOI over predefined angular sectors are constructed. Then, prime eigenvector of each signal corresponding to the maximum eigenvalue is utilized to estimate the steering vector of the desired signal and interferences. The method in [42] uses the same idea of the beamformer in [41].

However, in order to improve the reconstruction against large look direction errors, the authors exploit double estimation of the steering vector as an optimization programme tries to obtain accurate SOI's steering vector.

The adaptive beamformer in [32] uses sparsity to reconstruct the IPNC matrix by computing a weighted sum of the outer products of the interference steering vectors, the coefficients of which are estimated from a compressive sensing (CS) problem. In [35], the beamformer algorithm utilizes a pair of decomposed coprime subarrays to estimate the DOA and corresponding power for each signal source. These estimates later are used to reconstruct the IPNC matrix and the desired signal steering vector. To reduce the computational burden of solving the QCQP problem, a method has been proposed in [43] to estimate the desired signal's steering vector. The method uses correlations between the presumed steering vector of the SOI and the eigenvectors of the sample covariance matrix. This approach can not eliminate the subspace swap error in the case of low SNRs. An adaptive beamforming [44] has been proposed based on spatial power spectrum sampling (SPSS) which utilizes the Capon spectrum to reconstruct the IPNC matrix. Also, covariance matrix tapering is employed to improve performance. However, as the authors have shown in the method's derivation, the number of sensors must be sufficiently large.

On the other hand, there are yet many applications and signal scenarios such as nonstationary interference where existing methods are inadequate. When the interference waveform or distribution change with time or location by antenna platform vibration, propagation channel variation, conventional adaptive cancelers might perform poorly. One of the most popular approaches to adaptive beamforming

is the so-called MVDR processor, which minimizes the array output power while maintaining a distortionless mainlobe response toward the desired signal [20]. However, in most of the conventional adaptive beamformers, a narrow null is designed to cancel an interference by making the array's response to that interference zero [11], [22]. With multiple interferences, multiple similar constraints are imposed, which lead to the Linearly Constrained Minimum Variance (LCMV) beamformer [45]. However, this approach does not perform well with an interference whose direction-of-arrival varies quickly with time. Unlike the LCMV methods, in the null broadening approach [46] a transformation is applied to the sample covariance matrix in order to extend a greater angular. Algorithm in [47] provides a null region to interferences by introducing the concept of CMT. A multi-parametric quadratic programming method is presented to control the null level of the adaptive antenna array [48]. However, when the null width is broadened, there exist high sidelobes and the depth becomes shallower.

Several methods have been proposed based on the CMT algorithm in order to overcome the pattern distortion which arises from the moving interference. However, these methods retain similar performance in the output in [49], where a beamforming method is proposed based on the IPNC matrix reconstruction which imposes the null toward the angular sector of a moving interference. This algorithm involves solution by the QCQP technique. In the large aperture scenario, the deviation of the interference location presents a serious problem because the directional pattern nulls are sharp and interference may move out of the nulls region [50]. Also, the multiparametric quadratic programming for covariance matrix taper minimum variance distortionless response beamformer is proposed to resolve null-broading and

sidelobe control problem in [51]. Nevertheless, the sidelobe domain constraint is obviously broadening the mainlobe beam pattern which decreases array gain.

Moreover, the null-broadening method of derivative constraint was proposed in [52], [53], but has more computational complexity than [46]. In [54] the quadratic constraint of the optimization problem [55] is replaced by a set of linear constraints to produce a widened null sector over moving interferences. Also, the adaptive array with troughs produced by dispersion synthesis approach is proposed in [56]. On the other hand, the minimum dispersion distortionless response beamformer is proposed in [57] which tries to provide a sector over a predefined range of DOA. In [58] a technique is proposed based on projection matrix which is established by choosing eigenvectors corresponding to the large eigenvalue of the array correlation matrix. The steering vector correlation matrix is constructed in the pre-defined angular sectors of the interference direction. Moreover, diagonal loading approach is utilized to obtain the sample covariance matrix.

# Chapter 3

# MODIFIED ROBUST CAPON BEAMFORMING WITH APPROXIMATE ORTHOGONAL PROJECTION ONTO THE SIGNAL PLUS INTERFERENCE SUBSPACE

## 3.1 Introduction

In this chapter, we propose a method to estimate the desired signal steering vector based on the Robust Capon Beamformer (RCB) [19]. Moreover, this estimate is shown to approximate the orthogonal projection of the presumed steering vector onto the signal-plus-interference subspace. Meanwhile, determination of the optimal value for the diagonal loading factor is based on the Capon spectral estimator, which is used here to detect the beamformer output power that corresponds to the desired signal.

The desired signal's steering vector estimate can be further improved by estimating the DOA of the desired signal, whereby the presumed steering vector is updated as $\bar{\mathbf{a}} = \mathbf{a}(\hat{\theta}_\circ)$, $\hat{\theta}_\circ$ being the DOA estimate. A procedure based on the MUSIC method [12] and the steering vector estimate obtained from modified RCB is applied.

## 3.2 Mathematical Development of Modified RCB

The Modified RCB is obtained as the solution of the following optimization problem

$$\min_{\mathbf{a}} \mathbf{a}^{\mathrm{H}}(\hat{\mathbf{R}} - \zeta\mathbf{I})^{-1}\mathbf{a} \quad \text{s.t.} \quad \|\mathbf{a} - \bar{\mathbf{a}}\| = \varepsilon \tag{3.1}$$

which is the problem formulated in [19] and modified by subtracting a diagonal matrix from the sample covariance matrix. It should be noted that the parameter $\zeta$ is

assumed to be not equal to any eigenvalue of the covariance matrix, so that $(\hat{\mathbf{R}} - \zeta\mathbf{I})$ is nonsingular. The underlying motivation of this modification is that, with a proper choice of the parameter $\zeta$, the white noise component of the covariance matrix can be minimized. This would result in a steering vector solution residing in the signal-plus-interference subspace. Solution of (3.1) gives the following SOI steering vector estimate [19].

$$\hat{\mathbf{a}}_\circ = \bar{\mathbf{a}} - (1+\lambda\zeta)(\mathbf{I}+\lambda\hat{\mathbf{R}})^{-1}\bar{\mathbf{a}} \tag{3.2}$$

where $\lambda$ is the Lagrange multiplier. It will now be shown that the vector $\hat{\mathbf{a}}_\circ$, in the ideal case where the sample covariance matrix is replaced by the theoretical one (2.6), is approximately equal to the orthogonal projection of the presumed steering vector $\bar{\mathbf{a}}$ onto signal-plus-interference subspace.

*Proposition I*: The orthogonal projection of the presumed steering vector onto the signal-plus-interference subspace is given by

$$\mathbf{c}_\mathrm{p} = \eta_\circ\mathbf{a}_\circ + \mathbf{P}_i(\bar{\mathbf{a}} - \eta_\circ\mathbf{a}_\circ) \tag{3.3}$$

where

$$\eta_\circ = \frac{\mathbf{a}_\circ^\mathrm{H}(\mathbf{I}-\mathbf{P}_i)\bar{\mathbf{a}}}{\mathbf{a}_\circ^\mathrm{H}(\mathbf{I}-\mathbf{P}_i)\mathbf{a}_\circ} \tag{3.4}$$

and

$$\mathbf{P}_i = \mathbf{A}_i(\mathbf{A}_i^\mathrm{H}\mathbf{A}_i)^{-1}\mathbf{A}_i^\mathrm{H} \tag{3.5}$$

is the orthogonal projector onto the interference subspace.

*Proof*: The orthogonal projection of the presumed steering vector can be written as

$$\mathbf{c}_{\mathrm{p}} = \mathbf{A}_{\mathrm{s}}(\mathbf{A}_{\mathrm{s}}^{H}\mathbf{A}_{\mathrm{s}})^{-1}\mathbf{A}_{\mathrm{s}}^{\mathrm{H}}\bar{\mathbf{a}} \tag{3.6}$$

where $\mathbf{A}_{\mathrm{s}} = [\mathbf{a}_{\circ} \quad \mathbf{A}_i]$ contain the steering vectors of the desired and interference signals, assumed to be linearly independent. It is relatively simple to demonstrate that the projection matrix can also be expressed as (Appendix A)

$$\mathbf{A}_{\mathrm{s}}(\mathbf{A}_{\mathrm{s}}^{\mathrm{H}}\mathbf{A}_{\mathrm{s}})^{-1}\mathbf{A}_{\mathrm{s}}^{\mathrm{H}} = \mathbf{P}_i + \frac{1}{\mathbf{a}_{\circ}^{H}(\mathbf{I}-\mathbf{P}_i)\mathbf{a}_{\circ}}(\mathbf{I}-\mathbf{P}_i)\mathbf{a}_{\circ}\mathbf{a}_{\circ}^{\mathrm{H}}(\mathbf{I}-\mathbf{P}_i) \tag{3.7}$$

By substituting (3.7) into (3.6), the projection of the presumed steering vector is obtained as

$$\mathbf{c}_{\mathrm{p}} = \mathbf{P}_i\bar{\mathbf{a}} + \frac{\mathbf{a}_{\circ}^{H}(\mathbf{I}-\mathbf{P}_i)\bar{\mathbf{a}}}{\mathbf{a}_{\circ}^{H}(\mathbf{I}-\mathbf{P}_i)\mathbf{a}_{\circ}}(\mathbf{I}-\mathbf{P}_i)\mathbf{a}_{\circ} = \eta_{\circ}\mathbf{a}_{\circ} + \mathbf{P}_i(\bar{\mathbf{a}} - \eta_{\circ}\mathbf{a}_{\circ}) \tag{3.8}$$

It will be helpful to examine the structure of the projection vector in (3.8), which comprises two terms. The first one is a scaled version of the true steering vector $\mathbf{a}_{\circ}$ of the SOI, where the scaling factor $\eta_{\circ}$ is a complex scalar which approaches unity as $\bar{\mathbf{a}} \to \mathbf{a}_{\circ}$. The second term can be interpreted as the error of the projection vector with respect to $\mathbf{a}_{\circ}$. This term itself is the projection onto the interference subspace of the mismatch between the presumed and the scaled true steering vectors of the SOI. Hence, if this mismatch does not have a component in this subspace the error of the projection would be zero. Also, as the presumed steering vector approaches the true steering vector ($\bar{\mathbf{a}} \to \mathbf{a}_{\circ}$), then $\mathbf{c}_{\mathrm{p}} \to \mathbf{a}_{\circ}$, showing that $\mathbf{c}_{\mathrm{p}}$ is a consistent estimate under ideal conditions. However, if the difference between the presumed and true steering vectors is large, the error of the projection vector is likely to be large as well.

*Proposition II*: With the choice $\zeta = \sigma_{\mathrm{n}}^2$, the modified RCB estimate (3.2) can be

expressed as

$$\hat{\mathbf{a}}_\circ(\lambda) = \eta(\lambda)\mathbf{a}_\circ + \mathbf{P}(\bar{\mathbf{a}} - \eta(\lambda)\mathbf{a}_\circ) \tag{3.9}$$

where

$$\eta(\lambda) = \frac{\mathbf{a}_\circ^{\mathrm{H}}(\mathbf{I}-\mathbf{P})\bar{\mathbf{a}}}{\mu(\lambda) + \mathbf{a}_\circ^{\mathrm{H}}(\mathbf{I}-\mathbf{P})\mathbf{a}_\circ} \qquad , \qquad \mu(\lambda) = \frac{1+\lambda\sigma_{\mathrm{n}}^2}{\lambda\sigma_{\mathrm{s}}^2} \tag{3.10}$$

and $\mathbf{P}$ is given by

$$\mathbf{P} = \mathbf{A}_i((\lambda_{\mathrm{d}} + \sigma_{\mathrm{n}}^2)\mathbf{D}_i^{-1} + \mathbf{A}_i^{\mathrm{H}}\mathbf{A}_i)^{-1}\mathbf{A}_i^{\mathrm{H}} \tag{3.11}$$

*Proof*: The proof is given in Appendix B.

Note that the choice for $\zeta$ is not allowed by the requirement that the matrix $(\hat{\mathbf{R}} - \zeta\mathbf{I})$ be nonsingular. However, this choice may be regarded as a limiting case. It can be observed that the vector (3.9) has the same structure as the projection $\mathbf{c}_{\mathrm{p}}$ in (3.8). There are basically two differences between this expression and the projection $\mathbf{c}_{\mathrm{p}}$. The first is that $\mathbf{P}_i$ is replaced by $\mathbf{P}$. However, note that $\mathbf{P}$ becomes approximately equal to $\mathbf{P}_i$ for sufficiently large $\lambda$ and noise power much less than the interference signal powers. The second difference is that the factor $\eta(\lambda)$ has an additional term $\mu(\lambda)$ in its denominator. It can be easily shown that $\hat{\mathbf{a}}_\circ$ approaches $\mathbf{c}_{\mathrm{p}}$ as $\lambda \to \infty$ and $\sigma_{\mathrm{n}}^2 \to 0$. Hence, $\hat{\mathbf{a}}_\circ$ can be considered as a good approximation of $\mathbf{c}_{\mathrm{p}}$ for large values of $\lambda$ and high SNR.

A basic difference of the estimate in (3.2) from the robust Capon beamformer estimate is that the factor $(1+\lambda\zeta)$ with the proper choice of $\zeta$ makes the new estimate $\hat{\mathbf{a}}_\circ$ approach the orthogonal projection $\mathbf{c}_{\mathrm{p}}$. Furthermore, if the presumed steering vector is a good approximation of the true steering vector, then the approximate projection will be mainly in the subspace of the true steering vector, with a negligible component in the

interference subspace. The presumed steering vector can be improved by estimating the true DOA of the desired signal, as described in the next section.

## 3.3 DOA Estimation of the Desired Signal

In the MUSIC method for the estimation of the DOAs of signals impinging on an ULA, the following cost function is minimized with respect to the angle $\theta$.

$$F_{\text{MUSIC}}(\theta) = \|\mathbf{a}(\theta) - \sum_{r=1}^{R} (\mathbf{s}_r^{\text{H}}\mathbf{a}(\theta))\mathbf{s}_r\|^2 = \mathbf{a}^{\text{H}}(\theta)\mathbf{G}\mathbf{G}^{\text{H}}\mathbf{a}(\theta) \tag{3.12}$$

where $\|\cdot\|$ is the Euclidean norm, $\mathbf{a}(\theta)$ is the array steering vector, $\{\mathbf{s}_r\}_{r=1}^{R}$ are the signal subspace eigenvectors ($R$ is the number of signals), $\mathbf{G}\mathbf{G}^{\text{H}} = \mathbf{I} - \mathbf{S}\mathbf{S}^{\text{H}}$ and $\mathbf{S}$ is the matrix with columns which are the signal subspace eigenvectors. Note that the summation term in (3.12) is the orthogonal projection of the vector $\mathbf{a}(\theta)$ onto the signal subspace. A similar approach is applied to estimate the DOA of the SOI by minimizing the following cost function in the vicinity of the presumed DOA

$$\hat{F}(\theta) = \|\bar{\mathbf{a}}(\theta) - \mathbf{c}_{\text{p}}(\theta)\|^2 \tag{3.13}$$

where $\mathbf{c}_{\text{p}}(\theta)$ is the orthogonal projection of $\bar{\mathbf{a}}(\theta)$ onto the signal-plus-interference subspace. In the preceding section it was shown that this projection can be approximated by the vector $\hat{\mathbf{a}}_{\circ}(\lambda)$. Hence, using this vector instead of $\mathbf{c}_{\text{p}}(\theta)$ in (3.13) we get

$$\hat{F}(\theta) = \|\bar{\mathbf{a}}(\theta) - \hat{\mathbf{a}}_{\circ}(\lambda)\|^2 = (1+\lambda\zeta)^2\|(\mathbf{I}+\lambda\hat{\mathbf{R}})^{-1}\bar{\mathbf{a}}(\theta)\|^2 \tag{3.14}$$

Therefore, an estimate of the DOA of the desired signal can be obtained as the solution of the minimization problem

$$\hat{\theta}_{\circ} = \underset{\theta\in\Theta}{\text{argmin}}\|(\mathbf{I}+\lambda\hat{\mathbf{R}})^{-1}\bar{\mathbf{a}}(\theta)\|^2 \tag{3.15}$$

where $\Theta$ is an angular sector centered around the presumed DOA of the desired signal. The selection of the parameter $\lambda$ is discussed in the next section. The optimization problem (3.15) can be solved using a simple steepest descent approach, which is guaranteed to converge if the cost function is convex in the vicinity of the minimum.

A basic feature of this estimation method is that, unlike the MUSIC method there is no requirement for determining the signal subspace, since the orthogonal projection to this subspace is indirectly obtained from the modified RCB formulation. Hence, this ensures that the DOA estimate is not affected by low SNR conditions.

## 3.4 Principles of the Proposed Beamformer

For the implementation of the proposed beamforming method, the value of $\lambda$ which yields an optimal steering vector estimate should be determined. An approach different from the RCB approach in [19] is adopted. A major reason for the adoption of a different approach is that information regarding the uncertainties in the SOI steering vector, represented by the parameter $\varepsilon$ is generally unavailable. This inevitably leads to an educated guess in determining this parameter. The proposed approach is based on computing the output power of the beamformer. The beamformer weight vector using the steering vector estimate (3.9) is

$$\mathbf{w}_{\text{pro}} = \frac{\hat{\mathbf{R}}^{-1}\hat{\mathbf{a}}_{\circ}(\lambda)}{\hat{\mathbf{a}}_{\circ}^{\text{H}}(\lambda)\hat{\mathbf{R}}^{-1}\hat{\mathbf{a}}_{\circ}(\lambda)} \tag{3.16}$$

The beamformer output power is given by

$$P'_{\circ}(\lambda) = \mathbf{w}^{\text{H}}\hat{\mathbf{R}}\mathbf{w} = \frac{1}{\hat{\mathbf{a}}_{\circ}^{\text{H}}(\lambda)\hat{\mathbf{R}}^{-1}\hat{\mathbf{a}}_{\circ}(\lambda)} \tag{3.17}$$

Note that in computing the power output, the norm of the steering vector estimate must be normalized to have the theoretical value $\sqrt{N}$, since the norm of the steering vector estimate itself is a function of $\lambda$. After normalization the power becomes

$$P_{\circ}(\lambda) = \frac{\|\hat{\mathbf{a}}_{\circ}(\lambda)\|^2}{N} P'_{\circ}(\lambda) \tag{3.18}$$

The dependence of the power on $\lambda$ can be best understood by expressing it in terms of the Eigenvalue Decomposition (EVD) of $\hat{\mathbf{R}}$. Let the latter be expressed as

$$\hat{\mathbf{R}} = \sum_{j=1}^{N} \hat{q}_j \hat{\mathbf{e}}_j \hat{\mathbf{e}}_j^{\mathrm{H}} \tag{3.19}$$

where $\hat{q}_j$ and $\hat{\mathbf{e}}_j$ $(j = 1, ..., N)$ are the eigenvalues and eigenvectors of $\hat{\mathbf{R}}$, respectively. By computing

$$\hat{\mathbf{a}}_{\circ}^{\mathrm{H}}(\lambda) \hat{\mathbf{R}}^{-1} \hat{\mathbf{a}}_{\circ}(\lambda) = \sum_{j=1}^{N} \frac{1}{\hat{q}_j} \left(\frac{\lambda \hat{q}_j}{1 + \lambda \hat{q}_j}\right)^2 \left(1 - \frac{\zeta}{\hat{q}_j}\right)^2 |\hat{\mathbf{e}}_j^{\mathrm{H}} \, \bar{\mathbf{a}}|^2 \tag{3.20}$$

$$\|\hat{\mathbf{a}}_{\circ}(\lambda)\|^2 = \sum_{j=1}^{N} \left(\frac{\lambda \hat{q}_j}{1 + \lambda \hat{q}_j}\right)^2 \left(1 - \frac{\zeta}{\hat{q}_j}\right)^2 |\hat{\mathbf{e}}_j^{\mathrm{H}} \, \bar{\mathbf{a}}|^2 \tag{3.21}$$

and substituting into (3.18), it can be shown that the beamformer output power is a monotonically decreasing function of $\lambda$. The minimum is attained as $\lambda \to \infty$, which verifies the conclusion reached at the end of Section 3.2. This implies that $\lambda$ should be chosen sufficiently large so that the beamformer output power approaches its minimum. From (3.20) and (3.21) we may deduce that $\lambda$ should in general satisfy

$$\frac{\lambda \hat{q}_j}{1 + \lambda \hat{q}_j} \approx 1 \qquad j = 1, \ldots, N \tag{3.22}$$

A stricter rule can be obtained through the following reasoning. Note that the contribution of the noise terms in (3.20) and (3.21) would be considerably smaller

than those of the signal terms if $\zeta$ is chosen to be around the noise eigenvalues. Also, (3.22) would be satisfied for the interference eigenvalues, provided that they are much larger than the SOI and noise eigenvalues. Therefore, it would suffice if (3.22) is satisfied for the SOI eigenvalue. The minimum value of the power is

$$\lim_{\lambda\to\infty} P_{\circ}(\lambda) = \frac{1}{N}\frac{\sum_{j=1}^{N}[1-(\zeta/\hat{q}_j)]^2|\hat{\mathbf{e}}_j^{\mathrm{H}}\,\bar{\mathbf{a}}|^2}{\sum_{j=1}^{N}[1-(\zeta/\hat{q}_j)]^2|\hat{\mathbf{e}}_j^{\mathrm{H}}\,\bar{\mathbf{a}}|^2/\hat{q}_j} \tag{3.23}$$

An insight into the effectiveness of the proposed beamforming method can be gained by calculating the beamformer output power under the conditions cited above. To simplify the expressions, only one interference signal is considered. In the following, 's' and 'I ' indicate the desired and interference signals respectively. With $\hat{q}_j = \zeta$, $j = 1,\ldots,J$, $\hat{q}_I \gg \zeta, \sigma_{\mathrm{s}}^2$, and $\hat{q}_{\mathrm{s}} = N\sigma_{\mathrm{s}}^2 + \sigma_{\mathrm{n}}^2$ [12], we obtain

$$\lim_{\lambda\to\infty} P_{\circ}(\lambda) = (\sigma_{\mathrm{s}}^2 + \frac{\sigma_{\mathrm{n}}^2}{N})[1 + \frac{1}{\sigma_{\mathrm{s}}^2}(\sigma_{\mathrm{s}}^2 + \frac{\sigma_{\mathrm{n}}^2}{N})\frac{|\hat{\mathbf{e}}_{\mathrm{I}}^{\mathrm{H}}\,\bar{\mathbf{a}}|^2}{|\hat{\mathbf{e}}_{\mathrm{s}}^{\mathrm{H}}\,\bar{\mathbf{a}}|^2}] = (\sigma_{\mathrm{s}}^2 + \frac{\sigma_{\mathrm{n}}^2}{N})[1 + \frac{P_{\mathrm{ex}}}{\sigma_{\mathrm{s}}^2}] \tag{3.24}$$

In (3.24) the first term in the parenthesis can be shown to be the optimum beamformer output power. Then, $P_{\mathrm{ex}}$ is the excess power resulting from the noise-plus-interference that cannot be eliminated. It can be observed, however, that if the angular separation of the presumed steering vector from that of the interference steering vector is large, the ratio of the inner product terms would be of the order of $(1/N)$, leading to an output power very close to the ideal.

It should be noted that the criterion based on (3.22), with $\hat{q}_j$ standing for the SOI eigenvalue ($\hat{q}_{\mathrm{s}}$ ) is problematic at low SNR because of subspace swap. Hence, a procedure based on detecting the $\lambda$ value at which the relative change in the output power with respect to $\lambda$ is below a chosen threshold is adopted. It can be inferred from the discussions following (3.22) that the $\lambda$ value beyond which the power

approaches its limit value is of the order of $(1/\hat{q}_{\mathrm{s}})$. The choice for the initial value of $\lambda$ is based on this observation ($\hat{q}_{\mathrm{s}}$ can be taken to be the largest eigenvalue, after excluding the interference eigenvalues). Also, the parameter $\delta\lambda$ used in the algorithm below can be chosen as a small fraction of $(1/\hat{q}_{\mathrm{s}})$

The computational complexity of the desired signal steering vector estimation of the proposed algorithm is dominated by the eigenvalue decomposition of $\hat{\mathbf{R}}$ which is $O(N^3)$. The solution of the QCQP problem in [33] to obtain the final optimal weight vector has complexity of at least $O(N^{3.5})$. The beamformer in [43] has complexity of $O(N^2S)$ for IPNC matrix reconstruction, where $S$ ($S \gg N$), is the number of sampled points in the DOA region of the desired signal and $O(N^3)$ for the eigendecomposition operation on the covariance matrix $\hat{\mathbf{R}}$. Therefore the total complexity cost for beamformer in [43] is $O(N^2S)+O(N^3)$. The beamformer in [31] has the complexity $O(NK)$ for computing the covariance matrix by the shrinkage method and $O(N^3)$ in order to estimate the steering vector mismatch. Hence, the total cost will be $O(NK)+O(N^3)$.

## 3.5 The Algorithm of Proposed Modified RCB Method

*1:* ***Input:*** *array received signal* $\mathbf{x}(k)$.

*2:* ***Output:*** *Beamformer weight* $\mathbf{w}_{\mathrm{pro}}$.

*3:* ***Initialize:*** $\varepsilon$=0.001

*4: Calculate the eigendecomposition of* $\hat{\mathbf{R}}$

*5:* $\zeta$= *minimum eigenvalue of* $\hat{\mathbf{R}}$

*6:* $\lambda = \lambda_{\circ} = 1/(10\hat{q}_{\mathrm{s}})$, $\delta\lambda = 1/(100\hat{q}_{\mathrm{s}})$

*7:* ***for*** $k = 0:1,\ldots$ *Do*

*8: Calculate* $S_{\mathrm{p}}(k) = \dfrac{\Delta P_o(k)}{P_{\circ}(\lambda_k)} = \dfrac{P_{\circ}(\lambda_k) - P_{\circ}(\lambda_k + \delta\lambda)}{P_{\circ}(\lambda_k)}$

*9:* ***If*** $S_{\mathrm{p}}(k) < \varepsilon$ ***then***

*10:* *break;*

*11:* ***end if***

*12:* $\lambda_{k+1} = \lambda_k + \dfrac{\delta\lambda}{S_{\mathrm{p}}(k)}$

*13:* ***end for***

*14: Solve (3.15) for the desired signal's DOA estimate,* $\hat{\theta}_\circ$

*15: Update the presumed steering vector as* $\bar{\mathbf{a}}(\hat{\theta}_\circ) = [1\ e^{-j\hat{\theta}_\circ}\ \ldots\ e^{-j(N-1)\hat{\theta}_\circ}]^T$.

*16: Calculate* $\hat{\mathbf{a}}_\circ$ *using (3.2) with* $\bar{\mathbf{a}}$ *replaced by the update in step 15.*

*16: Calculate* $\mathbf{w}_{\mathrm{pro}}$ *by (3.16)*

## 3.6 Simulation Results

In all the simulation examples, we numerically evaluate the performance of the proposed beamforming algorithm. The uniform linear array has $N = 10$ omni-directional sensors spaced by half-wavelength. In all scenarios, there is one desired and two interfering sources with directions of arrival $5^\circ$ and $\{20^\circ, 30^\circ\}$, respectively. Also, the desired signal is always present in the training data. The interference power in each sensor is fixed at 30 dB above the desired signal power at all SNR values, except for the simulation where interference to noise ratio (INR) is fixed at 30 dB. The additive noise is modeled as a zero-mean complex symmetric Gaussian spatially and temporally white process that has identical variances in each array sensor. For each scenario, 200 Monte-Carlo runs are performed. In the performance comparison versus the input SNR, the number of snapshots is fixed at $K = 100$ and when comparing the performances of the adaptive beamformers in terms of the number of snapshots, the SNR in each sensor is set to -5 dB for all the scenarios considered.

The proposed beamformer is compared with the improved diagonal loading beamformer [24], the beamformer with modified projection [31], the robust Capon beamformer [19], the reconstruction based beamformer [33] and the correlation coefficient calculation based beamformer [43], the Adaptive Uncertainty based Iterative Robust Capon (AU-IRCB) beamformer [59]. The AUIRCB method is applied without signal subspace reconstruction proposed for low SNR, because the reconstruction procedure is very demanding computationally, causing this method's complexity to be much higher than those of the others. The angular sectors of the SOI and the interference plus noise part for [33] and [43] are defined as $\bar{\Theta} = (\bar{\theta} - 10^{\circ}, \bar{\theta} + 10^{\circ})$ and $[-90^{\circ}, \bar{\theta} - 10^{\circ}) \cup (\bar{\theta} + 10^{\circ}, 90^{\circ}]$, respectively. These angular sectors are uniformly sampled to the discrete sectors with the same angular interval $\triangle\theta = 0.5^{\circ}$. The parameter $\varepsilon = 7.5$ is used in the AU-IRCB based beamformer and $\rho = 0.7$ is considered in [31]. In the proposed method, the value of $\zeta$ is taken to be equal to the minimum noise eigenvalue of $\hat{\mathbf{R}}$.

### 3.6.1 Mismatch Due to Signal Look Direction Error

In the first simulation example, a scenario with only signal look direction mismatch is considered. We assume that both the presumed and actual signal spatial signatures are plane waves impinging from the directions of $0^{\circ}$ and $5^{\circ}$, respectively. This corresponds to a $5^{\circ}$ mismatch in the signal look direction. Fig. 3.1 compares the output SINRs of the aforementioned methods versus the number of snapshots. Also, the performance curves versus the input SNR are displayed in Fig. 3.2.

In Fig. 3.1, it can be observed that the proposed method performs better than the other tested beamformers for the number of snapshots more than 40. The slightly lower performance of the beamformer in [33] from the expected is due to the fact that the

DOA mismatch here is larger than those taken in [33].

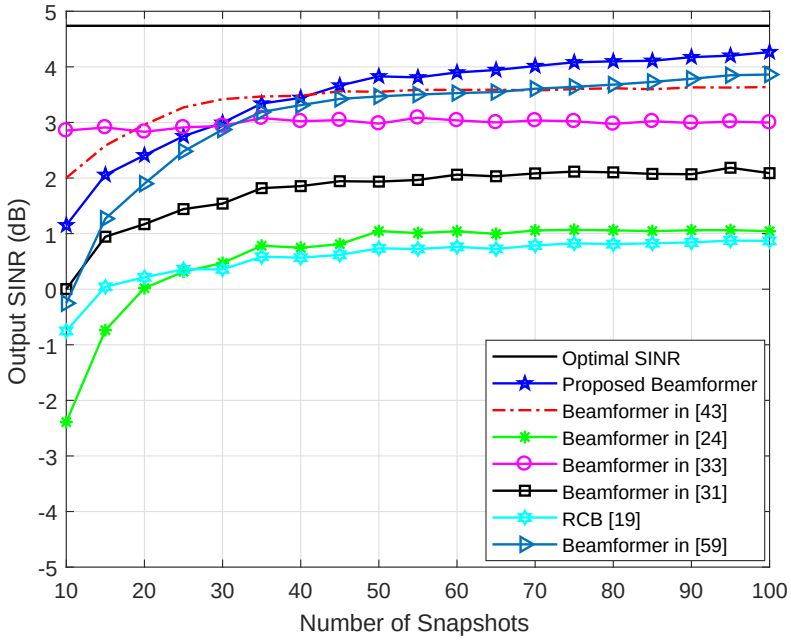


Figure 3.1: SINR vs number of snapshots in the case of look direction error

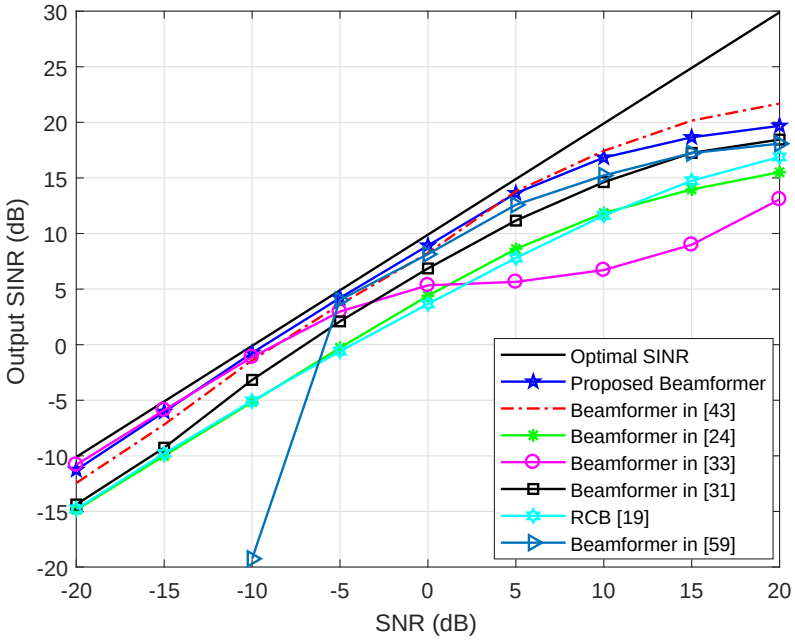


Figure 3.2: SINR vs SNR in the case of look direction error

In Fig. 3.2, again the proposed method's performance is higher than those of others except for the beamformer in [43] which has slightly higher SINR for values more than 10 dB. Also, the low performance of the AUIRCB method at low SNRs is due

to the absence of the subspace reconstruction procedure which is not applied in the simulations. In Fig. 3.3, INR is fixed to 30 dB and SINR versus SNR is shown for all methods. It can be observed that the performances of the proposed method and the algorithms of [33] and [43] remain the same as for fixed interference power, whereas the performances of the other methods are adversely affected.

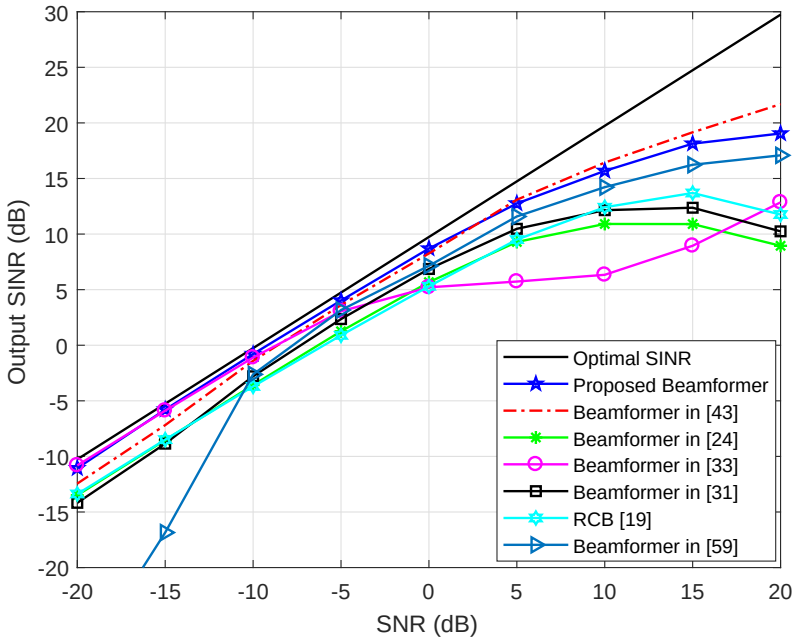


Figure 3.3: SINR vs SNR in the case of look direction error when INR=30

### 3.6.2 Mismatch Due to Array Calibration Errors

In the second example, we simulate the situation when the presumed and actual signal spatial signatures are plane waves impinging from the directions of 0° and 5°, respectively and the signal spatial signature is distorted by arbitrary array imperfections. We assume that the desired signal wavefront is distorted by a random error vector with zero mean and variance $\sigma_e^2 \mathbf{I}_{N\times 1}$. In each simulation run, each of the distortions (which remains fixed for all snapshots) is drawn from a Gaussian random generator with variance equal to 0.4. Fig. 3.4 shows the performances of the methods tested versus the number of snapshots for the fixed SNR. Similar to the previous

scenario the proposed method yields higher SINRs for number of training data more than 30. The improvement of the performance of the beamformer [43] for training data size less than 30 is due to higher calibration error in the signal SV. The performance of the beamformer in [33] does not appreciably improve with increased number of snapshots similar to the previous scenario.

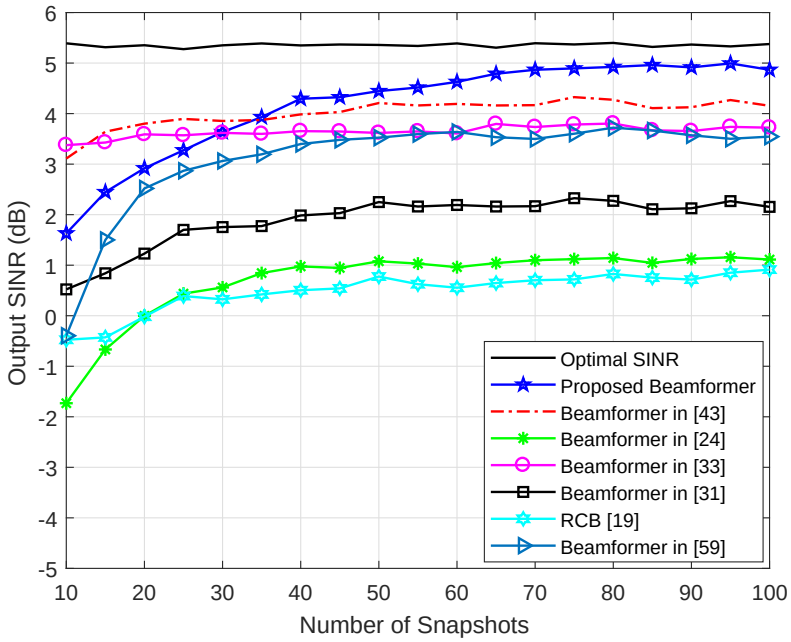


Figure 3.4: SINR vs number of snapshots in the case of calibration error

The performances of these techniques versus the SNR for the fixed training data size is shown in Fig. 3.5. It can be observed that the proposed method's performance is better for the SNR range from -15dB to 10 dB. It should be mentioned that the performance of the modified projection beamformer is decreased with respect to the previous scenario, possibly because of the increased calibration error. Also, note that the performance of the correlation coefficient method [43] is improved with respect to look direction error case. This is due to the advent of calibration error, which contributes to the increased performance of this method.

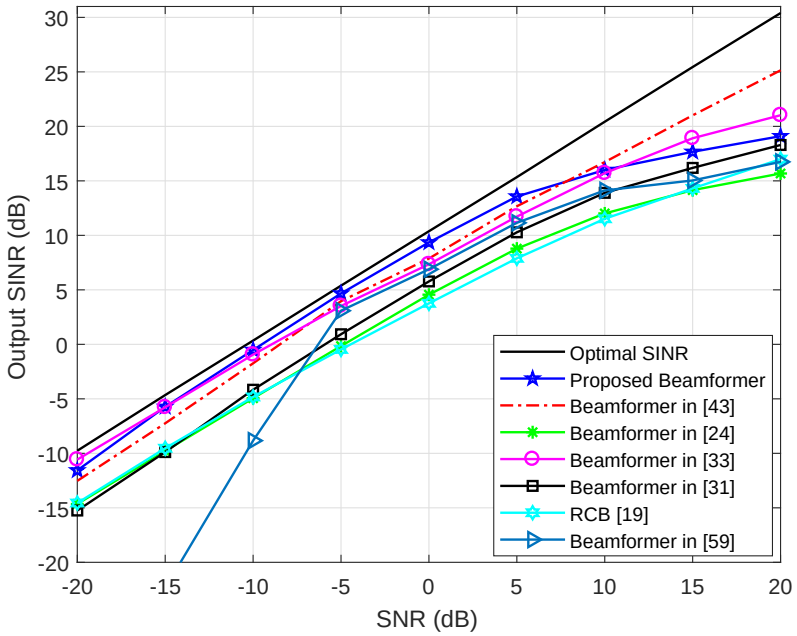

Figure 3.5: SINR vs SNR in the case of calibration error

### 3.6.3 Mismatch Due to Coherent Local Scattering

In the third scenario, the impact of the desired signal steering vector mismatch due to coherent local scattering [60] on array output SINR is considered. In this example, the presumed signal array is a plane wave impinging from $\theta_\circ = 5^\circ$, whereas the actual spatial signature is formed by five signal paths as

$$\tilde{\mathbf{a}} = \mathbf{a} + \sum_{i=1}^{4} e^{j\varphi_i}\mathbf{d}(\theta_i) \tag{3.25}$$

where $\mathbf{a}$ is the direct path and corresponds to the assumed signal steering vector, and $\mathbf{d}(\theta_i)$ represents the $i$th coherently scattered path with the direction $\theta_i$, $i = 1,2,3,4$ which varies in every run for constant number of snapshots and randomly distributed in a Gaussian distribution with mean $\theta_\circ$ and standard deviation $2^\circ$. Correspondingly, the parameters $\varphi_i$ denote the path phases which are changed from run to run for fixed snapshots, which can be drawn uniformly from $[0, 2\pi]$ in each simulation run.

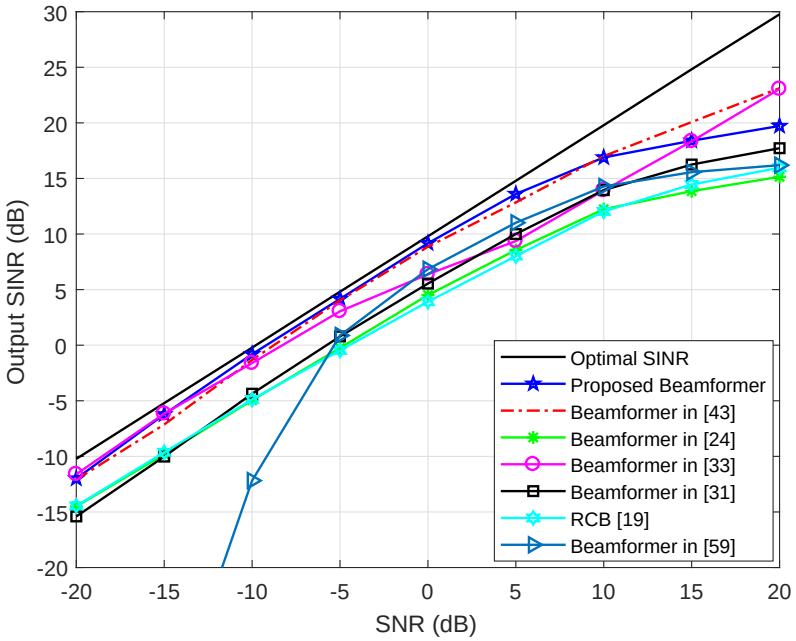


Figure 3.6: SINR vs SNR in the case of coherent local scattering

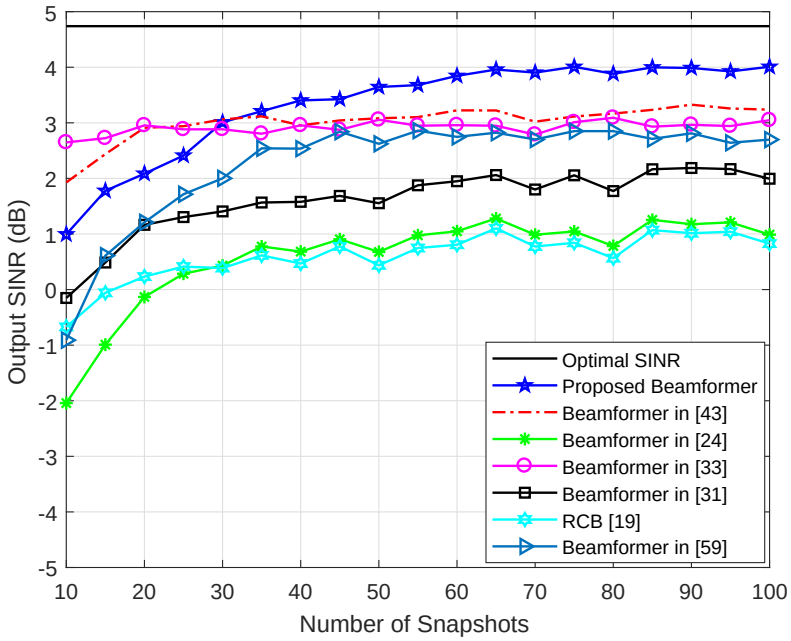


Figure 3.7: SINR vs number of snapshots in the case of coherent local scattering

The performance of the proposed method versus the number of snapshots $K$ with the fixed SNR is shown in Fig. 3.7. Although, the superiority of the proposed method over the methods of [33] and [43] deteriorates for $K < 30$, it is clear that the performance of the proposed method gets better as the number of snapshots is increased. Also, it can be observed that AUIRCB's performance for local scattering is worse than other

scenarios. In Fig. 3.6 the performance versus SNR with the fixed number of snapshots is shown. As can be seen, the proposed method has better performance for all SNRs less than 10dB.

### 3.6.4 DOA Estimation Results

The accuracy of the DOA estimation method introduced in (3.15) is evaluated by computing the estimation variance and average error. These are computed as averages over all runs of $(\theta_\circ - \hat{\theta}_\circ)$ versus input SNR given in Fig. 3.8, where it can be observed that the estimation variance (in dB) decreases almost linearly as SNR increases.

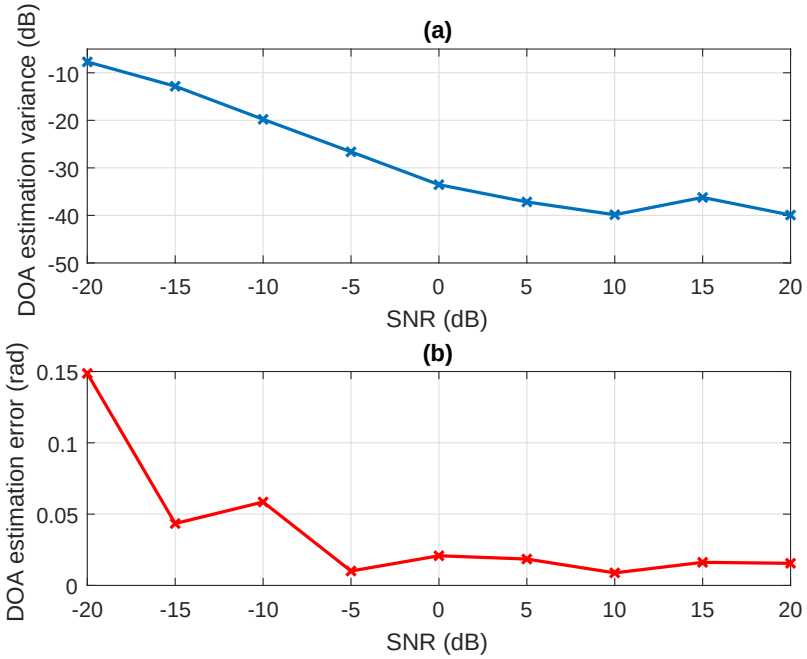


Figure 3.8: (a) DOA estimation variance, (b) DOA estimation average error vs SNR

## 3.7 Conclusion

In this chapter a modified robust Capon beamforming technique is introduced. It is shown that this method leads to a steering vector estimate which closely approximates the orthogonal projection estimate used in the eigenspace beamformer. Furthermore, this method, in conjunction with a MUSIC like approach allows estimation of the DOA

of the desired signal. Also, a methodology for the selection of the diagonal loading factor is developed which guides us to determine this factor in a more or less precise way. Simulation results indicate that the proposed method's performance is highly robust under a wide range of scenarios, and better than or comparable to some of the recently proposed methods.

# Chapter 4

# ADAPTIVE BEAMFORMING BASED ON THEORETICAL INTERFERENCE PLUS NOISE COVARIANCE MATRIX AND DIRECTION OF ARRIVAL ESTIMATION

## 4.1 Introduction

Adaptive beamformers suffer from output performance degradation in the presence of imprecise knowledge of the array steering vector and inaccurate estimation of the covariance matrix [11]. Classically the MVDR beamformer [61, 62] provides an acceptable solution to the problem of recovering the SOI in the array input while minimizing the array output power. However, in some non-ideal situations, the performance of the adaptive beamforming methods severely degrades since the desired signal component is present in the training snapshots.

In this chapter, a new approach for adaptive beamforming is proposed, where the eigenvalue decomposition of the received signal's covariance matrix is utilized to approximate the IPNC matrix very closely. Furthermore, a new technique, which uses as little as possible and easy to obtain imprecise prior information is introduced. The objective for estimating the steering vector is the maximization of the beamformer output to obtain DOA of the desired signal in a certain angular sector. This estimation is expected to be more robust against general mismatches such as coherent local scattering and calibration errors.

## 4.2 Problem Statement

Even though the reconstruction based estimation of the IPNC matrix is in general effective, it has a number of drawbacks. First, it makes the assumption that the array's response to a narrowband signal is the ideal steering vector, which cannot account for array or wavefront distortions. Second, approximation of the integral by a summation requires a large number of terms in order to be able to accurately synthesize powers from narrowband signals. However, recognition of the fact that the only function of the IPNC matrix is to generate notches in the array's directional response at angles that correspond to the narrowband interfering signals, makes it difficult to justify estimation procedures with high computational complexities. The IPNC matrix may be efficiently estimated under certain conditions by utilizing the eigenvalue decomposition of the received signal's covariance matrix, which is the approach adopted in the proposed beamforming method.

The main motivation of this work is to simplify the estimation of the IPNC matrix based on its theoretical expression. Also, it is aimed to avoid estimation of this matrix based on reconstruction in terms of the integral of rank-one matrices weighted by the corresponding incident power, obtained using the Capon spectral estimator [34].

On the other hand, estimation of the desired signal's steering vector is the second important aspect of the beamforming problem. In some of the recently proposed methods in the literature, this estimation is achieved by formulating the problem as a constrained optimization problem, with no analytical solution in general. Hence, the optimization problem is solved iteratively, with the associated increase in the computational burden of the method. The proposed method here offers a simple but effective method to arrive at an accurate estimate of the SOI's steering vector, with

minimal additional burden. Effectiveness of the proposed strategy comes from the fact that the steering vector estimate is sought in a subspace corresponding to the desired signal and the noise. This subspace can be accurately identified if the interference powers are much larger than the SOI's and the noise powers.

## 4.3 Proposed Adaptive Algorithm

We introduce an effective adaptive beamforming algorithm for covariance matrix construction and desired signal steering vector estimation based on projection processing. The IPNC matrix is approximated by utilizing the eigenvalue decomposition of the received signal's covariance matrix. Moreover, the DOA of the desired signal is estimated by maximizing the beamformer output power. Then, the estimated DOA leads to formulate the new desired signal's steering vector for general steering vector mismatches. In particular, the proposed method avoids the optimization problem.

### 4.3.1 Interference Plus Noise Covariance Matrix Estimation

The proposed method can be employed to obtain $\mathbf{R}_{\mathrm{i+n}}^{-1}$ from the eigenvalue decomposition of the received signal's covariance matrix. The inverse of $\mathbf{R}_{\mathrm{i+n}} = \sigma_{\mathrm{n}}^2\mathbf{I}_N + \mathbf{A}_i\mathbf{D}_i\mathbf{A}_i^{\mathrm{H}}$ can be obtained by the application of the well-known matrix inversion lemma (Woodbury) [63], which gives

$$\mathbf{R}_{\mathrm{i+n}}^{-1} = \frac{1}{\sigma_{\mathrm{n}}^2}\left[\mathbf{I}_N - \mathbf{A}_i(\sigma_{\mathrm{n}}^2\mathbf{D}_i^{-1} + \mathbf{A}_i^{\mathrm{H}}\mathbf{A}_i)^{-1}\mathbf{A}_i^{\mathrm{H}}\right] = \frac{1}{\sigma_{\mathrm{n}}^2}(\mathbf{I}_N - \mathbf{P}) \tag{4.1}$$

In order to express the matrix $\mathbf{P}$ in terms of the eigenvalues and eigenvectors of the covariance matrix $\hat{\mathbf{R}}$, it should be noticed that the eigenvectors of $\hat{\mathbf{R}}$ corresponding to the interferences are not exactly the same as those of $\mathbf{R}_{\mathrm{i+n}}$. However, if the desired signal power is much smaller than the interference signal powers, an interference signal eigenvector of $\mathbf{R}_{\mathrm{i+n}}$ is almost equal to the corresponding eigenvector of $\hat{\mathbf{R}}$ (Appendix

C). Then, interference-plus-noise covariance matrix can be approximated as

$$\hat{\mathbf{R}}_{\mathrm{i+n}} = \sigma_{\mathrm{n}}^2 \mathbf{I}_N + \sum_{j=J}^{\mathrm{N}} \tilde{\lambda}_j \mathbf{e}_j \mathbf{e}_j^{\mathrm{H}} = \sigma_{\mathrm{n}}^2 \mathbf{I}_N + \mathbf{E}_i \tilde{\Lambda}_i \mathbf{E}_i^{\mathrm{H}} \tag{4.2}$$

where $\mathbf{e}_j$ are the eigenvectors of $\hat{\mathbf{R}}$ corresponding to the interference signals and $J = N - L + 1$. This can be used to structure $\mathbf{E}_i$ which spans the estimated interference signal subspace as $\mathbf{E}_i = [\mathbf{e}_J, ..., \mathbf{e}_N]$ and $\tilde{\Lambda}_i = \Lambda_i - \Lambda_{\mathrm{n}}^{'}$, where $\Lambda_i$ denote the interference signal subspace eigenvalues of $\mathbf{R}_{\mathrm{i+n}}$ and $\Lambda_{\mathrm{n}}^{'} = \sigma_{\mathrm{n}}^2 \mathbf{I}_{N-L}$ [12]. Then, applying the matrix inversion lemma to (4.2) gives,

$$\hat{\mathbf{R}}_{\mathrm{i+n}}^{-1} = \frac{1}{\sigma_{\mathrm{n}}^2} \left[ \mathbf{I}_N - \mathbf{E}_i (\sigma_{\mathrm{n}}^2 \tilde{\Lambda}_i^{-1} + \mathbf{E}_i^{\mathrm{H}} \mathbf{E}_i)^{-1} \mathbf{E}_i^{\mathrm{H}} \right] \tag{4.3}$$

where

$$\mathbf{E}_i^{\mathrm{H}} \mathbf{E}_i = \mathbf{I}_L \ \text{ and } \ \sigma_{\mathrm{n}}^2 \tilde{\Lambda}_i^{-1} = \mathrm{diag} \left[ \frac{\tilde{\lambda}_j - \sigma_{\mathrm{n}}^2}{\tilde{\lambda}_j}, ..., \frac{\tilde{\lambda}_N - \sigma_{\mathrm{n}}^2}{\tilde{\lambda}_N} \right] \tag{4.4}$$

Note that $\tilde{\lambda}_j \cong \lambda_j$ , $j = J, ..., N$ (Appendix C).

By substituting (4.4) into (4.3), the interference-plus-noise covariance matrix estimation can be written as

$$\hat{\mathbf{R}}_{\mathrm{i+n}}^{-1} = \frac{1}{\sigma_{\mathrm{n}}^2} \left[ \mathbf{I}_N - \sum_{j=J}^{N} \mu_j \mathbf{e}_j \mathbf{e}_j^{\mathrm{H}} \right] \tag{4.5}$$

where $\mu_j = 1 - (\sigma_{\mathrm{n}}^2 / \tilde{\lambda}_j)$ and $\lambda_1$, the minimum eigenvalue of $\hat{\mathbf{R}}$ can be used as an estimate of $\sigma_{\mathrm{n}}^2$. The interference-plus-noise covariance matrix estimation-based beamformer weight vector can be written as

$$\mathbf{w}_{\mathrm{est}} = \frac{\hat{\mathbf{R}}_{\mathrm{i+n}}^{-1} \bar{\mathbf{a}}}{\bar{\mathbf{a}}^{\mathrm{H}} \hat{\mathbf{R}}_{\mathrm{i+n}}^{-1} \bar{\mathbf{a}}} \tag{4.6}$$

Note that the presumed steering vector of the SOI is used instead of the unknown true steering vector $\mathbf{a}_\circ$. However, it is possible to improve the presumed steering vector by estimating the desired signal's DOA. In order to achieve this improvement, the presumed steering vector can be replaced by the vector $\mathbf{a}(\theta)$. Then, the output power of the beamformer can be written as

$$\hat{P}_{\text{out}}(\theta) = \mathbf{w}_\circ^{\text{H}} \hat{\mathbf{R}} \mathbf{w}_\circ \tag{4.7}$$

The spectral decomposition of the matrix $\hat{\mathbf{R}}$ can also be written as

$$\hat{\mathbf{R}} = \mathbf{E}_i \Lambda_i \mathbf{E}_i^{\text{H}} + \mathbf{E}_{\text{sn}} \Lambda_{\text{sn}} \mathbf{E}_{\text{sn}}^{\text{H}} \tag{4.8}$$

where the eigenvectors and eigenvalues associated with the SOI and noise are the columns of $\mathbf{E}_{\text{sn}}$ and diagonal entries of $\Lambda_{\text{sn}}$, respectively. Also, $\mathbf{E}_i$ and $\mathbf{E}_{\text{sn}}$ satisfy $\mathbf{E}_i \mathbf{E}_i^{\text{H}} + \mathbf{E}_{\text{sn}} \mathbf{E}_{\text{sn}}^{\text{H}} = \mathbf{I}_N$. Inserting the proposed beamformer weight vector (4.6) and (4.8) into the output power (4.7), we readily find that the output power can be formulated as

$$\hat{P}_{\text{out}}(\theta) = \frac{\mathbf{a}^{\text{H}}(\theta) \mathbf{E}_{\text{sn}} \Lambda_{\text{sn}} \mathbf{E}_{\text{sn}}^{\text{H}} \mathbf{a}(\theta)}{|\mathbf{a}^{\text{H}}(\theta) \mathbf{E}_{\text{sn}} \mathbf{E}_{\text{sn}}^{\text{H}} \mathbf{a}(\theta)|^2} \tag{4.9}$$

which follows from the orthogonality of the eigenvectors. Maximum of the output power in (4.9) occurs when $\theta$ is very close to the true DOA of the SOI. This can be shown by substituting (2.4) and (2.10) into (4.7) and calculating the theoretical output power as

$$P_{\text{out}}(\theta) = \frac{1}{[\mathbf{a}^{\text{H}}(\theta)(\mathbf{I}-\mathbf{P})\mathbf{a}(\theta)]^2} \cdot \Big( \sigma_{\text{n}}^2 \mathbf{a}^{\text{H}}(\theta)(\mathbf{I}-\mathbf{P})^2 \mathbf{a}(\theta) + \sigma_{\text{s}}^2 |\mathbf{a}^{\text{H}}(\theta)(\mathbf{I}-\mathbf{P})\mathbf{a}(\theta)|^2 + \mathbf{a}^{\text{H}}(\theta)(\mathbf{I}-\mathbf{P})\mathbf{A}_i \mathbf{D}_i \mathbf{A}_i^{\text{H}} (\mathbf{I}-\mathbf{P}) \mathbf{a}(\theta) \Big) \tag{4.10}$$

Let us decompose the presumed signal steering vector as

$$\mathbf{a}(\theta) = \mathbf{A}_i\,\boldsymbol{\gamma}(\theta) + \mathbf{a}_\perp(\theta) \tag{4.11}$$

where $\boldsymbol{\gamma}$ contains the coordinates of $\mathbf{a}(\theta)$ in the interference subspace and $\mathbf{a}_\perp(\theta) = (\mathbf{I} - \mathbf{P}_i)\mathbf{a}(\theta)$ is orthogonal to this subspace, where $\mathbf{P}_i = \mathbf{A}_i(\mathbf{A}_i^{\mathrm{H}}\mathbf{A}_i)^{-1}\mathbf{A}_i^{\mathrm{H}}$ is the orthogonal projection matrix. Then, making the assumption

$$\mathbf{a}_\circ = \mathbf{a}(\theta_\circ) = \mathbf{A}_i\,\boldsymbol{\gamma}(\theta_\circ) + \mathbf{a}_\perp(\theta_\circ) \tag{4.12}$$

and the approximation $(\mathbf{I} - \mathbf{P})\mathbf{A}_i \simeq 0$, will result in

$$P_{\mathrm{out}}(\theta) = \frac{\sigma_{\mathrm{s}}^2 |\mathbf{a}_\perp^{\mathrm{H}}(\theta_\circ)\mathbf{a}_\perp(\theta)|^2}{\|\mathbf{a}_\perp(\theta)\|^4} + \frac{\sigma_{\mathrm{n}}^2}{\|\mathbf{a}_\perp(\theta)\|^2} \tag{4.13}$$

It can be shown in (4.13) that, if the angular separation between the interference signals and SOI steering vector is large enough, the maximum of $P_{\mathrm{out}}(\theta)$ occurs at $\theta = \theta_\circ$. Then, the DOA of the SOI is estimated as

$$\hat{\theta}_\circ = \underset{\theta \in \bar{\Theta}}{\operatorname{argmax}}\, \hat{P}_{\mathrm{out}}(\theta) \tag{4.14}$$

where $\bar{\Theta} = [\bar{\theta} - \triangle\bar{\theta}, \bar{\theta} + \triangle\bar{\theta}]$ is an angular sector centered around the presumed DOA $\bar{\theta}$ of the SOI. The parameter $\triangle\bar{\theta}$ is chosen such that the true DOA is within the sector $\bar{\Theta}$. A gradient algorithm can be employed to numerically obtain the maximum of $\hat{P}_{\mathrm{out}}(\theta)$ in a few iterations, where the computational load is negligible compared with the other computations in the algorithm.

### 4.3.2 Desired Signal Steering Vector Estimation

If the uncertainty in the desired signal's steering vector is not due to a simple mismatch in the true and the presumed DOAs, then estimation of the desired signal's

DOA may not be sufficient for estimating the SOI steering vector. Here, a new approach to estimating the desired signal's steering vector is described that is capable of improving the steering vector's estimation for other types of mismatches, such as array calibration errors and scattering of the incident signal.

First, we consider that part of the covariance matrix which corresponds to the SOI and the noise only as

$$\mathbf{R}_{\mathrm{s+n}} = \sigma_{\mathrm{n}}^2 \mathbf{I}_N + \sigma_{\mathrm{s}}^2 \mathbf{a}_\circ \mathbf{a}_\circ^{\mathrm{H}} \tag{4.15}$$

Then the theoretical estimate of the desired signal's steering vector $\mathbf{c}$ is defined as

$$\mathbf{c} = \left(\mathbf{R}_{\mathrm{s+n}} - \eta \mathbf{I}_N\right)\bar{\mathbf{a}} = \left(\sigma_{\mathrm{n}}^2 - \eta\right)\bar{\mathbf{a}} + \sigma_{\mathrm{s}}^2 \left(\mathbf{a}_\circ^{\mathrm{H}} \bar{\mathbf{a}}\right)\mathbf{a}_\circ \tag{4.16}$$

where $\bar{\mathbf{a}}$ is the assumed steering vector. Now, if $\eta = \sigma_{\mathrm{n}}^2$, then $\mathbf{c}$ becomes equal to a vector which differs from the desired signal's steering vector by a scalar factor. Therefore, the desired steering vector can be recovered from $\mathbf{c}$ as

$$\hat{\mathbf{a}}_\circ = \frac{\|\mathbf{a}_\circ\|}{\|\mathbf{c}\|}\mathbf{c} \tag{4.17}$$

The same idea can be applied to the approximate signal-plus-noise covariance matrix to obtain,

$$\hat{\mathbf{a}}_\circ = \frac{\|\mathbf{a}_\circ\|}{\|\hat{\mathbf{c}}\|}(\mathbf{E}_{\mathrm{sn}} \Lambda_{\mathrm{sn}} \mathbf{E}_{\mathrm{sn}}^{\mathrm{H}} - \eta \mathbf{I}_{\mathrm{N}})\bar{\mathbf{a}} \tag{4.18}$$

where the signal-plus-noise covariance matrix can be approximately obtained from the eigenvalue decomposition as

$$\hat{\mathbf{R}}_{\mathrm{s+n}} = \mathbf{E}_{\mathrm{sn}} \Lambda_{\mathrm{sn}} \mathbf{E}_{\mathrm{sn}}^{\mathrm{H}} \tag{4.19}$$

It is noticed that the parameter $\eta$ can be chosen to be equal to the minimum of the noise eigenvalues.

By inserting the estimated IPNC matrix (4.5) and approximated signal-plus-noise covariance matrix (4.19) into (2.10), the weight vector with the new estimated steering vector is obtained as

$$\mathbf{w}_{\text{prop}} = \frac{\|\hat{\mathbf{c}}\| \, (\hat{\mathbf{R}}_{\text{s+n}} - \eta\sigma_{\text{n}}^2 \hat{\mathbf{R}}_{\text{i+n}}^{-1})\bar{\mathbf{a}}(\hat{\theta}_{\circ})}{\|\mathbf{a}_{\circ}\| \, \bar{\mathbf{a}}^{\text{H}}(\hat{\theta}_{\circ})(\hat{\mathbf{R}}_{\text{s+n}} - \eta\mathbf{I}_N)^{\text{H}}(\hat{\mathbf{R}}_{\text{s+n}} - \eta\sigma_{\text{n}}^2 \hat{\mathbf{R}}_{\text{i+n}}^{-1})\bar{\mathbf{a}}(\hat{\theta}_{\circ})} \tag{4.20}$$

where $\hat{\theta}_{\circ}$ is the DOA estimate in (4.14). Note that $\|\mathbf{a}_{\circ}\|$ is in general unknown. However, its exact value does not affect the output SINR of the beamformer.

The proposed desired signal steering vector estimation method has advantages over the orthogonal projection method used in eigenspace-based beamformers, where the presumed steering vector is projected onto the signal subspace comprising the desired and interference signal eigenvectors. First, there is the possibility of a swap between the desired signal eigenvector and one of the noise subspace eigenvectors. The correlation based algorithm [43] can solve this problem to some degree. However, the success of this method depends on the accuracy with which the presumed steering vector represents the true steering vector of the desired signal. In other words, if the presumed steering vector is not a good approximation for the true steering vector, a noise eigenvector may lead to the maximum correlation with the presumed steering vector. This in turn degrades the SINR performance of the correlation-based steering vector estimation method.

## 4.4 Summary of the Proposed Algorithm

The proposed beamformer steps is summarized as follows:

*1: Compute the sample covariance matrix* $\hat{\mathbf{R}}$ *by using* (2.12).

*2: Reconstruct the IPNC matrix* $\hat{\mathbf{R}}_{\mathrm{i+n}}^{-1}$ *according to* (4.5).

*3: Estimate the desired signal's DOA, in* (4.14) *as the angle which maximizes the output power according to equation* (4.9).

*4: Estimate the steering vector of the desired signal by using* (4.18).

*5: Obtain the beamformer weight vector using equation* (4.20).

## 4.5 Computational Complexity

The computational complexity of the reconstruction of the IPNC matrix and desired signal steering vector estimation of the proposed algorithm is dominated by the eigenvalue decomposition of $\hat{\mathbf{R}}$ which is $O(N^3)$. The solution of the QCQP problem in [33] to obtain the final optimal weight vector has complexity of at least $O(N^{3.5})$. The beamformer in [43] has complexity of $O(N^2S)$ for IPNC matrix reconstruction, where $S$ ($S \gg N$), is the number of sampled points in the DOA region of the desired signal and $O(N^3)$ for the eigendecomposition operation on the covariance matrix $\hat{\mathbf{R}}$. Therefore the total complexity cost for beamformer in [43] is $O(N^2S) + O(N^3)$. The beamformer in [31] has the complexity $O(NK)$ for computing the covariance matrix by the shrinkage method and $O(N^3)$ in order to estimate the steering vector mismatch. Hence, the total cost will be $O(NK) + O(N^3)$.

## 4.6 Simulation

In all the simulation examples, we numerically evaluate the performance of the proposed beamforming algorithm. The uniform linear array has $N = 10$ omni-directional sensors spaced by half-wavelength. In all the scenarios, there is one desired and two interfering sources with directions of arrival $5^\circ$ and $\{-20^\circ, 30^\circ\}$,

respectively. Also, the desired signal is always present in the training data. The interference power in each sensor is fixed at 30 dB. The additive noise is modeled as a zero-mean complex symmetric Gaussian spatially and temporally white process that has identical variances in each array sensor. For each scenario, 200 Monte-Carlo runs are performed. In the performance comparison versus the input SNR, the number of snapshots is fixed at $K = 100$ and when comparing the performance of the adaptive beamformers in terms of the number of snapshots, the SNR in each sensor is fixed at 0 dB.

The proposed beamformer is compared with the improved diagonal loading beamformer [24], the beamformer with modified projection [31], the reconstruction based beamformer [33], the correlation coefficient calculation based beamformer [43], the orthogonal projection matrix beamformer [30] and the beamformer in [34] which is named as the SPSS beamformer. The angular sectors of the SOI and the interference-plus-noise part for [33] and [43] are defined as $\bar{\Theta} = (\bar{\theta} - 10^\circ, \bar{\theta} + 10^\circ)$ and $[-90^\circ, \bar{\theta} - 10^\circ) \cup (\bar{\theta} + 10^\circ, 90^\circ]$, respectively. These angular sectors are uniformly sampled to the discrete sectors with the same angular interval $\triangle\theta = 0.5^\circ$. CVX software [64] was used to solve this convex optimization problem. The parameter $\rho = 0.7$ is considered in the beamformers of [31] and [30].

### 4.6.1 Random Signal Look Direction Mismatch

In the first simulation example, a scenario with only random signal look direction mismatch is considered. We assume that the random direction mismatch of the desired signal and interferences are subject to uniform distribution in $[-5^\circ, 5^\circ]$ for each simulation run, which means that direction changes from run to run but kept fixed from snapshot to snapshot. Fig. 4.1 compares the output SINRs of the

aforementioned methods versus the input SNR. It can be observed in Fig. 4.1 that the proposed method, with and without steering vector estimation, performs significantly better than the other methods up to the SNR of 12 dB. Above this SNR, the proposed method is superior than all the methods except the QCQP beamformer.

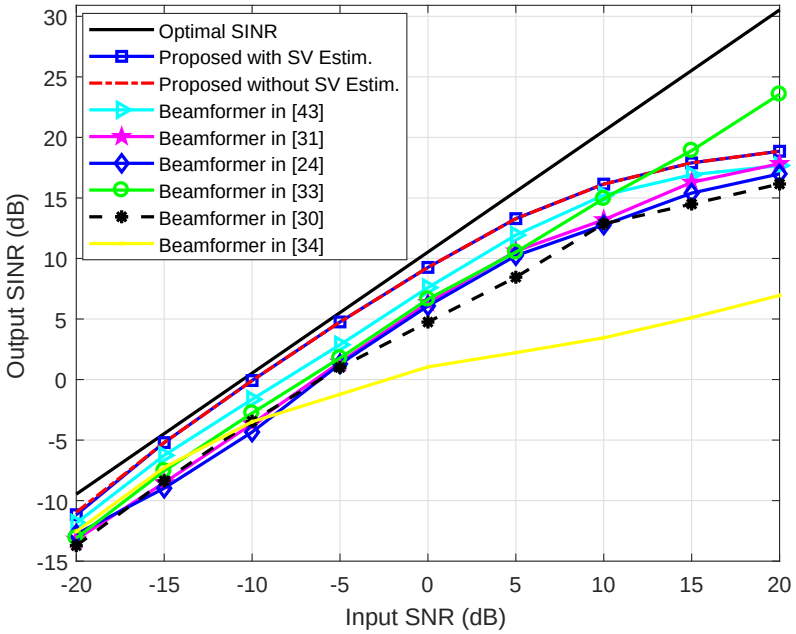

Figure 4.1: SINR versus SNR for look direction error

Also, we examine the performance of the beamformers as the number of snapshots $K$ increases which is demonstrated in Fig. 4.2. In this figure, the proposed method's performance versus number of snapshots is higher than all the other methods for number of snapshots in excess of 25. Below this number of snapshots, the beamformer in [43] performs better than the proposed. It can be put forward that, the generally higher performance of the proposed method is due to the better estimation of the SOI's steering vector and/or DOA. The accuracy of DOA estimation is further investigated in section 4.4. It should be noted that the performance of [33] is sensitive to some parameters of the beamforming scenario. Specifically, the interference signal powers here are kept constant at all SNR values, whereas the INR is fixed at 30 dB

in [33] so that the interference powers decrease as SNR increases. From the results shown in Figs. 4.1 and 2, it can be observed that the proposed method'performance has more robustness against look direction errors compared with the other tested beamformers.

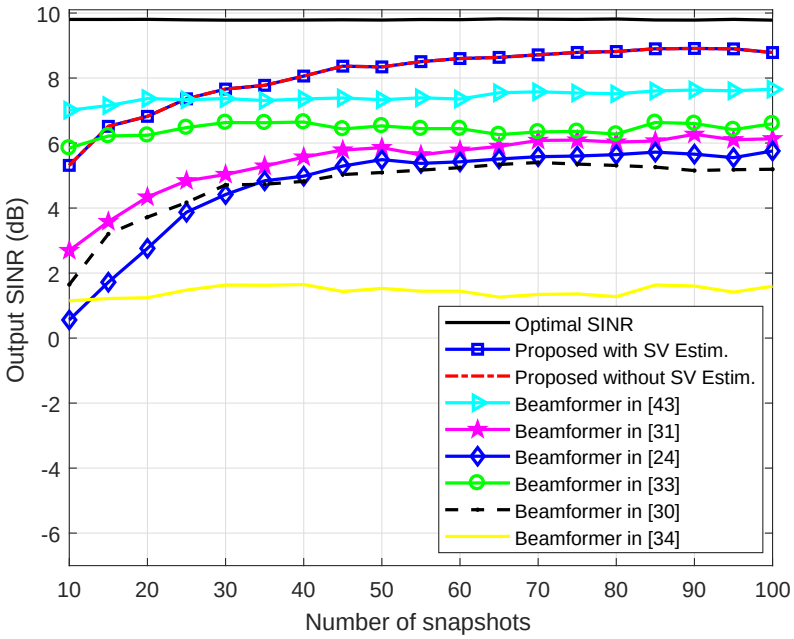

Figure 4.2: SINR versus number of snapshots for look direction error

### 4.6.2 Signal Mismatch Due to Coherent Local Scattering

In the second scenario, the impact of the desired signal steering vector mismatch due to coherent local scattering [60] on array output SINR is considered. In this example, the presumed signal is a plane wave impinging from $\bar{\theta}_o = 5^\circ$, whereas the actual spatial signature is formed by five signal paths as $\tilde{\mathbf{a}} = \mathbf{a} + \sum_{i=1}^{4} e^{j\varphi_i}\mathbf{d}(\theta_i)$, where $\mathbf{a}$ is the direct path and corresponds to the assumed signal steering vector, and $\mathbf{d}(\theta_i)$ represents the $i$th coherently scattered path with the direction $\theta_i$,($i$=1,2,3,4) which are randomly distributed in a Gaussian distribution with mean $\theta_\circ$ and standard deviation $2^\circ$. Correspondingly, the parameters $\varphi_i$ denote the path phases which are drawn uniformly from the interval $[0, 2\pi]$ in each simulation run. Note that $\theta_i$ and $\varphi_i$

($i$=1,2,3,4) only change from run to run while remaining fixed from snapshot to snapshot. In Fig. 4.3 the performance versus SNR with the fixed number of snapshots is shown. The performance of the proposed method versus the number of snapshots $K$ with fixed SNR is shown in Fig. 4.4. It is evident in these figures that the steering vector estimation of the proposed method has increased performance compared with DOA estimation only. Compared with the DOA mismatch case almost all methods show slight improvements particularly in the low SNR range.

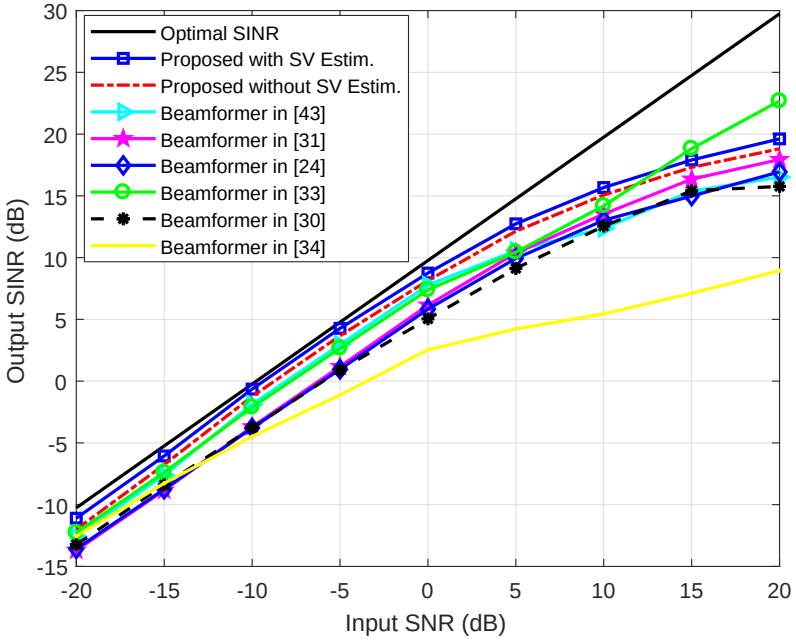

Figure 4.3: SINR versus SNR in the case of coherent local scattering

### 4.6.3 Mismatch Due to Array Calibration Errors

In the third example, we simulate the situation when the presumed and actual signal spatial signatures are plane waves impinging from the directions of 0° and 5°, respectively and the signal spatial signature is distorted by arbitrary array imperfections. We assume that the desired signal wavefront is distorted by a random error vector with zero mean and variance $\sigma_e^2\mathbf{I}_{N\times 1}$. In each simulation run, each of the distortions (which remains fixed for all snapshots) is drawn from a Gaussian random

generator with variance equal to 0.3. The performances of these techniques versus the SNR for fixed training data size are shown in Fig. 4.5. Fig. 4.6 shows the performances of the methods tested versus the number of snapshots for fixed SNR. The performance of the proposed approach is much better than that of the tested methods when arbitrary array errors are considered up to SNR=10 dB. This improvement is a result of the desired signal elimination in the covariance matrix reconstruction and array steering vector estimation. It should be mentioned that the performance of the modified projection beamformer is sensitive to the parameter ρ. In Fig. 4.6 the proposed method's performance is considerably better than the other methods over a large range of the number of snapshots. The results show that the proposed method yields better output SINR than all the other tested beamformers, because of the high estimation accuracy of both the IPNC matrix and the steering vector of the SOI.

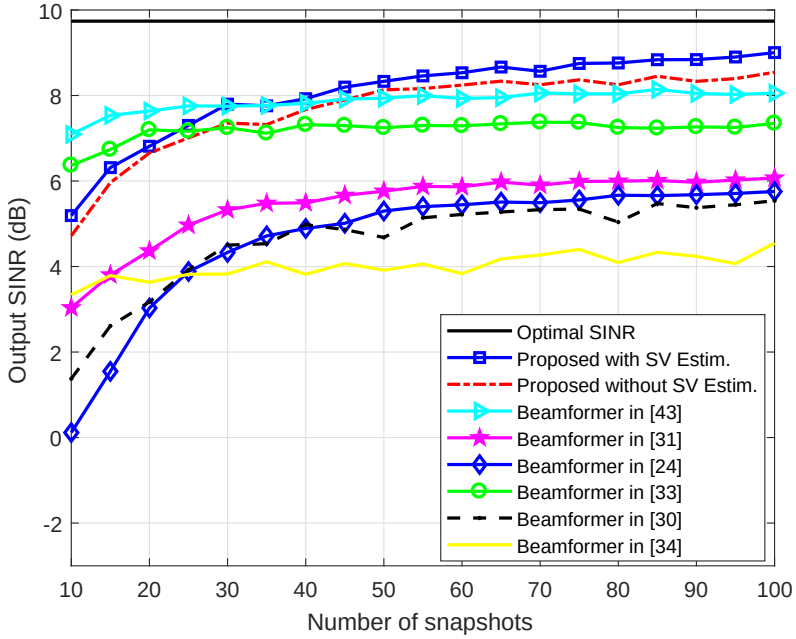


Figure 4.4: SINR versus number of snapshots in the case of coherent local scattering

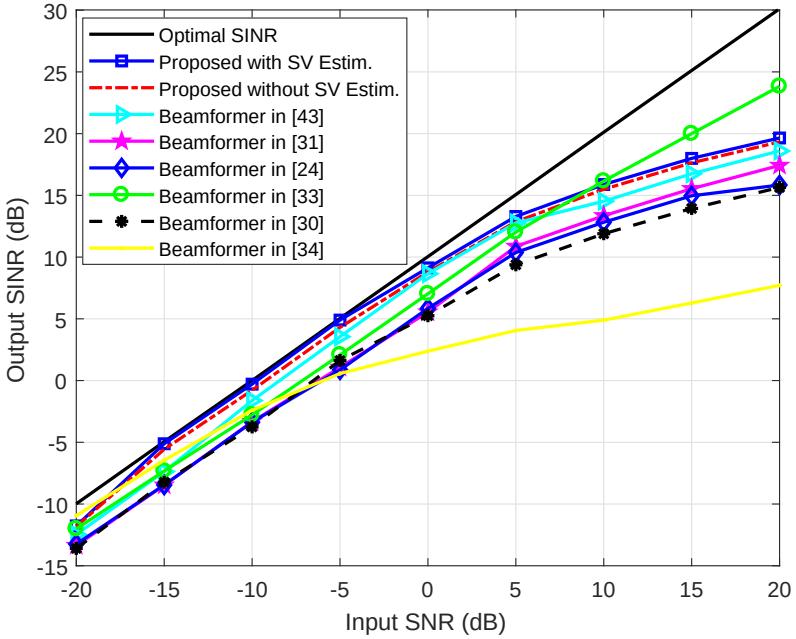


Figure 4.5: SINR versus SNR in the case of array calibration error

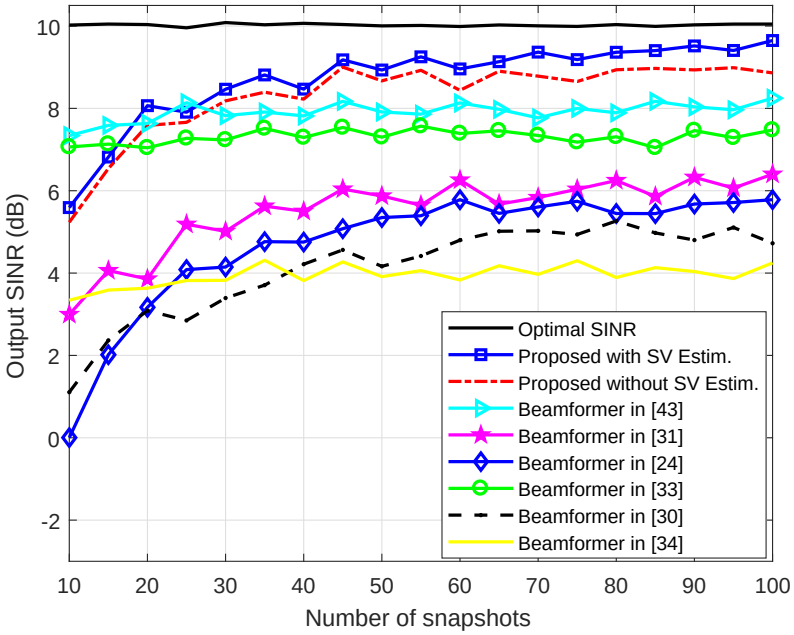


Figure 4.6: SINR versus number of snapshots in the case of array calibration error

### 4.6.4 DOA Estimation Results

The accuracy of the DOA estimation method introduced in (4.14) is evaluated by computing the estimation variance and average error. These are computed as averages over all runs of $(\theta_\circ - \hat{\theta}_\circ)$ versus input SNR and also as a function of the mismatch

between presumed and true DOAs of the desired signal. These are given in Fig. 4.7 and Fig. 4.8, where it can be observed that the estimation variance (in dB) decreases almost linearly as SNR increases. In order to give an insight into the accuracy of the estimates, we calculated the standard deviation of the DOA estimate at SNR=0 dB to be $3.2 \times 10^{-3}$ rad. ($0.1812^{\circ}$). The average estimation error at the same SNR is 0.03 rad.($1.72^{\circ}$) which is reasonably low considering that the DOA mismatch is $15.7^{\circ}$($5^{\circ}$ as AOA(Angle of Arrival)). In Fig. 4.8 it can be observed that the estimation variances are almost independent of the AOA mismatch which verifies the accuracy of the proposed estimation method.

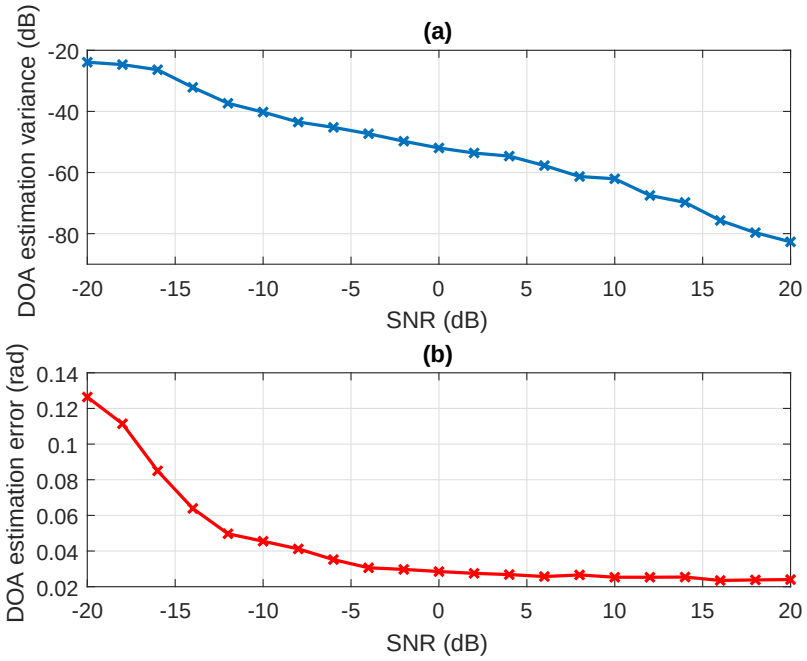


Figure 4.7: (a) DOA estimation variance, (b) DOA estimation average error vs SNR

## 4.7 Conclusion

In this chapter, a novel adaptive beamforming method is presented that is robust against both the covariance matrix uncertainty and signal steering vector mismatch. It is shown that the interference-plus-noise covariance matrix can be accurately estimated in terms of the noise power estimate and the eigenvectors of the array's

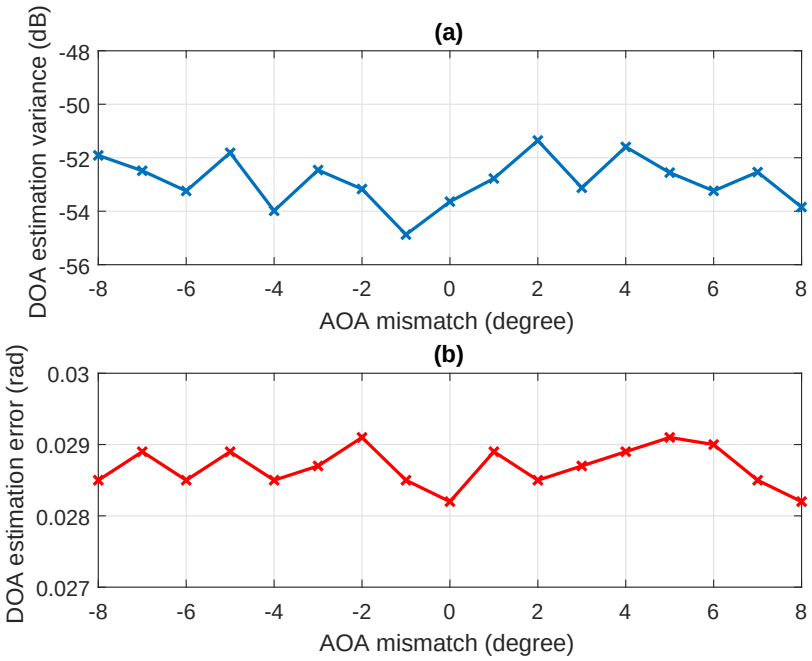


Figure 4.8: DOA estimation (a) variance, (b) average error versus AOA mismatch

covariance matrix corresponding to the interference signals. With the knowledge of the presumed DOA of the desired signal, the presumed steering vector of the signal can be improved to maximize the array output power. Also, a method for estimating the desired signal's steering vector is introduced for general steering vector mismatches. Simulation results demonstrate the effectiveness of the proposed algorithm compared with some of recent ones in the literature.

# Chapter 5

# ROBUST ADAPTIVE BEAMFORMING FOR FAST MOVING INTERFERENCE BASED ON COVARIANCE MATRIX RECONSTRUCTION

## 5.1 Introduction

We introduce a novel approach with respect to the time-varying DOA of a moving interference source. This interference is estimated during the period in which snapshots are taken. Then, the beamformer is designed to place a null region which spans the directions in which the interfering source moves. The IPNC matrix is replaced by another one derived from a simplified power spectral density function that can be used to shape the directional response of the beamformer. An expression for the inverse of this matrix is developed which facilitates fast calculation of the beamformer weight given the interference signal DOAs. In this work, the desired signal's DOA is assumed to be available, as the focus is on suppression of moving interferences.

## 5.2 Proposed Beamformer

Adaptive beamforming is a classic problem in array signal processing and has broad application prospects in radar, sonar and communications signal processing [65], [45]. Although, adaptive beamforming has been developed to extract the desired signal and suppress the interference as well as noise at the array output simultaneously [37], if the assumptions of the source, environment and antenna become imprecise, the performance of the adaptive beamforming degrades [20]. Variety of algorithms have been proposed to improve robustness against signal

steering vector mismatch and covariance matrix estimation inaccuracy [33], [66], and spatially cancel interfering signals [67], [11]. However, there are yet many applications and signal scenarios such as nonstationary interference where existing methods are inadequate. When the interference waveform or distribution change with time or location by antenna platform vibration, propagation channel variation, conventional adaptive cancelers might perform poorly. Since in general, these methods include additional constraints in the optimization problem for suppression of selected angular ranges and usually requiring online solutions.

In this research, we focus on the time-varying interference suppression problem, with interference-plus-noise covariance matrix reconstruction on the condition that target knowledge (interference DOA) is estimated. When the interference moves quickly or the antenna platform vibrates, continuously updating of the adaptive weight vector can be prohibitive; the mismatching between adaptive weight and data occurs due to the change of interference locations. We propose a beamformer that can flexibly adjust the null width and avoid the additional complexity of continuous updating.

### 5.2.1 Estimation of Time-Varying Interference DOA

Determination of the time-varying DOA of a moving interference during the interval in which snapshots are taken is crucial for the implementation of the proposed method. Here, a DOA estimation using correlation is adopted where inner products of the received vectors with the steering vector corresponding to a general direction of incidence are computed. The directions are chosen in the angular sector corresponding to the moving interference. First, a coarse estimate of the interference DOA is obtained from the discrete Fourier transform of the first received vector in the set of snapshots. Then, an angular sector centered on this estimate is scanned and the

angle which maximizes the magnitude of the inner product is taken as the DOA's estimate, as follows

$$\hat{\theta}_i(k) = \underset{\theta \in \Theta_{\text{int}}(k)}{\text{argmax}} \; \left| \mathbf{x}^{\text{H}}(k)\mathbf{a}(\theta) \right|, \quad k = 1, \cdots, K \tag{5.1}$$

where $\Theta_{\text{int}}(k)$ is the angular sector of the interference signal corresponding to $k$th received vector. This procedure is then repeated for the next vector in the snapshots. When all snapshot vectors are processed, a polynomial of sufficiently high degree can be fitted to the set of DOA estimates. The angular range of variation of the interference's DOA is determined using this polynomial. Aside from the correlation estimator (5.1), there are other methods which use low resolution direction finding [68].

It is noted that, the procedure enables the proposed method to adopt itself to the motion of interference by determining the angular region where the null in the beampattern is to be created. This is unlike most methods that provide null over a predefined range of the interference signal which is expected to move [57].

### 5.2.2 Interference-Plus-Noise Covariance Matrix Reconstruction

We propose to reconstruct the IPNC matrix using a weighted sum of the outer products of steering vectors, the coefficient of which can be estimated in the vicinity of the DOAs of the interferences as follows

$$\mathbf{C} = \int_{-\pi}^{\pi} \gamma(\theta)\mathbf{a}(\theta)\mathbf{a}^{\text{H}}(\theta)d\theta \tag{5.2}$$

where $\mathbf{a}(\theta)$ is the steering vector associated with a hypothetical direction $(\theta)$ based on the known array structure and $\gamma(\theta)$ may be interpreted as the spatial power spectrum of the interference-plus-noise component of the received signal. However, in lieu of

estimating this spectrum, a simplified approach is adopted where $\gamma(\theta)$ is chosen to have a piecewise constant form with only two levels.

Here, the choice of $\gamma(\theta)$ is based on the fact that the interference with higher power should be more suppressed. Hence, one level is assigned for the white noise ($\gamma_{\mathrm{L}}$), and the other for the interference signals ($\gamma_{\mathrm{H}}$). Since scaling of $\gamma(\theta)$ does not change the weight vector, the lower level can be fixed at unity. The higher level then can be chosen as the relative power of the strongest interference with respect to the noise.

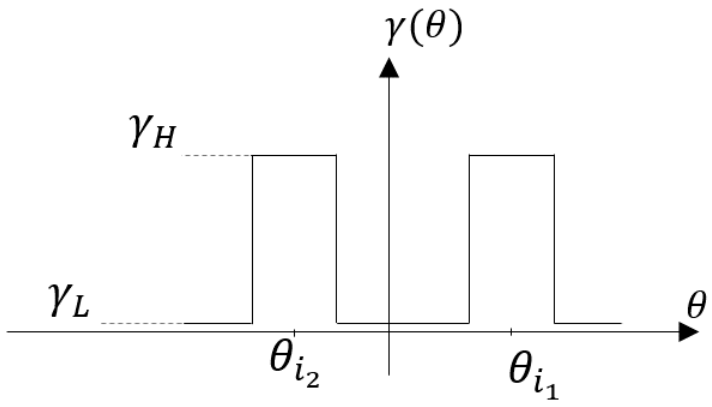

Figure 5.1: Weight function versus θ

In the following section, a procedure is described where the inverse of the IPNC matrix is simply computed. Considering the structured feature of the integral, the matrix $\mathbf{C}$ can be approximately calculated using a discrete sum

$$\mathbf{C} \cong \sum_{m=1}^{M} \gamma(\theta_m)\mathbf{a}(\theta_m)\mathbf{a}^{\mathrm{H}}(\theta_m) \quad \text{for} \quad M \gg N \tag{5.3}$$

and

$$\gamma(\theta_m) = \begin{cases} \gamma_{\mathrm{H}}, & \theta_m \in \bar{\Theta} \\ \gamma_{\mathrm{L}}, & \theta_m \in \Theta \end{cases} \tag{5.4}$$

where $\bar{\Theta}$ stands for the direction range of interferences and $\Theta$ is the complement sector

of $\bar{\Theta}$ in the whole spatial domain. This domain is discretized as follows

$$\theta_m = \theta_1 + (m-1)\Delta\theta, \quad \Delta\theta = 2\pi/M, \quad (m = 1, \cdots, M) \tag{5.5}$$

Therefore, equation (5.3) can be written in matrix form as

$$\mathbf{C} = \mathbf{E}\Gamma\mathbf{E}^{\mathrm{H}} \tag{5.6}$$

where $\mathbf{E} = [\mathbf{a}(\theta_1), \ldots, \mathbf{a}(\theta_M)] \in \mathbb{C}^{N\times M}$ and $\Gamma = \mathrm{diag}[\gamma(\theta_1), \ldots, \gamma(\theta_M)] \in \mathbb{C}^{M\times M}$

The matrix $\mathbf{E}$ can be factorized as

$$\mathbf{E} = \mathbf{F}_{\theta_1}\mathbf{F}_{\Delta\theta} \tag{5.7}$$

where $\mathbf{F}_{\Delta\theta}$ is a matrix with the following elements

$$[\mathbf{F}_{\Delta\theta}]_{n,m} = e^{-j(n-1)(m-1)\Delta\theta} \tag{5.8}$$

for $(n = 1, \ldots, N; m = 1, \ldots, M)$, and

$$\mathbf{F}_{\theta_1} = \mathrm{diag}[1, e^{-j\theta_1}, \ldots, e^{-j(N-1)\theta_1}] \tag{5.9}$$

Based on (5.7), the matrix $\mathbf{C}$ can be written as follows

$$\mathbf{C} = \mathbf{F}_{\theta_1}(\mathbf{F}_{\Delta\theta}\Gamma\,\mathbf{F}_{\Delta\theta}^{\mathrm{H}})\mathbf{F}_{\theta_1}^{\mathrm{H}} = \mathbf{F}_{\theta_1}\mathbf{F}_{\mathrm{D}}\mathbf{F}_{\theta_1}^{\mathrm{H}} \tag{5.10}$$

The matrix $\mathbf{F}_D$ is nonsingular by virtue of the fact that $\mathbf{F}_{\Delta\theta}$ has full row rank. The singular value decomposition (SVD) of $\mathbf{F}_{\Delta\theta}$ is

$$\mathbf{F}_{\Delta\theta} = \mathbf{U}\Sigma\mathbf{V}^{\mathrm{H}} \tag{5.11}$$

where $\mathbf{U} \in \mathbb{C}^{N\times N}$, $\mathbf{V} \in \mathbb{C}^{M\times M}$ and $\Sigma$ are unitary and diagonal matrices, respectively.

Column $i$ of the unitary matrix $\mathbf{U}$ is denoted as $\mathbf{u}_i$ and the $i$th diagonal element of the diagonal matrix $\Sigma$ denoted as $\sigma_i$, respectively. It is assumed that $\sigma_i$, $i = 1,\ldots,N$ are ordered in the descending order, i.e., $\sigma_i \geq \sigma_{i+1}$, $i = 1,\ldots,N-1$. The product $\mathbf{U}\Sigma$ in (5.11) may be partitioned into

$$\mathbf{U}\Sigma = [\sigma_1\mathbf{u}_1 \quad \ldots \quad \sigma_N\mathbf{u}_N| \quad \mathbf{0}] = [\mathbf{U}_\sigma \quad \mathbf{0}] = \tilde{\mathbf{U}}_\sigma \tag{5.12}$$

By utilizing (5.12), the matrix $\mathbf{F}_D$ from (5.10) becomes

$$\mathbf{F}_\mathrm{D} = \tilde{\mathbf{U}}_\sigma(\mathbf{V}^\mathrm{H}\Gamma\,\mathbf{V})\tilde{\mathbf{U}}_\sigma^\mathrm{H} \tag{5.13}$$

If the matrices $\mathbf{V}$ and $\Gamma$ are partitioned as

$$\mathbf{V} = \begin{pmatrix} \mathbf{V}_{11} & \mathbf{V}_{12} \\ \mathbf{V}_{21} & \mathbf{V}_{22} \end{pmatrix}, \quad \Gamma = \begin{pmatrix} \Gamma_{11} & 0 \\ 0 & \Gamma_{22} \end{pmatrix} \tag{5.14}$$

where $\mathbf{V}_{11}, \mathbf{V}_{22}$ are $N\times N, M\times M$ and $\mathbf{V}_{12}, \mathbf{V}_{21}$ are $, N\times(M-N), (M-N)\times N$ matrices respectively.

By substituting (5.14) in (5.13), the matrix $\mathbf{F}_D$ becomes

$$\mathbf{F}_\mathrm{D} = \mathbf{U}_\sigma(\mathbf{V}_{11}^\mathrm{H}\Gamma_{11}\boldsymbol{V}_{11} + \mathbf{V}_{21}^\mathrm{H}\Gamma_{22}\mathbf{V}_{21})\mathbf{U}_\sigma^\mathrm{H} = \mathbf{U}_\sigma\mathbf{B}\mathbf{U}_\sigma^\mathrm{H} \tag{5.15}$$

The diagonal matrices in (5.15) are chosen as

$$\Gamma_{11} = \gamma_\mathrm{L}\mathbf{I}_N, \quad \Gamma_{22} = \gamma_\mathrm{L}\mathbf{I}_{M-N} + \gamma_\mathrm{H}\Gamma_\mathrm{s} \tag{5.16}$$

where $\Gamma_\mathrm{s}$ is the diagonal matrix

$$\Gamma_\mathrm{s}(n,n) = \begin{cases} 1, & \bigcup_{i=1}^{P}\{n_i \leq n \leq n_i + L_i - 1\}, \\ 0, & \text{Otherwise.} \end{cases} \tag{5.17}$$

where $P$ is the number of interferences to be suppressed, and the range $(n_i \leq n \leq n_i + L_i - 1)$ corresponds to an angular sector centered on the DOA of the $i$th interference and the parameter $L_i$ determines the width of this range which are expected as follows, Given the angular range in which the interference DOA varies $\Delta\theta_{\text{int}}$, and the center of this range, $\theta_{\text{ic}}$, then

$$L_i = \text{ceil}(\frac{\Delta\theta_{\text{int}}}{2\pi/M}), \;\; N_{\text{ic}} = \text{ceil}(\frac{\theta_{\text{ic}}}{2\pi/M}) \tag{5.18}$$

where $\big($ceil(X) rounds each element of X to the nearest integer greater than or equal to that element and floor(X) rounds each element of X to the nearest integer less than or equal to that element$\big)$. Also $N_{ic}$ is the index of the angular intervals corresponding to the center of the range. Then, the index of the first angular interval of this range can be calculated as

$$n_i = \text{floor}(N_{\text{ic}} - \frac{1}{2}L_i) \tag{5.19}$$

The unitary property of $\mathbf{V}$ implies that

$$\mathbf{V}_{11}^{\text{H}}\mathbf{V}_{11} + \mathbf{V}_{21}^{\text{H}}\mathbf{V}_{21} = \mathbf{I}_N \tag{5.20}$$

Using (5.16-5.20), the matrix $\mathbf{B}$ in (5.15) becomes

$$\mathbf{B} = \gamma_{\text{L}}\mathbf{I}_N + \gamma_{\text{H}}\mathbf{V}_{21}^{\text{H}}\Gamma_{\text{s}}\mathbf{V}_{21} = \gamma_{\text{L}}\mathbf{I}_N + \gamma_{\text{H}}\mathbf{S}^{\text{H}}\mathbf{S} \tag{5.21}$$

where $\mathbf{S}$ is the matrix

$$\mathbf{S} = \begin{pmatrix} S_1 \\ \vdots \\ S_P \end{pmatrix}, \quad S_i = \begin{pmatrix} v_{21}(n_i) \\ \vdots \\ v_{21}(n_i + L_i - 1) \end{pmatrix} \tag{5.22}$$

and $v_{21}(n_i)$ is the $n_i^{\text{th}}$ row of $\mathbf{V}_{21}$. Application of the matrix inversion lemma (Woodbury) yields

$$\begin{aligned} \mathbf{B}^{-1} &= \frac{1}{\gamma_{\text{L}}}(\mathbf{I}_N + \frac{\gamma_{\text{H}}}{\gamma_{\text{L}}}\mathbf{S}^{\text{H}}\mathbf{S})^{-1} \\ &= \frac{1}{\gamma_{\text{L}}}[\mathbf{I}_N - \mathbf{S}^{\text{H}}(\frac{\gamma_{\text{L}}}{\gamma_{\text{H}}}\mathbf{I}_J + \mathbf{S}\mathbf{S}^H)^{-1}\mathbf{S}] \end{aligned} \tag{5.23}$$

where $J = \sum_{i=1}^{P} L_i$. Therefore, the inverse of the matrix $\mathbf{F}_D$ becomes

$$\mathbf{F}_{\text{D}}^{-1} = \frac{1}{\gamma_L}(\mathbf{U}_\sigma\mathbf{U}_\sigma^{\text{H}})^{-1} - \frac{1}{\gamma_L}\mathbf{U}_\sigma\mathbf{S}^{\text{H}}(\frac{\gamma_L}{\gamma_H}\mathbf{I}_J + \mathbf{S}\mathbf{S}^{\text{H}})^{-1}\mathbf{S}\mathbf{U}_\sigma^{\text{H}} \tag{5.24}$$

Finally, $\mathbf{C}^{-1}$ in the weight expression can be computed as

$$\mathbf{C}^{-1} = \mathbf{F}_{\theta_1}\mathbf{F}_{\text{D}}^{-1}\mathbf{F}_{\theta_1}^{\text{H}} \tag{5.25}$$

By substituting the matrix $\mathbf{C}^{-1}$ and the assumed steering vector, $\bar{\mathbf{a}}$ back into the objective function of (2.9), the proposed beamformer is obtained as

$$\mathbf{w}_{\text{pro}} = \frac{\mathbf{C}^{-1}\bar{\mathbf{a}}}{\bar{\mathbf{a}}^{\text{H}}\mathbf{C}^{-1}\bar{\mathbf{a}}} \tag{5.26}$$

It should be noted that the matrix $\mathbf{U}_\sigma$ depends only on $N$ and $M$, so that the first term on the right hand side of (5.24) can be computed once and stored. Similarly, the matrix $\mathbf{V}_{21}$ can be computed and stored.

## 5.3 Theoretical Derivation of the Array Gain Within a Notch

To investigate the performance of the proposed method, this section gives the directional response of the array in an angular interval corresponding to the interferences which can be analytically obtained for the single interference case. Also, this would be useful in understanding the relationship of the weights to the depth of the notch in the beampattern.

Let the angular interval be $[\theta_1, \theta_2]$ where a notch is to be created to suppress an interference having DOA in the middle of this range. Then, the matrix $\mathbf{C}$ in (5.2) can be written as

$$\begin{aligned}\mathbf{C} &= \gamma_{\mathrm{L}} \int_{-\pi}^{\pi} \mathbf{a}(\theta)\mathbf{a}^{\mathrm{H}}(\theta)d\theta + (\gamma_{\mathrm{H}} - \gamma_{\mathrm{L}}) \int_{\theta_1}^{\theta_2} \mathbf{a}(\theta)\mathbf{a}^{\mathrm{H}}(\theta)d\theta \\ &= 2\pi\gamma_{\mathrm{L}}\mathbf{I}_{\mathrm{N}} + \Delta\gamma\mathbf{C}_{\mathrm{I}} \end{aligned} \tag{5.27}$$

where $\mathbf{C}_{\mathrm{I}}$ defines a matrix in which the spatial region of the interference direction is located over a broad null. Let eigenvalue decomposition (EVD) of $\mathbf{C}_{\mathrm{I}}$ be

$$\mathbf{C}_{\mathrm{I}} = \mathbf{A}_i \Lambda_i \mathbf{A}_i^{\mathrm{H}} \tag{5.28}$$

where $\mathbf{A}_i = \left[\mathbf{e}_1 \cdots \mathbf{e}_R\right]$ and $\left\{\mathbf{e}_r\right\}_{r=1,\cdots,R}$ are the eigenvectors and diagonal matrix $\Lambda_i$ contains the eigenvalues of the matrix and $(R \leq N)$ denotes the rank of $\mathbf{C}_{\mathrm{I}}$. The rank $R$ depends on the width of the angular interval $[\theta_1, \theta_2]$, which goes to one as the width shrinks to zero. If the width is sufficiently small, majority of the eigenvalues would be zero, and the dominant eigenvalue would be of the order of $\lambda_{max} \approx N(\theta_2 - \theta_1)$ . Using (5.28) the inverse of $\mathbf{C}$ can be obtained as

$$\mathbf{C}^{-1} = \frac{1}{2\pi\gamma_{\mathrm{L}}}\left[\mathbf{I}_N - \mathbf{A}_i\left(\frac{2\pi\gamma_{\mathrm{L}}}{\Delta\gamma}\Lambda_i^{-1} + \mathbf{A}_i^{\mathrm{H}}\mathbf{A}_i\right)^{-1}\mathbf{A}_i^{\mathrm{H}}\right] \tag{5.29}$$

The beampattern obtained with the beamformer weight (5.26) is given by

$$\mathbf{D}(\theta) = \left|\mathbf{w}_{\text{pro}}^{\text{H}}\mathbf{a}(\theta)\right| = \left|\frac{\mathbf{a}^{\text{H}}(\theta)\mathbf{C}^{-1}\bar{\mathbf{a}}}{\bar{\mathbf{a}}^{\text{H}}\mathbf{C}^{-1}\bar{\mathbf{a}}}\right| \tag{5.30}$$

By substituting (5.29) into (5.30), the numerator can be written as

$$\left|\mathbf{a}^{\text{H}}(\theta)\mathbf{C}^{-1}\bar{\mathbf{a}}\right| = \frac{1}{2\pi\gamma_{\text{L}}}\left|\mathbf{a}^{\text{H}}(\theta)\bar{\mathbf{a}} - \mathbf{a}^{\text{H}}(\theta)\mathbf{A}_i\left(\frac{2\pi\gamma_L}{\Delta\gamma}\Lambda_i^{-1} + \mathbf{I}_R\right)^{-1}\mathbf{A}_i^{\text{H}}\bar{\mathbf{a}}\right| \tag{5.31}$$

where the fact that $\mathbf{A}_i^{\text{H}}\mathbf{A}_i = \mathbf{I}_R$ is used. Note that the steering vector $\mathbf{a}(\theta)$ can be expressed as $\mathbf{a}(\theta) = \mathbf{A}_i\mathbf{h}(\theta)$ for $\theta_1 < \theta < \theta_2$.

Defining the vector

$$\mathbf{A}_i^{\text{H}}\bar{\mathbf{a}} = \mathbf{u} = [u_1, \cdots, u_R]^T \tag{5.32}$$

which is the orthogonal projection of $\bar{\mathbf{a}}$ onto the subspace spanned by the eigenvectors $\{\mathbf{e}_r\}_{r=1,\cdots,R}$, (5.31) can be simplified as

$$\begin{aligned}\left|\mathbf{a}^{\text{H}}(\theta)\mathbf{C}^{-1}\bar{\mathbf{a}}\right| &= \frac{1}{2\pi\gamma_{\text{L}}}\left|\mathbf{h}^{\text{H}}(\theta)\mathbf{u} - \mathbf{h}^{\text{H}}(\theta)\left(\frac{2\pi\gamma_L}{\Delta\gamma}\Lambda_i^{-1} + \mathbf{I}_R\right)^{-1}\mathbf{u}\right| \\ &= \left|\sum_{l=1}^{R} h_l^*(\theta)u_l\left(\frac{1}{2\pi\gamma_L + \lambda_l\Delta\gamma}\right)\right|\end{aligned} \tag{5.33}$$

Also, The denominator of (5.30) can similarly be shown as

$$\left|\bar{\mathbf{a}}^{\text{H}}\mathbf{C}^{-1}\bar{\mathbf{a}}\right| = \frac{1}{2\pi\gamma_L}\left[\,\|\,\bar{\mathbf{a}}\,\|^2 - \sum_{l=1}^{R}|\,u_l\,|^2\left(\frac{\lambda_l\Delta\gamma}{2\pi\gamma_L + \lambda_l\Delta\gamma}\right)\right] \tag{5.34}$$

The norm of the projection $\mathbf{u}$ can be expected to be significantly smaller than the norm of $\bar{\mathbf{a}}$ on the basis that the angular direction of the SOI is sufficiently separated from the region $[\theta_1, \theta_2]$. Furthermore, most of the eigenvalues $\lambda_l$ of $\mathbf{C}_{\text{I}}$ would be either zero or much smaller than the dominant one. Based on these facts, the summation term in

(5.34) can be omitted. Then, the beampattern becomes

$$\mathbf{D}(\theta) = \frac{2\pi\gamma_{\mathrm{L}}}{\| \bar{\mathbf{a}} \|^2} \Big| \sum_{l=1}^{R} h_l^*(\theta) u_l \Big( \frac{1}{2\pi\gamma_{\mathrm{L}} + \lambda_l \Delta\gamma} \Big) \Big| \quad (\theta_1 < \theta < \theta_2) \tag{5.35}$$

This result indicates that the array gain within the notch can be made arbitrarily small by choosing large values for $\Delta\gamma$. However, since the array gain at angles outside the interference sector is also affected by $\Delta\gamma$, an unnecessarily large value may increase the gain at these angles. Hence, it should be chosen large enough to annihilate the interference without affecting array gain at other angles.

## 5.4 Computational Complexity of the Proposed Method

The computational complexity of the calculation of $\mathbf{C}^{-1}$ in (5.25) is considerably lower than when $\mathbf{C}$ is computed from (5.3) and then inverted. In (5.3), the rank-one matrices $\mathbf{a}(\theta_m)\mathbf{a}^{\mathrm{H}}(\theta_m)$ must be first calculated and those matrices which correspond to the angles belonging to $\bar{\Theta}$ are multiplied by $\gamma_{\mathrm{H}}$. These calculations involve $(M+J)N^2$ operations. On the other hand, calculation of $\mathbf{F}_{\mathrm{D}}^{-1}$ in (5.24) involves inversion of a $J \times J$ matrix, where $J$ is an integer of the order of N. The computational complexity of the JMB approach is $O(2N^3 + 2N^2)$. The complexity of the SMI beamformer is $O(N^3)$. The beamformer in MDDR beamformer has a complexity of $O(N^3 + KN)$. The QCQP method has a computational complexity of $O(N^{3.5} + N^2)$ and the complexity in the SVE method is $O(N^3 + N^2 S)$, where $S$ is the number of sampled points in the DOA region of the desired and interference signals.

## 5.5 Summary of the Proposed Algorithm

The proposed algorithm is summarized as follows:

*1: Evaluate* $\mathbf{F}_{\Delta\theta}$ *and* $\mathbf{F}_{\theta_1}$ *by* (5.8) *and* (5.9).

*2: Compute SVD of* $\mathbf{F}_{\Delta\theta}$ *by* (5.11).

*3: Calculate* $\mathbf{U}_\sigma$ *from* (5.12).

*4: Calculate* $\mathbf{S}$ *matrix by* (5.22).

*5: Calculate* $\mathbf{F}_{\mathrm{D}}^{-1}$ *using* (5.24).

*6: Compute covariance matrix inverse by* (5.25).

*7: Calculate the robust adaptive beamformer weight as* (5.26)

## 5.6 Simulation Results

In all simulations, a ULA of $N = 30$ sensors with a half-wavelength spacing is considered. The additive noise is modeled as independent spatially white Gaussian with zero-mean. We assume that the incident angle of the desired signal is known or previously estimated to the array receiver, which is set to be $\theta_{\mathrm{s}} = 2^{\circ}$ while the actual one is $0^{\circ}$. This corresponds to a $2^{\circ}$ mismatch in the signal look direction. The INRs of the interferences are both 30 dB. For each scenario, 200 Monte-Carlo runs are performed.

The proposed beamformer is compared with the following beamformers: the reconstruction based (QCQP) [33], the correlation coefficient based (SVE) [43], minimum dispersion distortionless response (MDDR) [57], steering vector estimation against jammer motion (JMB) [58] and sample covariance matrix (SMI). The number of the base vectors, width of the null and diagonal loading factor for method in [58] are set to be 6, $10^{\circ}$ and 0.01 respectively. In the proposed method, the parameter $M$ is assumed to be 720 and $\gamma_{\mathrm{L}}$ and $\gamma_{\mathrm{H}}$ are the minimum and maximum eigenvalue of the sample covariance matrix. Note that these methods are chosen for comparison based on our assumption that there is no prior information on whether interferences move or not.

### 5.6.1 Beampattern of Beamformers

In the first example, we compared the beampattern of the aforementioned methods in two scenarios. First, in Fig. 5.2 we assume that two independent interferences are from the fixed directions $-30^\circ$ and a moving one is initially located at $40^\circ$ and moves with $0.02^\circ$ per snapshots, which means the interference is moving with the time varying directions $\theta_i(k) = 40^\circ + 0.02^\circ k$.

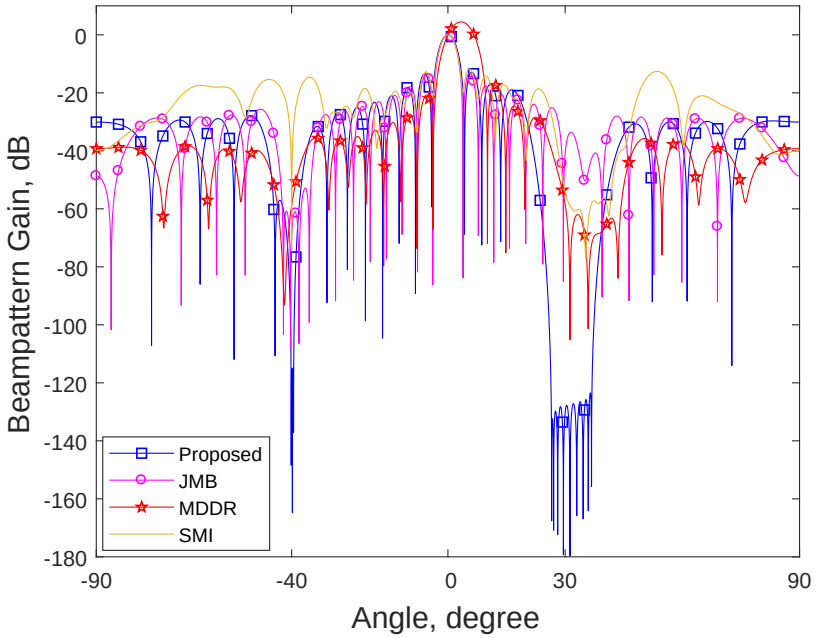


Figure 5.2: Beampattern of the beamformers for moving interference from $30^\circ$

Then, in Fig. 5.3 it is assumed that two time varying interferences are from $-30^\circ$ and $40^\circ$ and the fixed one is from $70^\circ$ direction. Also, the input SNR is 0 dB and the number of snapshots is 100. It is found that the JMB and MDDR methods are not able to broaden the interference nulls, especially for moving interferences more than two in numbers. However, in the proposed method it is indicated that the moving interference is successfully suppressed by the deep null created to span the range of DOAs in which it moves. It should be noted that, most of compared methods (except in MDDR and JMB) are based on covariance matrix reconstruction to suppress the

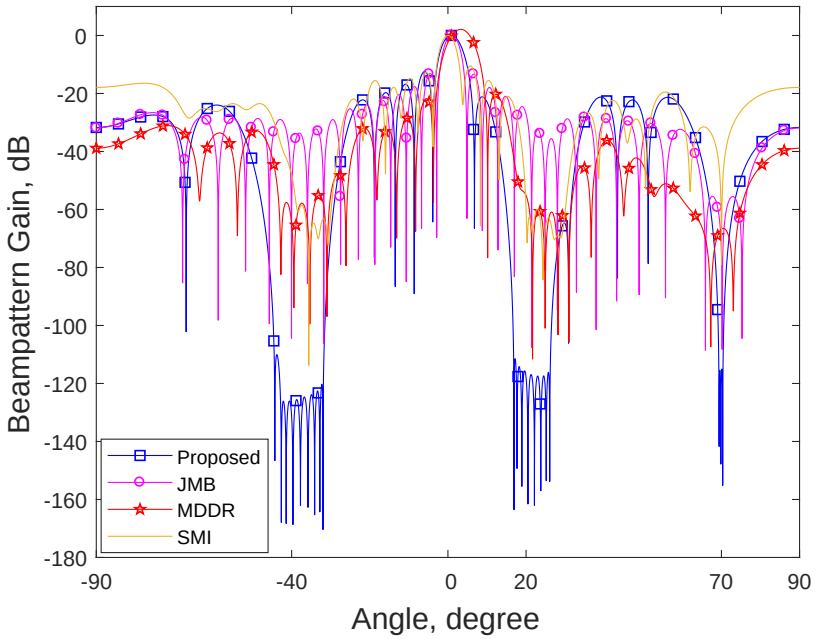

Figure 5.3: Beampattern of the beamformers for moving interferences from $20^\circ$, $-40^\circ$

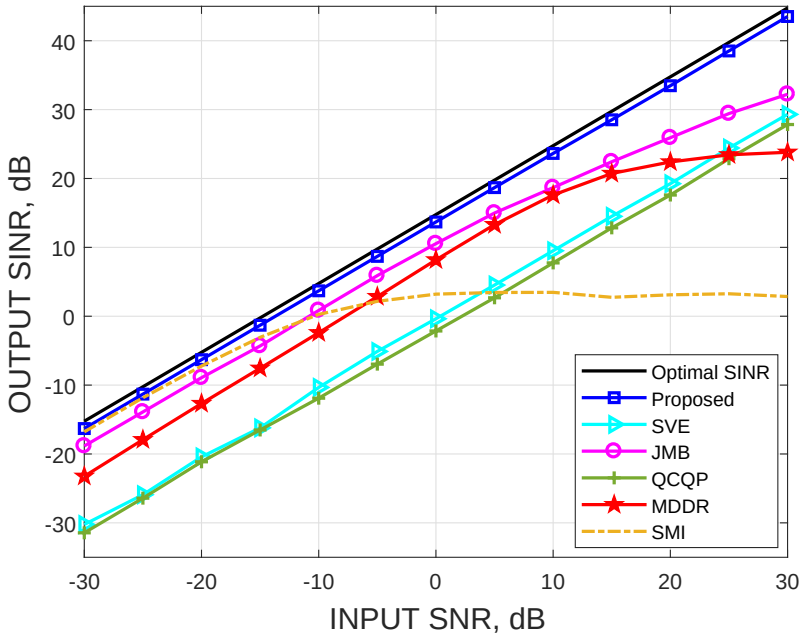

Figure 5.4: SINR versus input SNR for moving interference from $30^\circ$

interference signals. However, in the case of fast moving interference their performance deteriorates drastically.

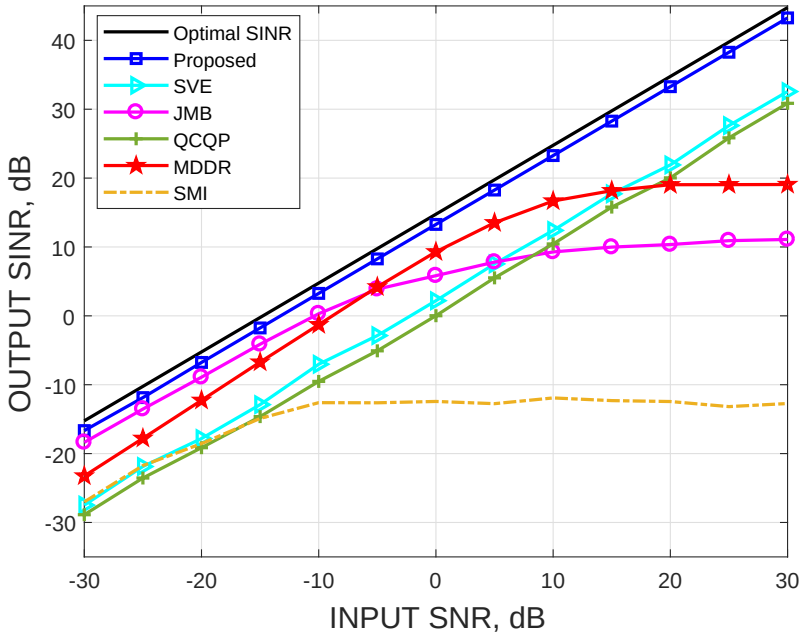

Figure 5.5: SINR versus input SNR for for moving interferences from $20°$, $-40°$

In Fig. 5.4 and Fig. 5.5, the output SINR of the aforementioned beamformers versus input SNRs is compared. As can be seen, the proposed method has better performance than other tested methods over a wide range of SNR. By contrast, the JMB method suffers a significant performance degradation due to the presence of two time varying interferences. while the other methods do not change very sensibly.

### 5.6.2 Effect of Error Due to Wavefront Mismatch

In this scenario, we investigate the impact of the mismatch when the wave propagation distortion affects the spatial signal in an homogeneous medium. It is assumed that the SOI's steering vector is distorted by a random error vector in which phase increments are fixed in each simulation and chosen independently from a Gaussian random generator with zero mean and variance $\sigma_n^2 \mathbf{I}_{M\times 1}$. We assume herein that the mismatch errors are random with zero-mean and second-order moments $\sigma_n^2 = 0.4$ and uncorrelated with the noise where the number of snapshots is fixed in $K = 100$.

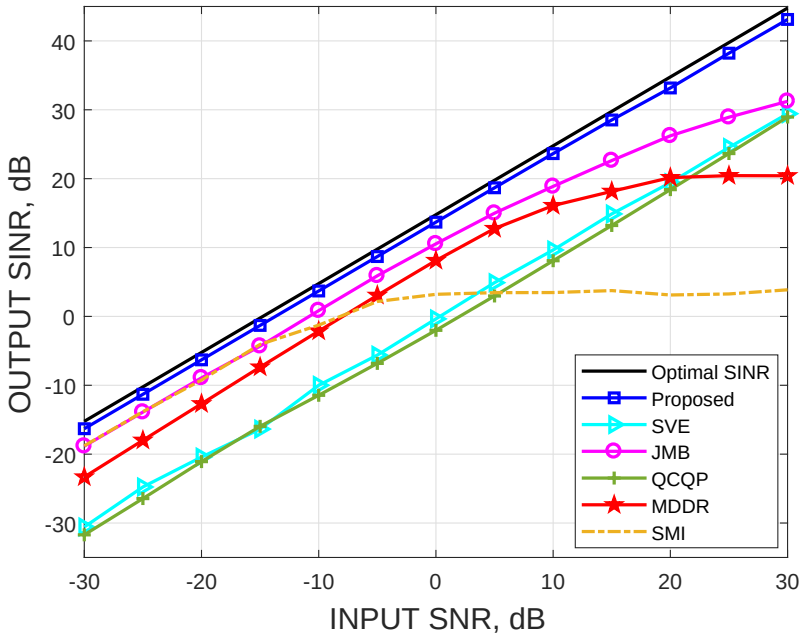

Figure 5.6: SINR versus input SNR in the case of wavefront mismatch

Fig. 5.6 compares the performances of the proposed method and other techniques with respect to the input SNRs. It is seen that the QCQP and SVE methods suffer severe performance degradation due to the inaccurate estimate of steering vector in the presence of time varying interferences. It is clearly seen that the proposed algorithm has the best performance compared to the other beamformers in wavefront mismatches. Obviously, it is very close to the optimal value, whether in high or low SNRs.

We consider the normalized beampattern of proposed method versus the other tested beamformers while SNR is fixed at 5 dB. It can be seen from Fig. 5.7 that the SMI beamformer fails in wavefront distortion. The performance of the MDDR is better than the JMB. However, its interference rejection level is degraded since the null is not deep enough. The proposed method exhibits excellent performance than other methods in interference suppression, providing wide and deep nulls in the direction of interferences.

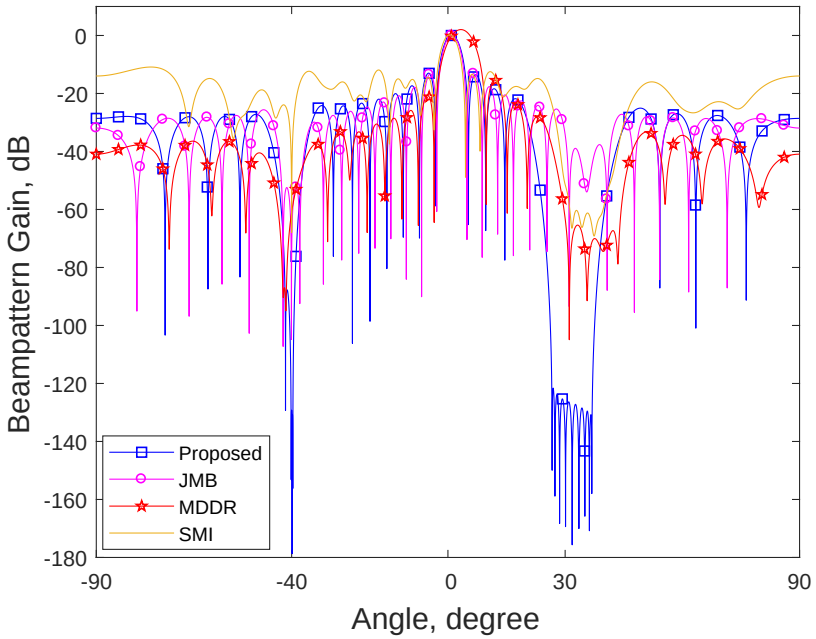

Figure 5.7: Beampattern the beamformers in the case of wavefront mismatch

### 5.6.3 Coherent Local Scattering Error for Desired Signal Steering Vector

In this simulation, the steering vector of the SOI is disturbed by local scattering effects so that the true steering vector is formed by five signal paths and is given by

$$\tilde{\mathbf{a}} = \mathbf{a} + \sum_{i=1}^{4} e^{j\psi_i} \mathbf{d}(\theta_i) \tag{5.36}$$

where $\mathbf{a}$ corresponds to the direct path, and $\mathbf{d}(\theta_i)$ ($i$=1,2,3,4) corresponds to the coherently scattered paths. We model the $i$ th path as a plane wave impinging on the array from the direction $\theta_i$. The parameters $\theta_i$ varies in every run for constant number of snapshots and randomly distributed in a Gaussian distribution with mean $\theta_s$ and standard deviation $2^\circ$. Correspondingly, the parameters $\psi_i$ denote the path phases which are changed from run to run for fixed snapshots, which can be drawn uniformly from $[0, 2\pi]$ in each simulation run. This case corresponds to the so-called coherent scattering [60]. Fig. 5.8 depicts the output SINR of the tested beamformers versus the input SNRs for the fixed training data size $K = 100$. It can be observed that the proposed beamformer still has better performance compared to the other methods

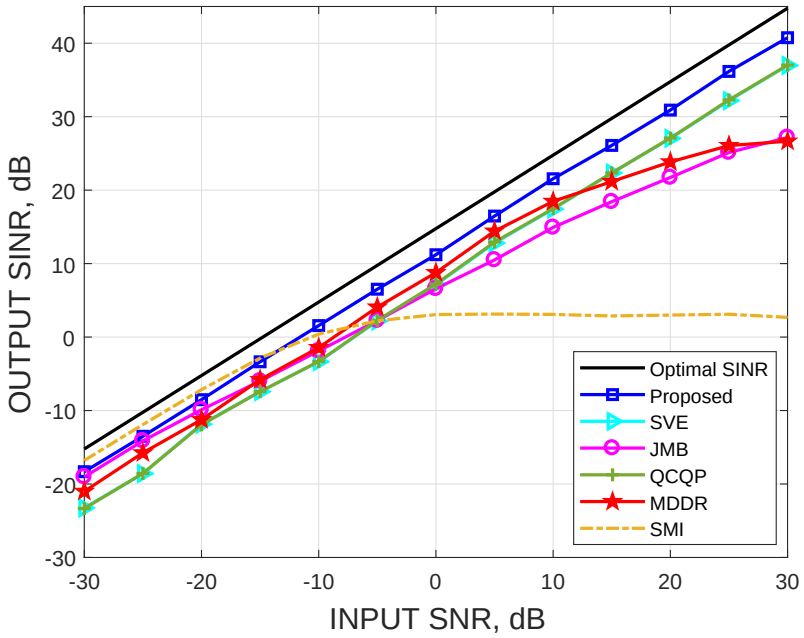

Figure 5.8: SINR versus input SNR in the case of local scattering

except the SMI method which is slightly better than the proposed method for SNRs less than -20 dB. Also, the performance of the QCQP and SVE methods have been improved where as the JMB method degrades from optimal SINR compared to before scenarios. As shown in Fig. 5.9, the proposed method's beampattern places deep nulls at the DOAs of the interference signals and maintain distortionless response for the SOI. However, the SMI method is not able to follow the DOAs of the SOI and interferences and it has high sidelobe levels.

### 5.6.4 Output SINR Versus the Number of Snapshots

We examine the performance of the beamformers as the number of snapshots $K$ is varied. It is assumed that, there is one moving interference which is from 30° direction. The other parameters remain the same as in example 1. In Fig. 5.10 the SNR is fixed at 0 dB. As shown in this figure, the SINR of the proposed method is close to the optimal one for all number of snapshots. This is the result of the proposed method's ability to adjust the widths of the notches in the directional response to correspond to the

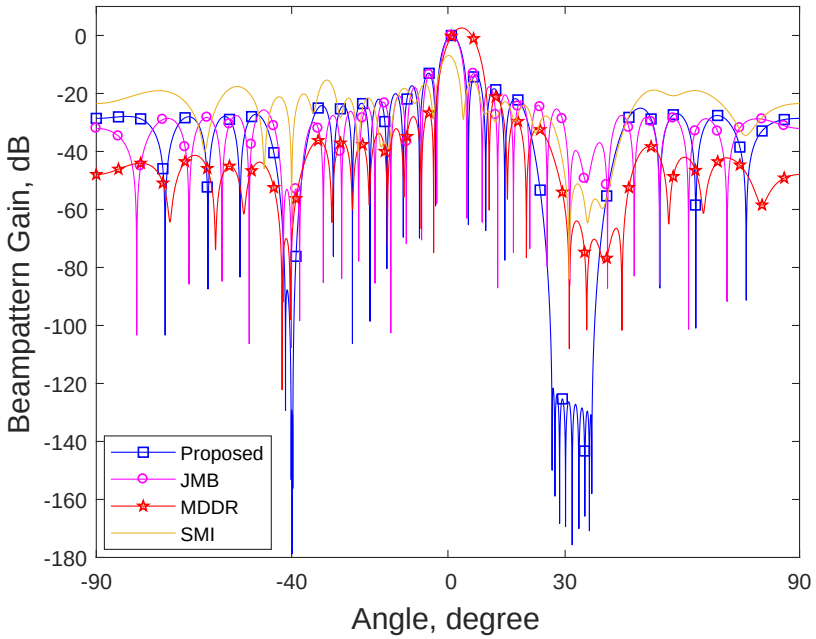

Figure 5.9: Beampattern of the beamformers in the case of local scattering

total angular variation of the moving interference. Although the JMB method shows fast convergence rate, it suffers from performance degradation mainly due to increased number of training data. The QCQP, SVE and SMI beamformers are sensitive to the nonstationary interference. Moreover it seems that the SMI beamformer requires a large number of snapshots. The performance of the MDDR method is expected to increase as snapshots are increased. However, it does not show this tendency because of its inability to create broad notches at moving interference directions.

### 5.6.5 Effect of Parameter M on Performance

The aim of this simulation is to investigate the effect of the parameter $M$. We assume that interferences are the same as in example 1, the number of snapshots is 100 and the input SNR is fixed at 0 dB while the parameter $M$ is varied. The beampattern of the proposed method with varying $M$ is shown in Fig. 5.11. It is clearly evident that the value of the parameter $M$ does not affect the performance of the proposed method. The width and depth of the notches almost always are the same for different values of

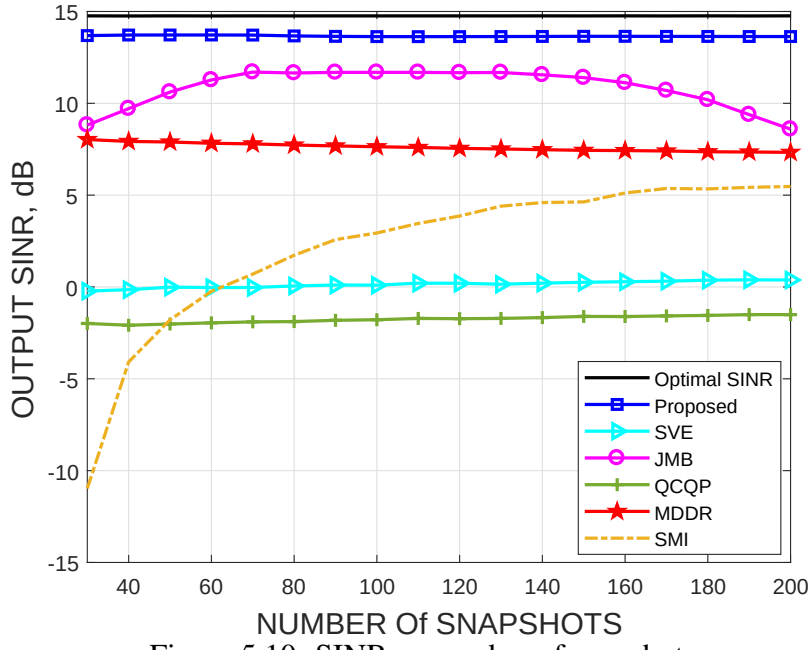

Figure 5.10: SINR vs number of snapshots

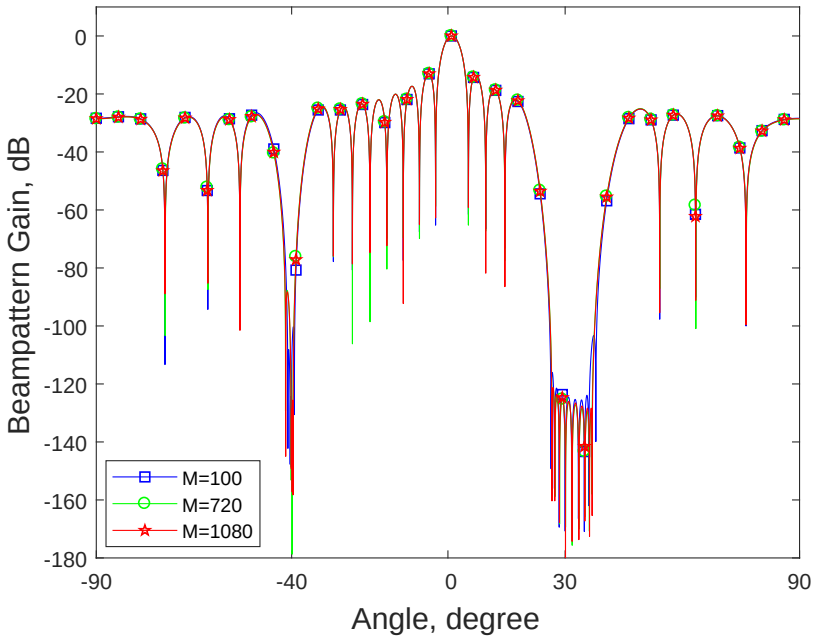

Figure 5.11: Beampatterns of the proposed method for different M values

*M* and the interferences are suppressed deeply enough.

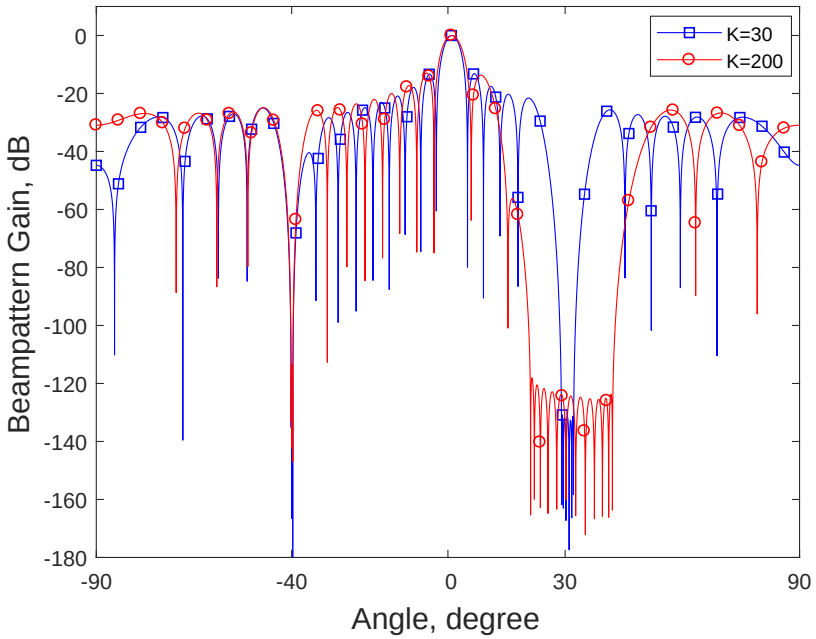

Figure 5.12: The effect of the number of snapshots on beampattern plots

### 5.6.6 Impact of the Number of Snapshots on Interference Suppression

If the number of snapshots used in the calculation of the sample covariance matrix is large enough, the spatial signature of an interference signal would become blurred. This, in turn, would deteriorate the interference rejection capability of the beamformer. Also, it implies that the number of snapshots ought to be small enough to enable tracking of a fast-moving interference, in which case SINR performance is likely to be adversely affected. However, in the proposed method varying the snapshots do not affect the output SINR. In order to show this, beampattern of the proposed method is evaluated for two different numbers of snapshots, which are demonstrated in Fig. 5.12. We assume that the input SNR is 0 dB and the parameter M is set to 720. It is clearly demonstrated that the angular range in which the interference moves when $K = 200$ is more than that of when $K = 30$. The proposed method detects the total angular range of motion and automatically adjusts the width of the corresponding notch in the directional response.

## 5.7 Conclusion

Most of interference signals encountered in real-world applications are unknown, whether they are fixed or time-varying. In this Chapter, a novel adaptive beamforming method is presented for moving interferences. The method is based on designing a weight vector which can be computed in an efficient way given the estimated DOAs of the moving interference. Simulation results have demonstrated that the proposed algorithm works effectively in generating broad notches corresponding to the time-varying DOA of a moving interference. Comparisons indicate that the proposed method outperforms some existing beamforming methods in the literature.

# Chapter 6

# CONCLUSIONS AND FUTURE WORK

## 6.1 Conclusion

Adaptive beamforming is quite sensitive to slight mismatches between the presumed and actual steering vectors. Such mismatches can occur as a result of environmental nonstationarities, look direction errors, imperfect array calibration as well as distortion caused by source spreading and local scattering. In this thesis, we present a number of new beamforming algorithms for the class of beamformers based on generalized approaches in the presence of the aforementioned problems.

In the first algorithm, we propose a new robust adaptive beamforming technique based on development of the RCB, attempting to determine the DL factor to improve steering vector estimation. Meanwhile, the DOA of the presumed SOI is updated every time through a MUSIC-like procedure by projecting it onto the signal subspace. With respect to performance, the proposed method outperforms most existing methods in a wide range of scenarios as well as low SNRs, which shows great improvement in overcoming the problem of low SNR subspace swap.

The proposed algorithm in the second method is based on projection processing. The IPNC matrix and the steering vector of the desired signal are estimated on the condition that interference signals have stronger power. In this accordance, we aimed to avoid estimation of this matrix based on reconstruction in terms of the integral of

rank-one matrices weighted by the corresponding incident power from direction $\theta$, obtained using the Capon spectral estimator. The simulation results indicate that the proposed method is robust against both the covariance matrix uncertainty and signal steering vector mismatch compared to existing methods.

Traditional adaptive beamforming's performance degrades with time-varying interferences, since they are designed to suppress interferences from fixed directions. Therefore, in the array observation vector interferences are time-varying, and consequently time-varying beamforming weights are required to achieve adequate interference cancellation. In the third approach, we investigate a robust adaptive beamformer which considers fast moving interferences. The resulting beamformer places a null region which spans the directions where the interfering sources move. The proposed method can generate notches with controllable widths and depths to suppress moving and/or stationary interference signals. Also, the beamformer weight vector is calculated directly using the inverse of the simplified covariance matrix. Simulation results have demonstrated that the proposed algorithm works effectively in different scenarios and conditions by generating broad notches corresponding to the time-varying DOA of a moving interference.

As a general conclusion, the resulting beamformers are seen to bring considerable improvement in the output SINR performance compared to some well-known approaches in the simulations.

## 6.2 The Future Work

Although, the treatment and provided analyses of proposed methodologies have shown that they constitute a set of powerful approaches for array of sensors, there are still some issues that require extensive studies for further improvement. Some of them

can be summarized as below:

- In this thesis, uniform linear arrays are considered. Further work can be extended to other array geometries such as planar and circular arrays.
- The signals induced in each array element and the reference signal are assumed uncorrelated in this work. Assuming the signals to be correlated is another challenge. Thus the work can be extended for correlated signals.
- The coupling effect between antennas in this work is not considered. Thus the work can be extended by including coupling effect.
- Narrowband signals are considered in this work. Thus, wideband signals can be considered for further studies.

Also, we aim to utilize a novel technique such as the Maximum Entropy Method (MEM) instead of the Capon estimator to optimize the SINR performance of adaptive beamforming.

# REFERENCES


[1] R. A. Monzingo and T. W. Miller, *Introduction to Adaptive Arrays*. SciTech, New York, 2004.

[2] D. G. Manolakis, V. K. Ingle, and S. M. Kogon, *Statistical and Adaptive Signal Processing: Spectral Estimation, Signal Modeling, Adaptive Filtering, and Array Processing*. McGraw-Hill, Boston, 2000.

[3] H. Cox, "Resolving power and sensitivity to mismatch of optimum array processors," *Journal of the Acoustical Society of America*, vol. 54, no. 3, pp. 771–785, 1973.

[4] M. A. Richards, *Fundamentals of Radar Signal Processing*. McGraw-Hill, New York, 2005.

[5] A. Aragon-Zavala, *Antennas and Propagation for Wireless Communication Systems*. John Wiley & Sons, New York, 2008.

[6] J. Boccuzzi, *Signal Processing for Wireless Communications*. McGraw-Hill, New York, 2008.

[7] P. S. Naidu, *Sensor Array Signal Processing*. CRC press, Washington, 2009.

[8] C. Farsakh and J. A. Nossek, "Spatial covariance based downlink beamforming in an sdma mobile radio system," *IEEE Transactions on Communications*, vol. 46,

no. 11, pp. 1497–1506, 1998.

[9] T. W. Parks and C. S. Burrus, *Digital Filter Design*. Wiley, Michigan, 1987.

[10] B. Van Veen and K. Buckley, "Beamforming techniques for spatial filtering," *Digital Signal Processing Handbook*, pp. 61–1, 1997.

[11] H. L. Van Trees, *Detection, Estimation, and Modulation Theory*. John Wiley & Sons, New York, 2004.

[12] P. Stoica and R. L. Moses, *Spectral Analysis of Signals*. Pearson Prentice Hall, New Jersy, 2005, vol. 452.

[13] M. H. Er and B. Ng, "A new approach to robust beamforming in the presence of steering vector errors," *IEEE Transactions on Signal Processing*, vol. 42, no. 7, pp. 1826–1829, 1994.

[14] A. Elnashar, S. M. Elnoubi, and H. A. El-Mikati, "Further study on robust adaptive beamforming with optimum diagonal loading," *IEEE Transactions on Antennas and Propagation*, vol. 54, no. 12, pp. 3647–3658, 2006.

[15] X. Mestre and M. A. Lagunas, "Finite sample size effect on minimum variance beamformers: Optimum diagonal loading factor for large arrays," *IEEE Transactions on Signal Processing*, vol. 54, no. 1, pp. 69–82, 2006.

[16] B. D. Carlson, "Covariance matrix estimation errors and diagonal loading in

adaptive arrays," *IEEE Transactions on Aerospace and Electronic Systems*, vol. 24, no. 4, pp. 397–401, 1988.

[17] J. Hudson, *Adaptive Array Principles*. Peregrinus LTD, London, 1991, vol. 11.

[18] Y. I. Abramovich and A. Nevrev, "An analysis of effectiveness of adaptive maximization of the signal to noise ratio which utilizes the inversion of the estimated correlation matrix," *Radio Engineering and Electronic Physics*, vol. 26, no. 12, pp. 67–74, 1981.

[19] J. Li, P. Stoica, and Z. Wang, "On robust capon beamforming and diagonal loading," *IEEE Transactions on Signal Processing*, vol. 51, no. 7, pp. 1702–1715, 2003.

[20] S. A. Vorobyov, A. B. Gershman, and Z.-Q. Luo, "Robust adaptive beamforming using worst case performance optimization: A solution to the signal mismatch problem," *IEEE Transactions on Signal Processing*, vol. 51, no. 2, pp. 313–324, 2003.

[21] S. E. Nai, W. Ser, Z. L. Yu, and H. Chen, "Iterative robust minimum variance beamforming," *IEEE Trans. Signal Processing*, vol. 59, no. 4, pp. 1601–1611, 2011.

[22] O. Kukrer and S. Mohammadzadeh, "Generalised loading algorithm for adaptive beamforming in ulas," *Electronics Letters*, vol. 50, no. 13, pp. 910–912, 2014.

[23] A. Khabbazibasmenj, S. A. Vorobyov, and A. Hassanien, "Robust adaptive beamforming based on steering vector estimation with as little as possible prior information," *IEEE Trans. Signal Processing*, vol. 60, no. 6, pp. 2974–2987, 2012.

[24] L. Du, J. Li, and P. Stoica, "Fully automatic computation of diagonal loading levels for robust adaptive beamforming," *IEEE Transactions on Aerospace and Electronic Systems*, vol. 46, no. 1, pp. 449–458, 2010.

[25] C. Gong, L. Huang, D. Xu, and Z. Ye, "Knowledge aided robust adaptive beamforming with small snapshots," *Electronics Letters*, vol. 49, no. 20, pp. 1258–1259, 2013.

[26] H. Ruan and R. C. de Lamare, "Robust adaptive beamforming using a low-complexity shrinkage based mismatch estimation algorithm." *IEEE Signal Process. Lett.*, vol. 21, no. 1, pp. 60–64, 2014.

[27] D. D. Feldman and L. J. Griffiths, "A projection approach for robust adaptive beamforming," *IEEE Transactions on Signal Processing*, vol. 42, no. 4, pp. 867–876, 1994.

[28] C. C. Lee and J.-H. Lee, "Eigenspace based adaptive array beamforming with robust capabilities," *IEEE Transactions on Antennas and Propagation*, vol. 45, no. 12, pp. 1711–1716, 1997.

[29] L. Chang and C. C. Yeh, "Performance of dmi and eigenspace based

beamformers," *IEEE Transactions on Antennas and Propagation*, vol. 40, no. 11, pp. 1336–1347, 1992.

[30] W. Jia, W. Jin, S. Zhou, and M. Yao, "Robust adaptive beamforming based on a new steering vector estimation algorithm," *Signal Processing*, vol. 93, no. 9, pp. 2539–2542, 2013.

[31] F. Huang, W. Sheng, and X. Ma, "Modified projection approach for robust adaptive array beamforming," *Signal Processing*, vol. 92, no. 7, pp. 1758–1763, 2012.

[32] Y. Gu, N. A. Goodman, S. Hong, and Y. Li, "Robust adaptive beamforming based on interference covariance matrix sparse reconstruction," *Signal Processing*, vol. 96, pp. 375–381, 2014.

[33] Y. Gu and A. Leshem, "Robust adaptive beamforming based on interference covariance matrix reconstruction and steering vector estimation," *IEEE Transactions on Signal Processing*, vol. 60, no. 7, pp. 3881–3885, 2012.

[34] X. Yuan and L. Gan, "Robust adaptive beamforming via a novel subspace method for interference covariance matrix reconstruction," *Signal Processing*, vol. 130, pp. 233–242, 2017.

[35] C. Zhou, Y. Gu, S. He, and Z. Shi, "A robust and efficient algorithm for coprime array adaptive beamforming," *IEEE Transactions on Vehicular Technology*, vol. 67, no. 2, pp. 1099–1112, 2018.

[36] C. Zhou, Z. Shi, and Y. Gu, "Coprime array adaptive beamforming with enhanced degrees of freedom capability," in *Radar Conference, 2017 IEEE*. IEEE, 2017, pp. 1357–1361.

[37] J. Zhuang and A. Manikas, "Interference cancellation beamforming robust to pointing errors," *IET Signal Processing*, vol. 7, no. 2, pp. 120–127, 2013.

[38] S. D. Somasundaram and A. Jakobsson, "Degradation of covariance reconstruction based robust adaptive beamformers," in *Sensor Signal Processing for Defence (SSPD)*. IEEE, 2014, pp. 1–5.

[39] J. Xie, H. Li, Z. He, and C. Li, "A robust adaptive beamforming method based on the matrix reconstruction against a large doa mismatch," *EURASIP Journal on Advances in Signal Processing*, vol. 2014, no. 1, p. 91, 2014.

[40] F. Shen, F. Chen, and J. Song, "Robust adaptive beamforming based on steering vector estimation and covariance matrix reconstruction," *IEEE Communications Letters*, vol. 19, no. 9, pp. 1636–1639, 2015.

[41] X. Yuan and L. Gan, "Robust algorithm against large look direction error for interference plus noise covariance matrix reconstruction," *Electronics Letters*, vol. 52, no. 6, pp. 448–450, 2016.

[42] H. Yang, W. Li, and D. Cao, "A modified robust algorithm against large look direction error based on interference plus noise covariance matrix reconstruction and steering vector double estimation," in *Progress in Electromagnetics Research*

*Symposium-Fall (PIERS-FALL), 2017*. IEEE, 2017, pp. 615–620.

[43] F. Chen, F. Shen, and J. Song, "Robust adaptive beamforming using low complexity correlation coefficient calculation algorithms," *Electronics Letters*, vol. 51, no. 6, pp. 443–445, 2015.

[44] Z. Zhang, W. Liu, W. Leng, A. Wang, and H. Shi, "Interference plus noise covariance matrix reconstruction via spatial power spectrum sampling for robust adaptive beamforming," *IEEE Signal Processing Letters*, vol. 23, no. 1, pp. 121–125, 2016.

[45] S. A. Vorobyov, "Principles of minimum variance robust adaptive beamforming design," *Signal Processing*, vol. 93, no. 12, pp. 3264–3277, 2013.

[46] R. Mailloux, "Covariance matrix augmentation to produce adaptive array pattern troughs," *Electronics Letters*, vol. 31, no. 10, pp. 771–772, 1995.

[47] J. R. Guerci, "Theory and application of covariance matrix tapers for robust adaptive beamforming," *IEEE Transactions on Signal Processing*, vol. 47, no. 4, pp. 977–985, 1999.

[48] F. Liu, J. Wang, C. Sun, and R. Du, "Robust mvdr beamformer for nulling level control via multi-parametric quadratic programming," *Progress In Electromagnetics Research*, vol. 20, pp. 239–254, 2011.

[49] J. Qian, Z. He, J. Xie, and Y. Zhang, "Null broadening adaptive beamforming

based on covariance matrix reconstruction and similarity constraint," *Eurasip Journal on Advances in Signal Processing*, no. 1, p. 1, 2017.

[50] B. D. Jeffs and K. F. Warnick, "Bias corrected psd estimation for an adaptive array with moving interference," *IEEE Transactions on Signal Processing*, vol. 56, no. 7, pp. 3108–3121, 2008.

[51] F. Liu, P.-p. Chen, J.-k. Wang, and L. Peng, "Null broadening and sidelobe control method based on multi-parametric quadratic programming," *Journal of Northeastern University (Natural Science)*, vol. 11, 2012.

[52] A. B. Gershman, U. Nickel, and J. F. Bohme, "Adaptive beamforming algorithms with robustness against jammer motion," *IEEE Transactions on Signal Processing*, vol. 45, no. 7, pp. 1878–1885, 1997.

[53] A. B. Gershman, G. V. Serebryakov, and J. F. Bohme, "Constrained hung turner adaptive beamforming algorithm with additional robustness to wideband and moving jammers," *IEEE Transactions on Antennas and Propagation*, vol. 44, no. 3, pp. 361–367, 1996.

[54] A. Amar and M. A. Doron, "A linearly constrained minimum variance beamformer with a pre specified suppression level over a pre defined broad null sector," *Signal Processing*, vol. 109, pp. 165–171, 2015.

[55] J. Riba, J. Goldberg, and G. Vazquez, "Robust beamforming for interference rejection in mobile communications," *IEEE Transactions on Signal Processing*,

vol. 45, no. 1, pp. 271–275, 1997.

[56] M. Zatman, "Production of adaptive array troughs by dispersion synthesis," *Electronics Letters*, vol. 31, no. 25, pp. 2141–2142, 1995.

[57] L. Zhang, B. Li, L. Huang, T. Kirubarajan, and H. C. So, "Robust minimum dispersion distortionless response beamforming against fast-moving interferences," *Signal Processing*, vol. 140, pp. 190–197, 2017.

[58] X. Mao, W. Li, Y. Li, Y. Sun, and Z. Zhai, "Robust adaptive beamforming against signal steering vector mismatch and jammer motion," *International Journal of Antennas and Propagation*, vol. 2015, 2015.

[59] J. P. Lie, W. Ser, and C. M. S. See, "Adaptive uncertainty based iterative robust capon beamformer using steering vector mismatch estimation," *IEEE Transactions on Signal Processing*, vol. 59, no. 9, pp. 4483–4488, 2011.

[60] J. Goldberg and H. Messer, "Inherent limitations in the localization of a coherently scattered source," *IEEE Trans. on Signal Processing*, vol. 46, no. 12, pp. 3441–3444, 1998.

[61] L. Ehrenberg, S. Gannot, A. Leshem, and E. Zehavi, "Sensitivity analysis of mvdr and mpdr beamformers," in *Electrical and Electronics Engineers in Israel (IEEEI), 2010 IEEE 26th Convention of*. IEEE, 2010, pp. 416–420.

[62] M. Wax and Y. Anu, "Performance analysis of the minimum variance

beamformer," *IEEE Transactions on Signal Processing*, vol. 44, no. 4, pp. 928–937, 1996.

[63] C. Y. Deng, "A generalization of the sherman morrison woodbury formula," *Applied Mathematics Letters*, vol. 24, no. 9, pp. 1561–1564, 2011.

[64] M. Grant, S. Boyd, and Y. Ye, "Cvx: Matlab software for disciplined convex programming," 2008.

[65] J. Li and P. Stoica, *Robust Adaptive Beamforming*. John Wiley & Sons, New York, 2005, vol. 88.

[66] S. Mohammadzadeh and O. Kukrer, "Adaptive beamforming based on theoretical interference plus noise covariance and direction of arrival estimation," *IET Signal Processing*, vol. 12, no. 7, pp. 819–825, 2018.

[67] B. D. Van Veen and K. M. Buckley, "Beamforming: A versatile approach to spatial filtering," *IEEE ASSP Magazine*, vol. 5, no. 2, pp. 4–24, 1988.

[68] L. Huang, J. Zhang, X. Xu, and Z. Ye, "Robust adaptive beamforming with a novel interference plus noise covariance matrix reconstruction method," *IEEE Trans. Signal Processing*, vol. 63, no. 7, pp. 1643–1650, 2015.

# APPENDICES

## Appendix A: The Orthogonal Projection Matrix

The following inverse of a partitioned matrix [11] can be used to evaluate the inverse on the left-hand-side of (3.7)

$$\begin{pmatrix} \mathbf{A} & \mathbf{C} \\ \mathbf{D} & \mathbf{B} \end{pmatrix}^{-1} = \begin{pmatrix} 0 \\ \mathbf{I} \end{pmatrix} \mathbf{B}^{-1} \begin{pmatrix} 0 & \mathbf{I} \end{pmatrix} + \begin{pmatrix} \mathbf{I} \\ -\mathbf{B}^{-1}\mathbf{D} \end{pmatrix} (\mathbf{A}-\mathbf{C}\mathbf{B}^{-1}\mathbf{D})^{-1} \begin{pmatrix} \mathbf{I} & -\mathbf{C}\mathbf{B}^{-1} \end{pmatrix} \tag{A.1}$$

where $\mathbf{A} \in \mathbb{C}^{m\times m}$ ,$\mathbf{B} \in \mathbb{C}^{n\times n}$, $\mathbf{C} \in \mathbb{C}^{m\times n}$, $\mathbf{D} \in \mathbb{C}^{n\times m}$. We need to find the inverse $(\mathbf{A}_{\mathrm{s}}^{\mathrm{H}}\mathbf{A}_{\mathrm{s}})^{-1}$ as follows

$$(\mathbf{A}_{\mathrm{s}}^{\mathrm{H}}\mathbf{A}_{\mathrm{s}})^{-1} = \begin{pmatrix} \|\mathbf{a}_{\circ}\|^2 & \mathbf{a}_{\circ}^{\mathrm{H}}\mathbf{A}_i \\ \mathbf{A}_i^{\mathrm{H}}\mathbf{a}_{\circ} & \mathbf{A}_i^{\mathrm{H}}\mathbf{A}_i \end{pmatrix}^{-1} \tag{A.2}$$

with the appropriate associations

$$\begin{aligned}(\mathbf{A}_{\mathrm{s}}^{\mathrm{H}}\mathbf{A}_{\mathrm{s}})^{-1} = {} & \begin{pmatrix} 0 \\ \mathbf{I} \end{pmatrix} (\mathbf{A}_i^{\mathrm{H}}\mathbf{A}_i)^{-1} \begin{pmatrix} 0 & \mathbf{I} \end{pmatrix} + \frac{1}{\|\mathbf{a}_{\circ}\|^2 - \mathbf{a}_{\circ}^{\mathrm{H}}\mathbf{A}_i(\mathbf{A}_i^{\mathrm{H}}\mathbf{A}_i)^{-1}\mathbf{A}_i^{\mathrm{H}}\mathbf{a}_{\circ}} \\ & \cdot \begin{pmatrix} 1 \\ -(\mathbf{A}_i^{\mathrm{H}}\mathbf{A}_i)^{-1}\mathbf{A}_i^{\mathrm{H}}\mathbf{a}_{\circ} \end{pmatrix} \begin{pmatrix} 1 & -\mathbf{a}_{\circ}^{\mathrm{H}}\mathbf{A}_i(\mathbf{A}_i^{\mathrm{H}}\mathbf{A}_i)^{-1} \end{pmatrix}\end{aligned} \tag{A.3}$$

Multiplying the left-hand side of (A.3) by $\mathbf{A}_{\mathrm{s}}$ and the right-hand side by $\mathbf{A}_{\mathrm{s}}^{\mathrm{H}}$ and rearranging (A.3) will be expressed as (3.7).

## Appendix B: Computation of Approximated Desired signal's SV

The matrix $(\mathbf{I}+\lambda\mathbf{R})$ can be written as

$$\mathbf{I}+\lambda\mathbf{R} = (1+\lambda\sigma_{\mathrm{n}}^2)\mathbf{I}+\lambda\sigma_{\mathrm{s}}^2\mathbf{a}_{\circ}\mathbf{a}_{\circ}^{\mathrm{H}}+\lambda\mathbf{A}_i\mathbf{D}_i\mathbf{A}_i^{\mathrm{H}} = \mathbf{R}_{\mathrm{n}\lambda}+\lambda\sigma_{\mathrm{s}}^2\mathbf{a}_{\circ}\mathbf{a}_{\circ}^{\mathrm{H}} \tag{B.1}$$

where $\mathbf{R}_{\mathrm{n}\lambda} = (1+\lambda\sigma_{\mathrm{n}}^2)\mathbf{I}+\lambda\mathbf{A}_i\mathbf{D}_i\mathbf{A}_i^{\mathrm{H}}$.

Using the well-known matrix inversion lemma, the inverse becomes

$$(\mathbf{I}+\lambda\mathbf{R})^{-1} = (\mathbf{R}_{\mathrm{n}\lambda}+\lambda\sigma_{\mathrm{s}}^2\mathbf{a}_{\circ}\mathbf{a}_{\circ}^{\mathrm{H}})^{-1} = \mathbf{R}_{\mathrm{n}\lambda}^{-1}-\mathbf{R}_{\mathrm{n}\lambda}^{-1}\big(\frac{\lambda\sigma_{\mathrm{s}}^2\mathbf{a}_{\circ}\mathbf{a}_{\circ}^{\mathrm{H}}}{1+\lambda\sigma_{\mathrm{s}}^2\mathbf{a}_{\circ}^{\mathrm{H}}\mathbf{R}_{\mathrm{n}\lambda}^{-1}\mathbf{a}_{\circ}}\big)\mathbf{R}_{\mathrm{n}\lambda}^{-1} \tag{B.2}$$

Again by using the same lemma the inverse of $\mathbf{R}_{\mathrm{n}\lambda}$ can be written as

$$\mathbf{R}_{\mathrm{n}\lambda}^{-1} = \frac{1}{1+\lambda\sigma_{\mathrm{n}}^2}\big[\mathbf{I}-\mathbf{A}_i((\lambda_{\mathrm{d}}+\sigma_{\mathrm{n}}^2)\mathbf{D}_i^{-1}+\mathbf{A}_i^{\mathrm{H}}\mathbf{A}_i)^{-1}\mathbf{A}_i^{\mathrm{H}}\big] = \frac{1}{1+\lambda\sigma_{\mathrm{n}}^2}(\mathbf{I}-\mathbf{P}) \tag{B.3}$$

where $\mathbf{P}$ is the second term within the square brackets and $\lambda_{\mathrm{d}} = 1/\lambda$. By substituting (B.3) into (B.2) , multiplying both sides by $\bar{\mathbf{a}}$ and simplifying gives

$$(\mathbf{I}+\lambda\mathbf{R})^{-1}\bar{\mathbf{a}} = \frac{1}{1+\lambda\sigma_{\mathrm{n}}^2}\big[(\mathbf{I}-\mathbf{P})\bar{\mathbf{a}}-\frac{\mathbf{a}_{\circ}^{\mathrm{H}}(\mathbf{I}-\mathbf{P})\bar{\mathbf{a}}}{\mu(\lambda)+\mathbf{a}_{\circ}^{\mathrm{H}}(\mathbf{I}-\mathbf{P})\mathbf{a}_{\circ}}(\mathbf{I}-\mathbf{P})\mathbf{a}_{\circ}\big]$$

$$\begin{aligned}(1+\lambda\sigma_{\mathrm{n}}^2)(\mathbf{I}+\lambda\mathbf{R})^{-1}\bar{\mathbf{a}} &= (\mathbf{I}-\mathbf{P})\big[\bar{\mathbf{a}}-\eta(\lambda)\mathbf{a}_{\circ}\big]\\ &= \bar{\mathbf{a}}-\big[\eta(\lambda)\mathbf{a}_{\circ}+\mathbf{P}(\bar{\mathbf{a}}-\eta(\lambda)\mathbf{a}_{\circ})\big]\end{aligned} \tag{B.4}$$

where $\mu(\lambda) = (1+\lambda\sigma_{\mathrm{n}}^2)/(\lambda\sigma_{\mathrm{s}}^2)$ and $\eta(\lambda) = \mathbf{a}_{\circ}^{\mathrm{H}}(\mathbf{I}-\mathbf{P})\bar{\mathbf{a}}/(\mu(\lambda)+\mathbf{a}_{\circ}^{\mathrm{H}}(\mathbf{I}-\mathbf{P})\mathbf{a}_{\circ})$. From (B.4) we obtain

$$\hat{\mathbf{a}}_{\circ}(\lambda) = \eta(\lambda)\mathbf{a}_{\circ}+\mathbf{P}(\bar{\mathbf{a}}-\eta(\lambda)\mathbf{a}_{\circ}) = \bar{\mathbf{a}}-(1+\lambda\sigma_{\mathrm{n}}^2)(\mathbf{I}+\lambda\mathbf{R})^{-1}\bar{\mathbf{a}} \tag{B.5}$$

Note that the noise power $\sigma_{\mathrm{n}}^2$ can be estimated from the eigenvalue decomposition of the covariance matrix. Here, the minimum of eigenvalues is taken as an estimate of the noise power.

## Appendix C: Interference Eigenvectors of SCM and IPNC

Let the theoretical covariance matrix of the signal received by the beamformer be written as

$$\hat{\mathbf{R}} = \sigma_s^2 \mathbf{a}_\circ \mathbf{a}_\circ^H + \mathbf{R}_{i+n} \tag{C.1}$$

The problem is to derive the relationship between the eigenvectors of $\hat{\mathbf{R}}$ and those of $\mathbf{R}_{i+n}$ corresponding to the interference signals. Let's write the EVD of $\mathbf{R}_{i+n}$ as

$$\mathbf{R}_{i+n} = \sum_{j=N-L+1}^{N} \tilde{\lambda}_j \tilde{\mathbf{e}}_j \tilde{\mathbf{e}}_j^H = \tilde{\mathbf{E}} \tilde{\Lambda} \tilde{\mathbf{E}}^H \tag{C.2}$$

Also, let $\mathbf{e}$ be an eigenvector of $\hat{\mathbf{R}}$ with corresponding eigenvalue $\lambda$. The representations of $\mathbf{e}$ and $\mathbf{a}_\circ$ with respect to the basis vectors of $C^{N\times 1}$ which are the eigenvectors in $\tilde{\mathbf{E}}$, can be expressed as

$$\mathbf{e} = \tilde{\mathbf{E}}\alpha, \qquad \mathbf{a}_\circ = \tilde{\mathbf{E}}\beta, \qquad \|\mathbf{e}\|^2 = \|\alpha\|^2 = 1 \qquad \|\beta\|^2 = \|\mathbf{a}_\circ\|^2 \tag{C.3}$$

Then, by inserting (C.3) into and (C.1) and post multiplying that by $\mathbf{e}$, it can be written as

$$\begin{aligned}
\hat{\mathbf{R}}\mathbf{e} &= (\sigma_s^2 \mathbf{a}_\circ \mathbf{a}_\circ^H + \mathbf{R}_{i+n})\mathbf{e} \\
&= \sigma_s^2 (\tilde{\mathbf{E}}\beta)(\tilde{\mathbf{E}}\beta)^H \tilde{\mathbf{E}}\alpha + \mathbf{R}_{i+n}\tilde{\mathbf{E}}\alpha \\
&= (\sigma_s^2 \beta^H \alpha)\tilde{\mathbf{E}}\beta + \mathbf{R}_{i+n}\tilde{\mathbf{E}}\alpha \\
&= (\sigma_s^2 \beta^H \alpha)\tilde{\mathbf{E}}\beta + \tilde{\mathbf{E}}\tilde{\Lambda}\alpha \\
&= \tilde{\mathbf{E}}[(\sigma_s^2 \beta^H \alpha)\beta + \tilde{\Lambda}\alpha] \\
&= \lambda \tilde{\mathbf{E}}\alpha
\end{aligned} \tag{C.4}$$

Since $\tilde{\mathbf{E}}$ in nonsingular, then $\tilde{\Lambda}\alpha + \sigma_s^2(\beta^H\alpha)\beta = \lambda\alpha$, and (C.4) implies that

$$(\lambda\mathbf{I} - \tilde{\Lambda})\alpha = (\sigma_s^2\beta^H\alpha)\beta \tag{C.5}$$

If $(\lambda, \mathbf{e})$ is not an eigenpair of $\mathbf{R}_{i+n}$ then $(\lambda\mathbf{I} - \tilde{\Lambda})$ is nonsingular. Solving for $\alpha$

$$\alpha = (\sigma_s^2\beta^H\alpha)(\lambda\mathbf{I} - \tilde{\Lambda})^{-1}\beta \tag{C.6}$$

Premultiplying (C.6) by $\beta^H$, and assuming that $\mathbf{a}_\circ$ is not orthogonal to $\mathbf{e}$ (so that $\beta^H\alpha \neq 0$)

$$\beta^H\alpha = (\sigma_s^2\beta^H\alpha)\beta^H(\lambda\mathbf{I} - \tilde{\Lambda})^{-1}\beta \qquad \Rightarrow \qquad \sigma_s^2\beta^H(\lambda\mathbf{I} - \tilde{\Lambda})^{-1}\beta = 1 \tag{C.7}$$

which is written explicitly as

$$\sigma_s^2 \sum_{i=1}^{N} \frac{|\beta_i|^2}{\lambda - \tilde{\lambda}_i} = 1 \tag{C.8}$$

Solution of (C.8) gives the eigenvalues of $\hat{\mathbf{R}}$ which are not common with those of $\mathbf{R}_{i+n}$. Note that if $\hat{\mathbf{R}}$ has $J$ eigenvalues corresponding to the noise only, then $\mathbf{R}_{i+n}$ has $J+1$ noise eigenvalues [12].

After solving for the eigenvalue $\lambda$, the corresponding eigenvector $\mathbf{e}$ should be determined by solving for $\alpha$. For this the fact that $\|\alpha\| = 1$ is used, giving

$$\sigma_s^2|\beta^H\alpha| = [\sum_{i=1}^{N} \frac{|\beta_i|^2}{(\lambda - \tilde{\lambda}_i)^2}]^{-1/2} \tag{C.9}$$

Let $\lambda = \lambda_k$ correspond to either an interference or the desired signal, with the corresponding eigenvalue $\tilde{\lambda}_k$ of $\mathbf{R}_{i+n}$. Note that if $\lambda_k$ corresponds to the desired

signal, then $\tilde{\lambda}_k = \sigma_{\mathrm{n}}^2$. The eigenvector $\mathbf{e}_k$ is obtained as

$$\mathbf{e}_j = \tilde{\mathbf{E}}\alpha = \sigma_{\mathrm{s}}^2(\beta^{\mathrm{H}}\alpha)\{\frac{\beta_j}{\lambda_j - \tilde{\lambda}_j}\tilde{\mathbf{e}}_j + \sum_{i=1, i\neq j}^{N} \frac{\beta_i}{\lambda_j - \tilde{\lambda}_i}\,\tilde{\mathbf{e}}_i\} \tag{C.10}$$

It can be observed that, when the desired signal power is sufficiently smaller than the interference signal powers, $\lambda_k - \tilde{\lambda}_k$ will be much smaller than $\lambda_j - \tilde{\lambda}_i, i \neq j$. This in turn makes the coefficient of $\tilde{\mathbf{e}}_j$ in (C.10) much larger than those of $\tilde{\mathbf{e}}_i$. It is impossible to solve for the eigenvalues of $\hat{\mathbf{R}}$ in terms of those of $\mathbf{R}_{\mathrm{i+n}}$ for the general case of multiple interferences, making it difficult for a quantitative assessment of the difference between the eigenvectors of $\hat{\mathbf{R}}$ and $\mathbf{R}_{\mathrm{i+n}}$ corresponding to an interference. However, closed form solution of the eigenvalues is possible in the case of a single interference. For this case, the interference eigenvalue and eigenvector of $\hat{\mathbf{R}}$ can be obtained approximately. Let assume that $\tilde{\lambda}_i = \sigma_{\mathrm{n}}^2$ for $i = 1, ..., N-1$ and $\tilde{\lambda}_N$ is the interference of $\mathbf{R}_{\mathrm{i+n}}$

$$\sigma_{\mathrm{s}}^2\Big(\frac{|\beta_N|^2}{\lambda - \tilde{\lambda}_N} + \sum_{i=1}^{N-1}\frac{|\beta_i|^2}{\lambda - \sigma_{\mathrm{n}}^2}\Big) = 1 \tag{C.11}$$

Let $\rho = \sum_{i=1}^{N-1}|\beta_i|^2$

$$\sigma_{\mathrm{s}}^2\Big(\frac{|\beta_N|^2}{\lambda - \tilde{\lambda}_N} + \frac{\rho}{\lambda - \sigma_{\mathrm{n}}^2}\Big) = 1 \Rightarrow$$

$$\lambda^2 - [\tilde{\lambda}_N + \sigma_{\mathrm{n}}^2 + \sigma_{\mathrm{s}}^2\|\mathbf{a}_\circ\|^2]\lambda + [(\sigma_{\mathrm{n}}^2 + \sigma_{\mathrm{s}}^2\rho)\tilde{\lambda}_N + \sigma_{\mathrm{n}}^2\sigma_{\mathrm{s}}^2|\beta_N|^2] = 0 \tag{C.12}$$

By solving (C.12) for the interference eigenvalue $\lambda_N$ of $\hat{\mathbf{R}}$

$$\lambda_N = \frac{1}{2}(\tilde{\lambda}_N + \sigma_{\mathrm{n}}^2 + \sigma_{\mathrm{s}}^2\|\mathbf{a}_\circ\|^2)\Big[1 + \sqrt{1 - \frac{4(\sigma_{\mathrm{n}}^2 + \sigma_{\mathrm{s}}^2\rho)\tilde{\lambda}_N + \sigma_{\mathrm{n}}^2\sigma_{\mathrm{s}}^2|\beta_N|^2}{(\tilde{\lambda}_N + \sigma_{\mathrm{n}}^2 + \sigma_{\mathrm{s}}^2\|\mathbf{a}_\circ\|^2)^2}}\Big] \tag{C.13}$$

If $\tilde{\lambda}_N \gg \sigma_n^2 + \sigma_s^2 \parallel \mathbf{a}_\circ \parallel^2$ then

$$\begin{aligned}\lambda_N &\cong \tilde{\lambda}_N + \sigma_n^2 + \sigma_s^2 \|\mathbf{a}_\circ\|^2 - \frac{(\sigma_n^2 + \sigma_s^2\rho)\tilde{\lambda}_N + \sigma_n^2\sigma_s^2|\beta_N|^2}{\tilde{\lambda}_N + \sigma_n^2 + \sigma_s^2\|\mathbf{a}_\circ\|^2} \\ &\cong \tilde{\lambda}_N + \sigma_s^2(\|\mathbf{a}_\circ\|^2 - \rho) - \frac{\sigma_n^2\sigma_s^2|\beta_N|^2}{\tilde{\lambda}_N} \\ &\cong \tilde{\lambda}_N + \sigma_s^2|\beta_N|^2\big(1 - \frac{\sigma_n^2}{\tilde{\lambda}_N}\big) \end{aligned} \tag{C.14}$$

and the eigenvector is

$$\mathbf{e}_N = \sigma_s^2(\beta^H\alpha)\{\frac{\beta_N}{\lambda_N - \tilde{\lambda}_N}\tilde{\mathbf{e}}_N + \sum_{i=1}^{N-1}\frac{\beta_i}{\lambda_N - \tilde{\lambda}_i}\,\tilde{\mathbf{e}}_i\} \tag{C.15}$$

Assume that $\tilde{\lambda}_i = \sigma_n^2$ and from (C.14), we have

$$\lambda_N - \tilde{\lambda}_N = \sigma_s^2|\beta_N|^2\big(1 - \frac{\sigma_n^2}{\tilde{\lambda}_N}\big) \tag{C.16}$$

then

$$\mathbf{e}_N = \sigma_s^2(\beta^H\alpha)\Big(\frac{\beta_N}{\sigma_s^2|\beta_N|^2\big(1 - \frac{\sigma_n^2}{\tilde{\lambda}_N}\big)}\tilde{\mathbf{e}}_N + \frac{1}{\lambda_N - \sigma_n^2}\sum_{i=1}^{N-1}\beta_i\tilde{\mathbf{e}}_i\Big) \tag{C.17}$$

In order to simplify (C.17), we utilize $\|\alpha\|^2 = 1$

$$\|\alpha\|^2 = \sigma_s^4|\beta^H\alpha|^2\sum_{i=1}^{N}\frac{|\beta_i|^2}{(\lambda - \tilde{\lambda}_i)^2} = 1 \tag{C.18}$$

By assuming $\lambda = \lambda_N$ we have

$$\begin{aligned}\sum_{i=1}^{N}\frac{|\beta_i|^2}{(\lambda_N - \tilde{\lambda}_i)^2} &= \sum_{i=1}^{N-1}\frac{|\beta_i|^2}{(\lambda_N - \sigma_n^2)^2} + \frac{|\beta_N|^2}{(\lambda_N - \tilde{\lambda}_N)^2} \\ &= \frac{\rho}{(\lambda_N - \sigma_n^2)^2} + \frac{1}{\sigma_s^4|\beta_N|^2\big(1 - \frac{\sigma_n^2}{\tilde{\lambda}_N}\big)^2}\end{aligned} \tag{C.19}$$

By substituting in (C.18)

$$\frac{\sigma_s^4|\beta^H\alpha|^2\rho}{(\lambda_N-\sigma_n^2)^2}+\frac{|\beta^H\alpha|^2}{|\beta_N|^2\big(1-\frac{\sigma_n^2}{\tilde{\lambda}_N})^2}=1 \tag{C.20}$$

Using (C.19), (C.20) can be written as

$$|\beta^H\alpha|^2\Big(\frac{\sigma_s^4\rho}{(\tilde{\lambda}_N+\sigma_s^2|\beta_N|^2)^2}+\frac{1}{|\beta_N|^2)^2}\Big)=(1-\frac{\sigma_n^2}{\tilde{\lambda}_N})^2 \tag{C.21}$$

By neglecting the first part, we can claim that

$$|\beta^H\alpha|\cong|\beta_N|(1-\frac{\sigma_n^2}{\tilde{\lambda}_N}) \tag{C.22}$$

and finally, the eigenvector of $\hat{\mathbf{R}}$ will be

$$\mathbf{e}_N\cong\tilde{\mathbf{e}}_N+|\beta_N|(\frac{\sigma_s^2}{\tilde{\lambda}_N})(\frac{\tilde{\lambda}_N-\sigma_n^2}{\lambda_N-\sigma_n^2})\sum_{i=1}^{N-1}\beta_i\tilde{\mathbf{e}}_i \tag{C.23}$$

where $\tilde{\lambda}_N\gg\sigma_n^2+\sigma_s^2\parallel\mathbf{a}_\circ\parallel^2$ and $(1-x)^{1/2}\simeq 1-(x/2)$ have been made. It is clear from (C.23) that if $\sigma_s^2\ll\tilde{\lambda}_N$ then $\mathbf{e}_N\cong\tilde{\mathbf{e}}_N$.